

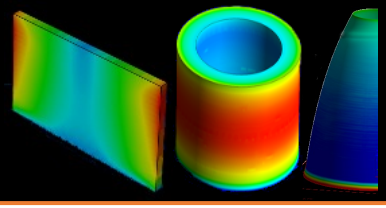
National Aeronautics and
Space Administration

Game Changing Development Program Office

Modeling & Simulation RAMPT Closeout Review

December 7, 2023

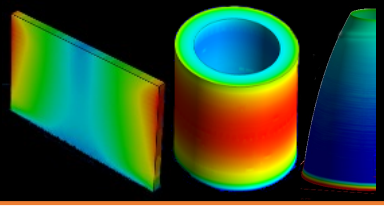
Authors:
Kevin R. Wheeler – NASA ARC
Vasyl Hafiychuk – KBR Wyle Services, LLC NASA ARC
Halyna Hafiychuk – KBR Wyle Services, LLC NASA ARC



Modeling

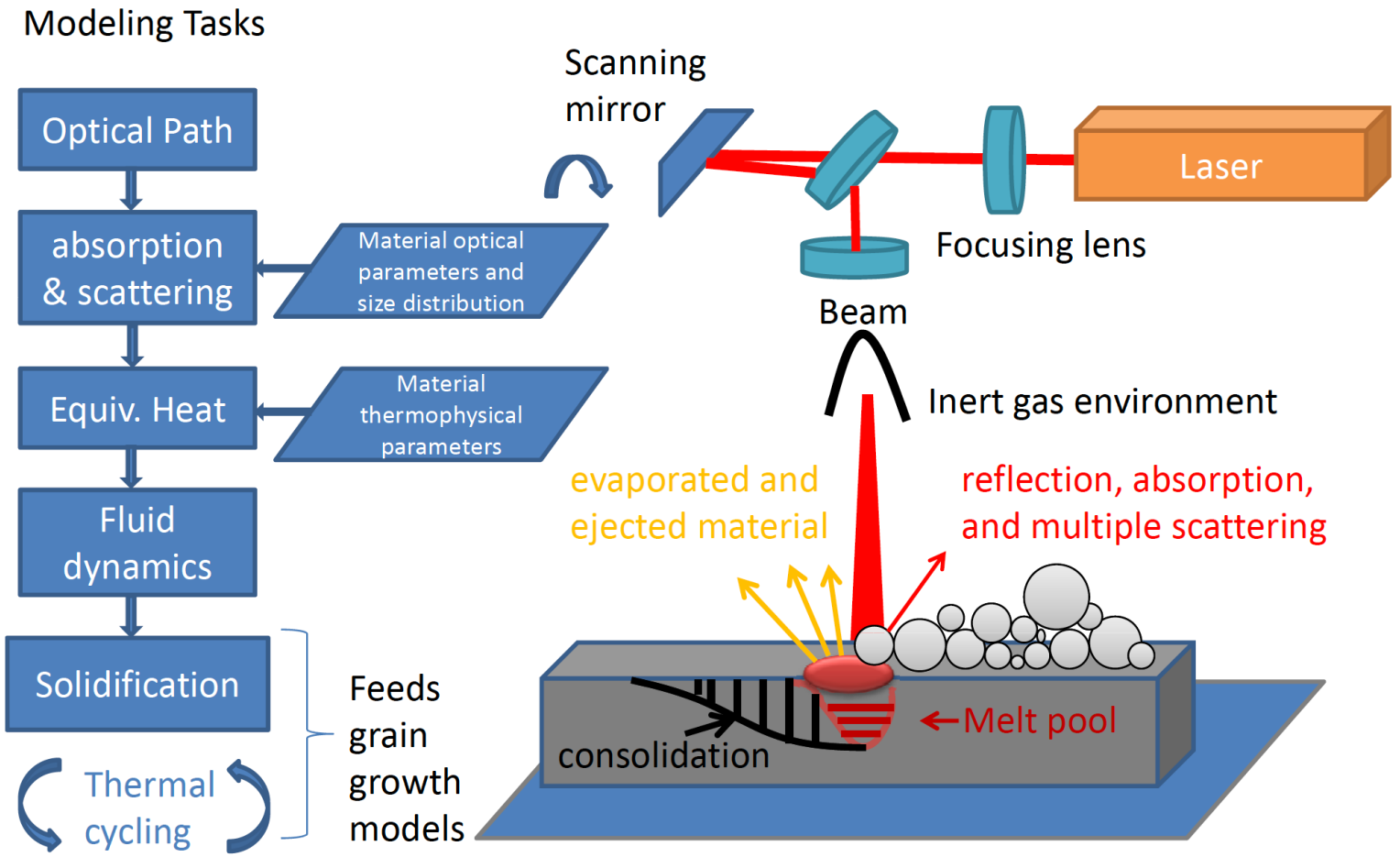
RAMPT Modeling Topics:

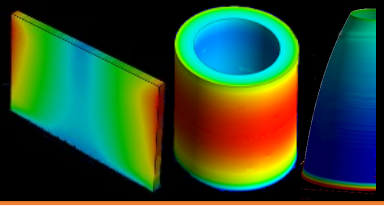
- Melt-pool with validation
  - Material Curves
  - Thermal model/Evaporation
  - Scaling – pragmatic method
- 3 Coupons for validation
  - Geometries
  - Models across scales
- X-ray diffraction and neutron source
  - X-ray vs neutron
- Validation – with NIST Data
- Scaling up modeling
  - Thermal lumped layers
  - Inherent Strain
  - Utilizing G-code
- Full-scale RS-25 Nozzle
- Bi-metallics
  - Cylinder coupons
  - Model analyses
  - Nickel layer analysis
- Conclusions



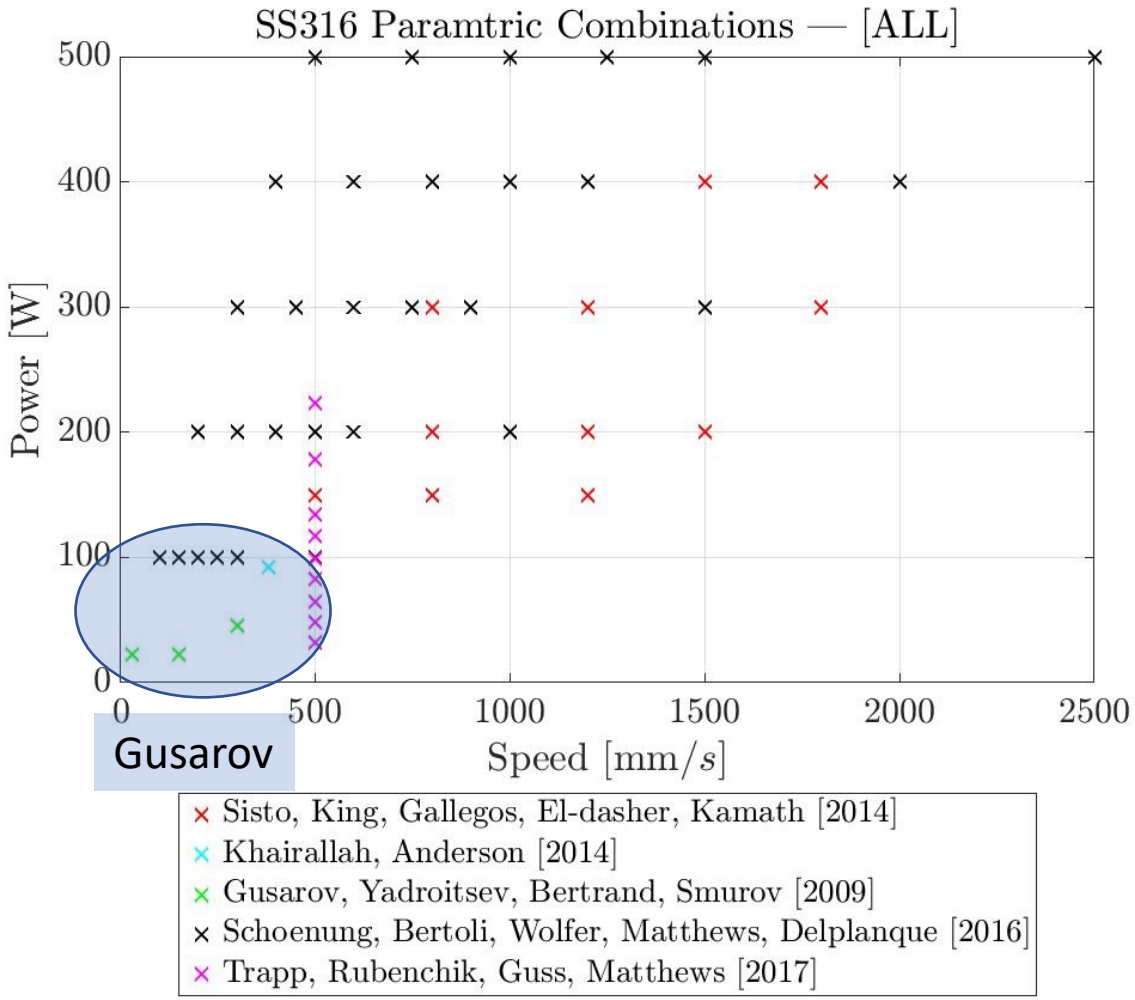
Details of melt-pool physics

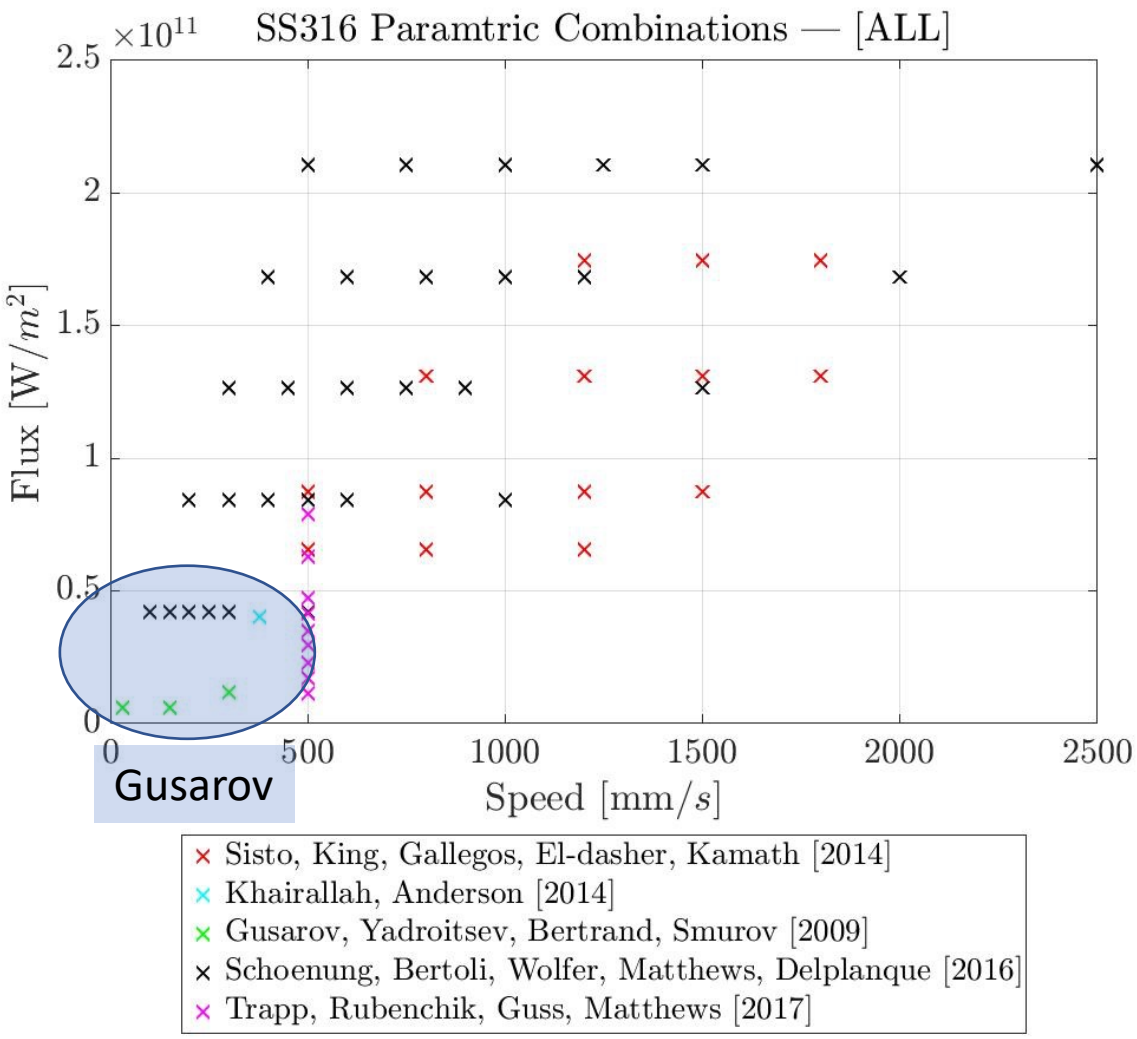
- Optical
  - Powder absorptivity
- Phase-state
  - Powder state - Phase change of powder from particles to liquid
- Thermal
  - Heat source
  - Phase changes (solid, fluid, boil)
  - Mass flux from evaporation
  - Conduction
  - Convection
  - Cooling rates & solidification
- Fluid
  - Velocity of melt-pool currents
  - Evaporation recoil pressure
  - Viscosity surface tension of temperature
- Multi-physics
  - Maragoni flow (surface tension as function of temperature)
  - Non-isothermal flow
- Geometric Deformation/moving mesh



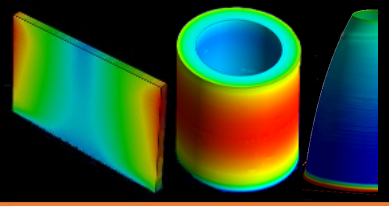


SS316 Melt-pool Dimensions

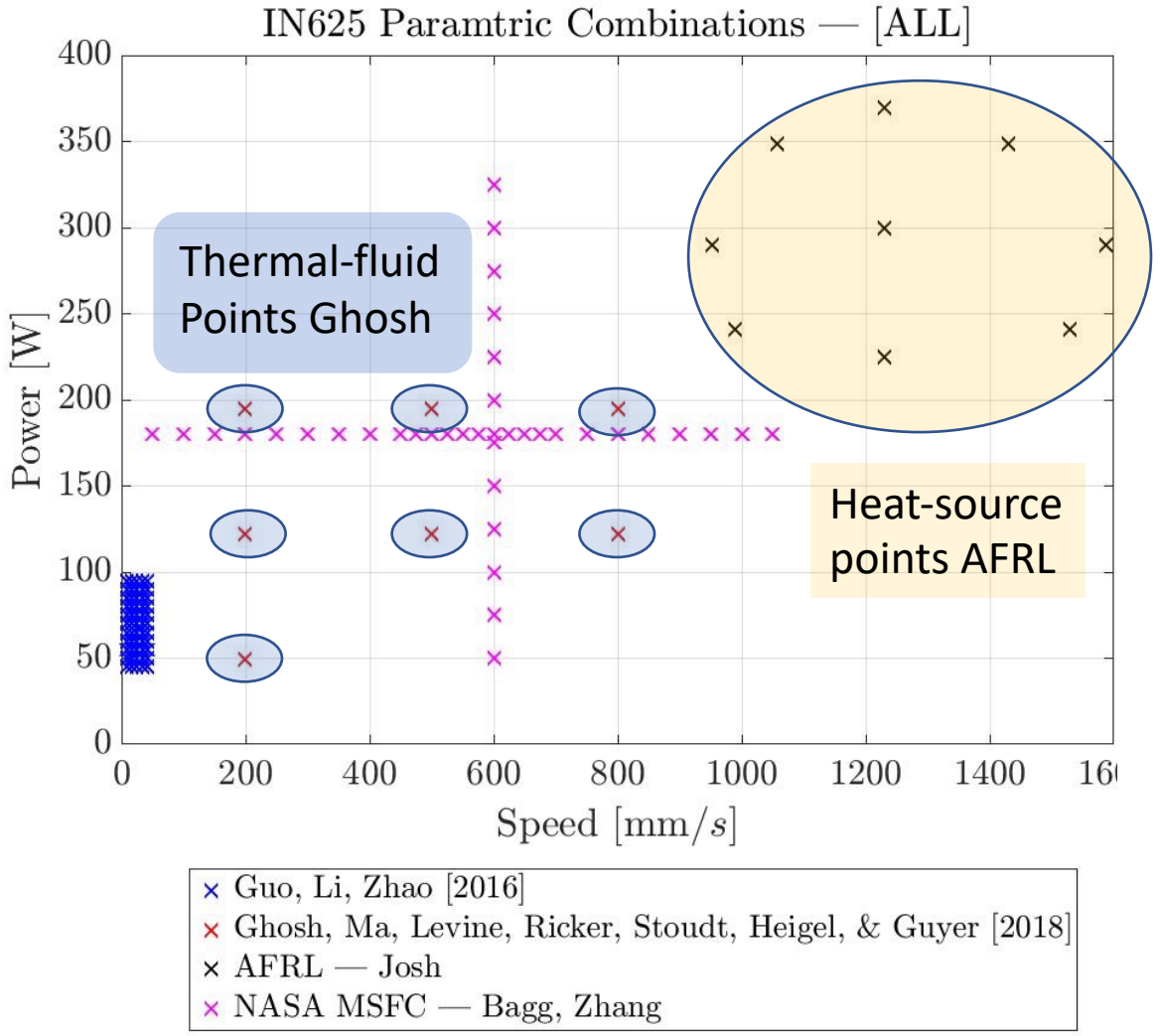


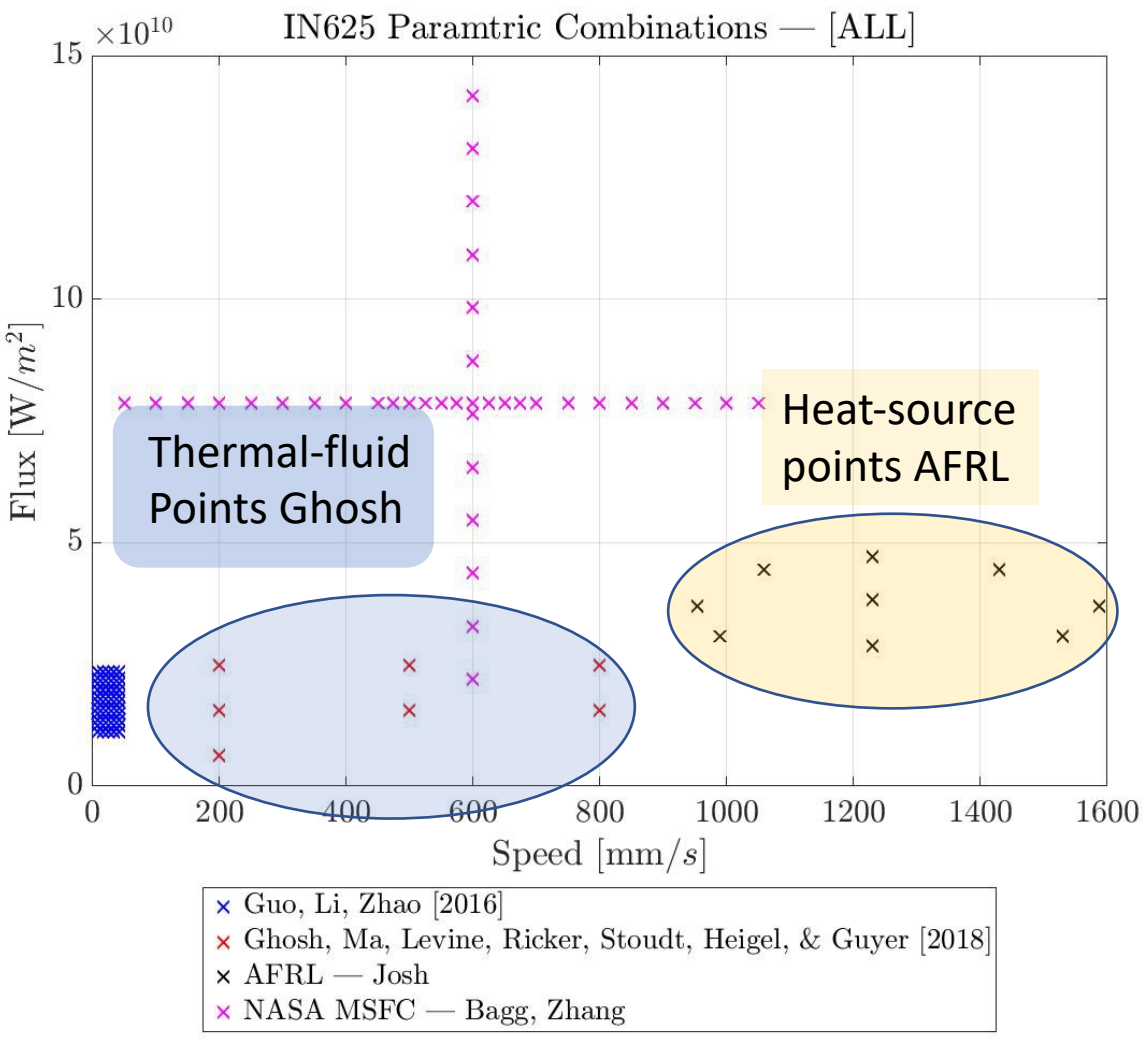


All of the data except for Trapp, et al. (the only non-powder study) looks to be good for model verification.



IN-625 Melt-pool Dimensions

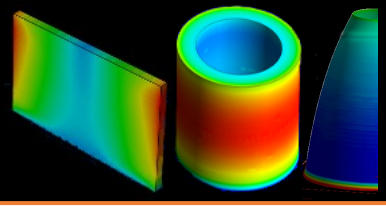




All of the data except for Guo and some outliers in the AFRL data look to be good for model verification. Recommended points are given only as an effort to expedite this process for largest spread of data with minimal effort. Other points may be more efficient due to modeling constraints.

PRIMARY RECOMMENDATION RATIONALE

- [Bagg, et al] has the largest span in terms of speed and flux as well as a second datapoint from the same study in close proximity which can help double-validate the datapoint.
- A secondary recommendation will be made due to the fact that there is not depth data to compare to for this set.



Validation Data

- AFRL Challenge Data[1]
  - Available melt pool measurements for SLM single track deposits of IN625
  - Various combinations of power and speed
  - Layer thickness = 40 um
  - Track length = 20 mm
  - Laser spot diameter = 0.1 mm

AFRL Data for $W_{measured}$ and $D_{measured}$

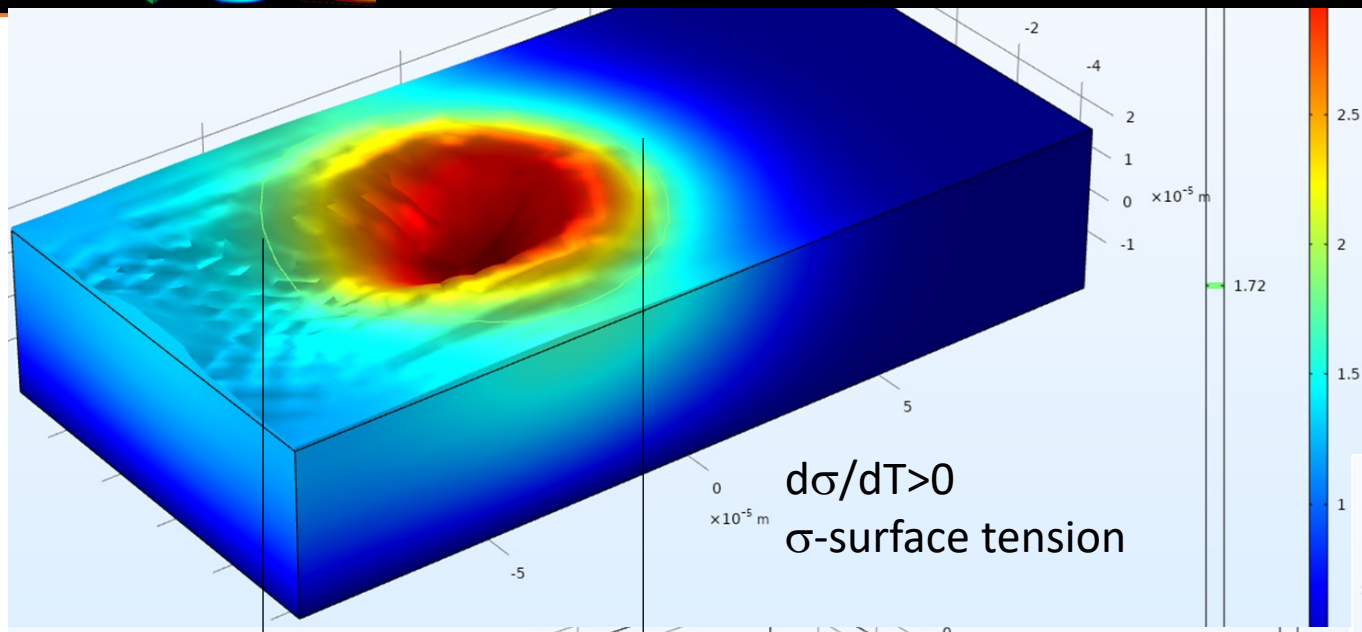
Track Id	Power	Speed	Top-Down Width [µm] µ, σ	Cross-section Width [µm] µ, σ	Cross-section Max. Width [µm] µ, σ	Cross-section Depth [µm] µ, σ	Cross-section Height [µm] µ, σ
B10	300	1230	112.0, 11.1	86.9, 10.4	98.3, 13.4	26.9, 5.4	62.2, 18.3
B11	300	1230	112.0, 11.9	89.5, 11.8	97.4, 15.5	25.0, 6.1	60.3, 14.9
B12	290	953	127.6, 7.0	125.2, 6.6	128.3, 8.1	75.9, 7.6	66.0, 15.5
B13	370	1230	122.9, 8.4	130.1, 6.7	130.1, 6.7	72.0, 7.4	68.1, 9.2
B14	225	1230	96.0, 13.9	107.1, 9.9	109.4, 11.5	52.3, 9.0	65.7, 21.8
B15	290	1588	97.9, 14.0	112.9, 9.6	115.6, 9.8	54.3, 9.0	59.1, 12.3
B16	241	990	112.0, 13.0	110.8, 7.9	117.1, 12.7	42.5, 6.6	61.2, 11.9
B17	349	1430	110.7, 11.3	109.4, 10.7	111.4, 8.6	58.5, 4.6	60.1, 15.9
B18	300	1230	112.7, 12.7	109.7, 8.7	113.0, 12.0	46.9, 9.3	68.8, 25.9
B19	349	1058	129.9, 7.0	130.1, 7.1	134.4, 14.1	84.0, 8.9	63.5, 17.8
B20	241	1529	89.3, 12.8	83.5, 7.0	87.1, 11.2	20.1, 7.1	56.3, 18.1

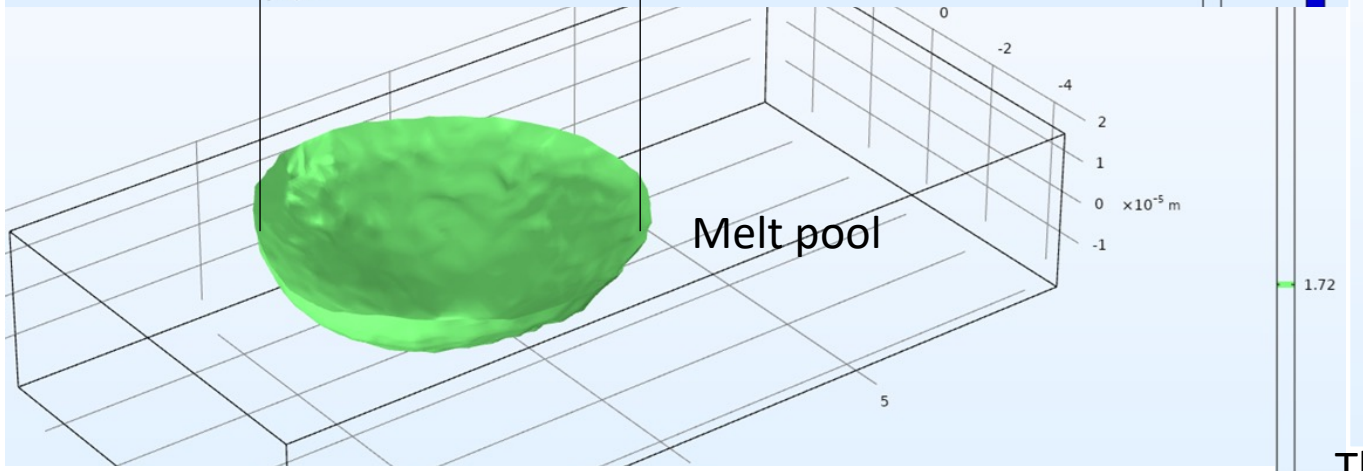
High fidelity model

[1] AFRL AM Modeling Challenge Series (http)

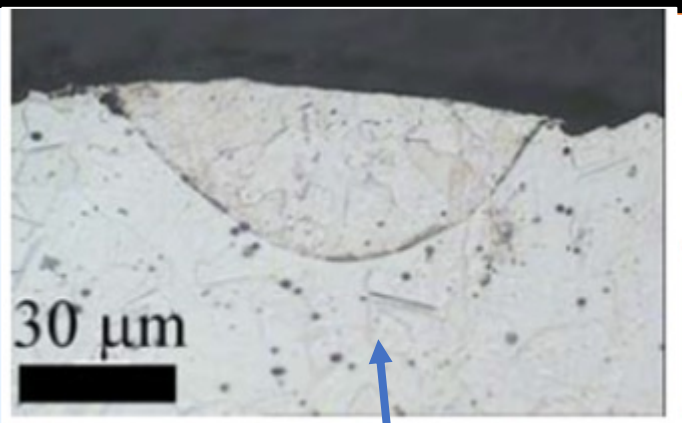
Melt pool size comparison with SS316 experiment

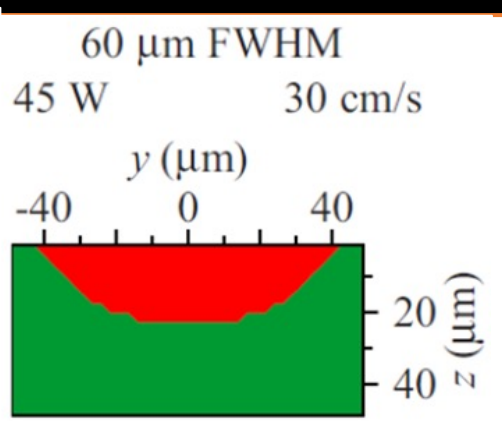
$\alpha \cdot I = 6 \cdot 10^9\ W/m^3$ v=300mm/s, if α=0.135 Power=45W



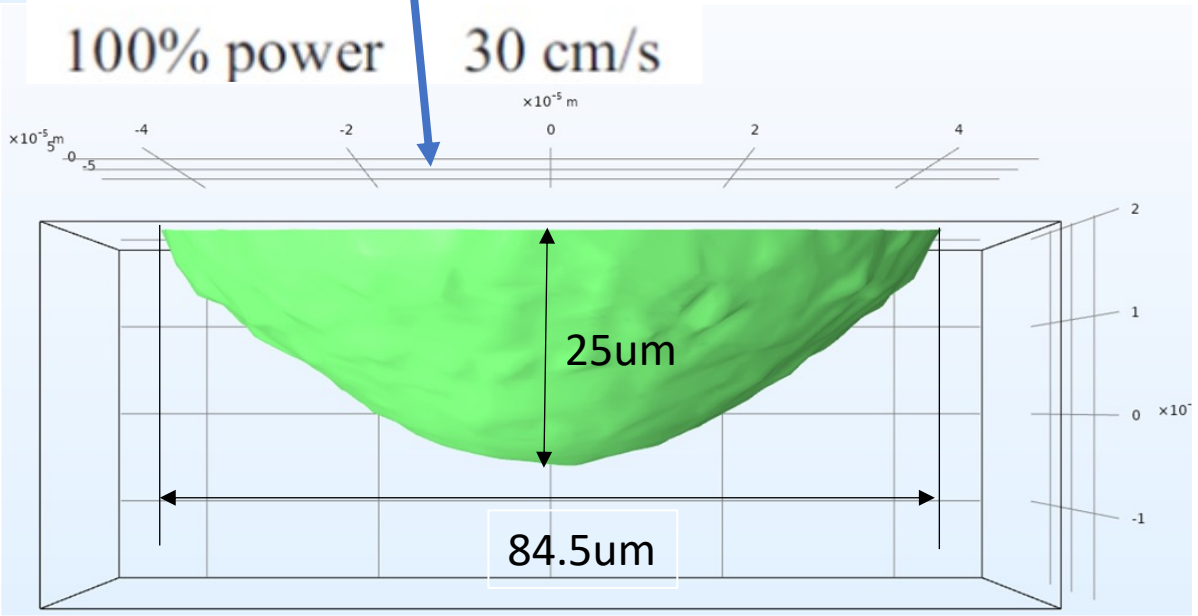


A.V.Gusarov at al. Modeling the interaction of laser radiation with powder bed at selective laser melting Journal of Heat Transfer, 2009 by ASME JULY 2009, Vol. 131 / 072101-1

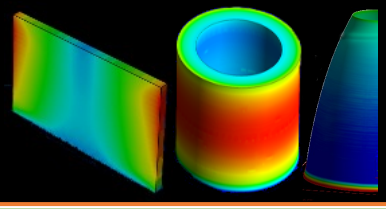




100% power 30 cm/s

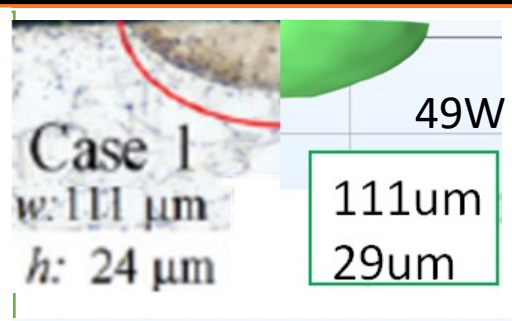


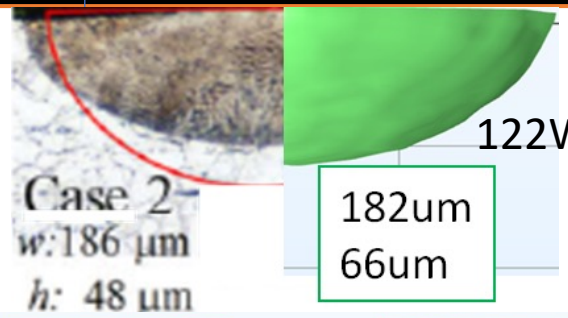
The power increase by 2 leads to keyhole formation, despite velocity is 2 times larger as well. Width is about 2 times wider, but depth is about 25um (fits the experiment).

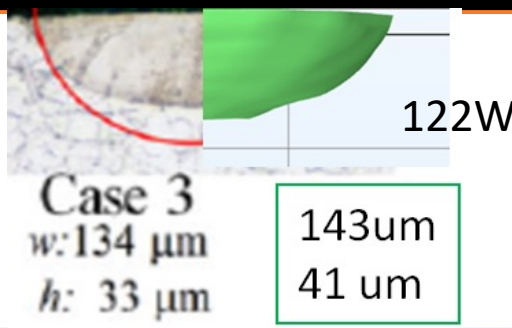


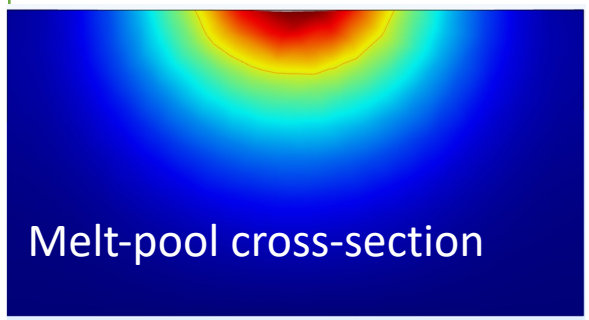
Melt-pool simulation comparison IN-625 SLM

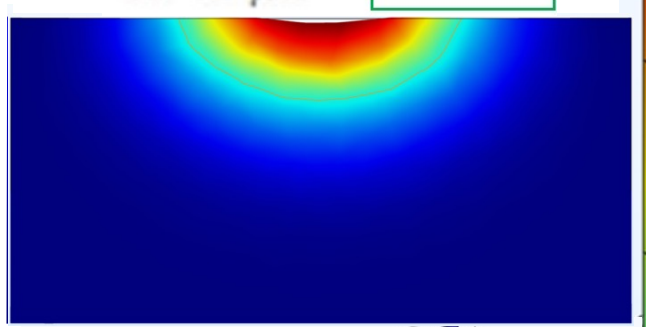
- Simulation results for melt-pool dimensions (green boxes). Temperature distributions are in 2nd and 3d rows, 4th row represents melt pool shape.
- The laser beam has a Gaussian power distribution with $1=e^2$ radius of 70 um, scanned along a length.
- Inconel 625 material parameters were used.
- Physics: Laminar Fluid with Marangoni Effect, Arbitrary Lagrange-Euler Moving Mesh, Heat Transfer in Fluids with Phase Changes
- Simulation performed for absorption power using the Beer-Lambert Law with α=2e6/m.

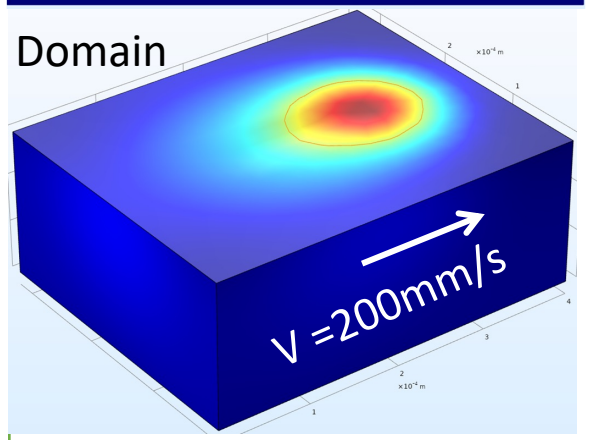


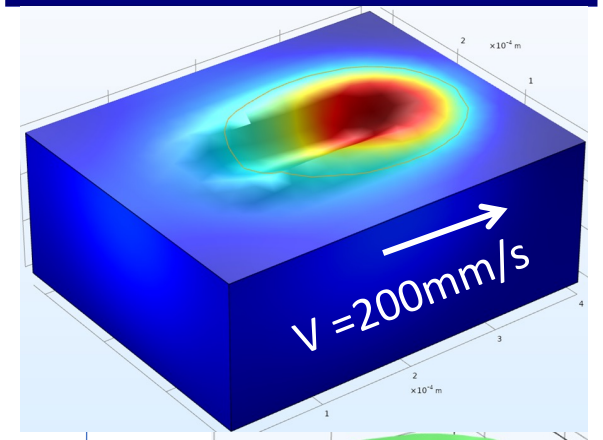


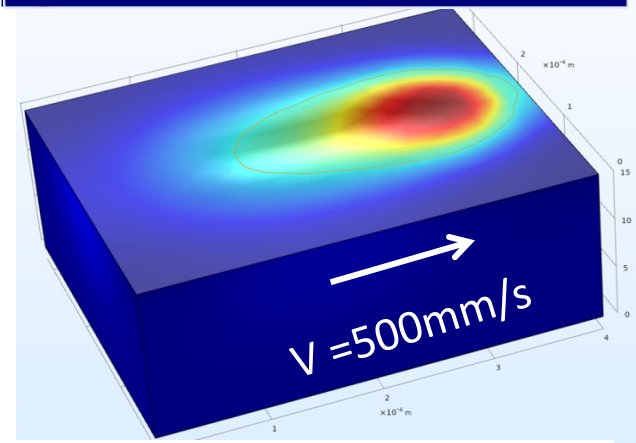


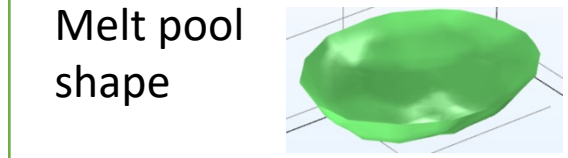


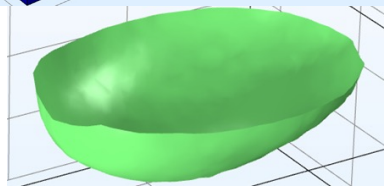


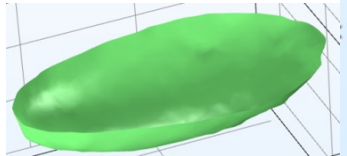


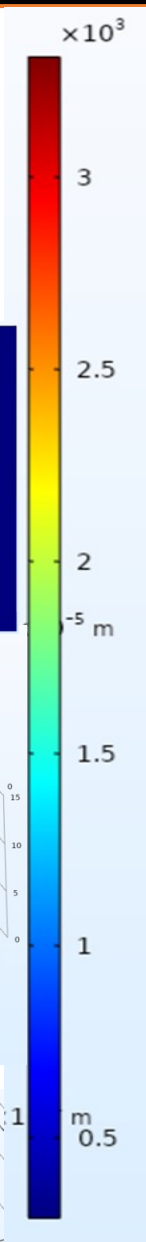


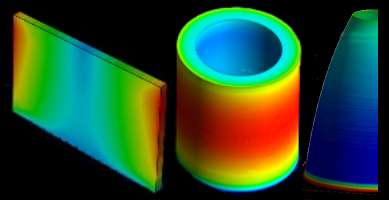




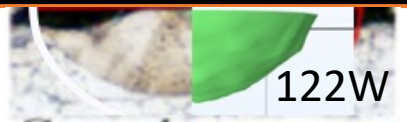






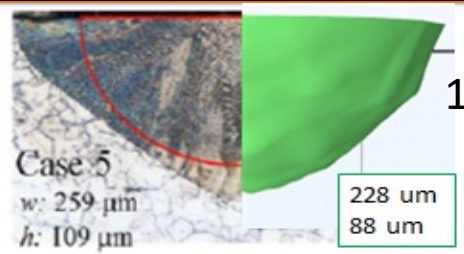


Melt-pool simulation comparison for IN-625



122W

128um
34 um



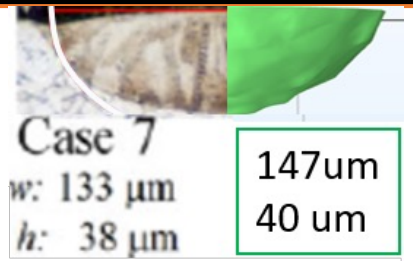
195W

228 um
88 um



195W

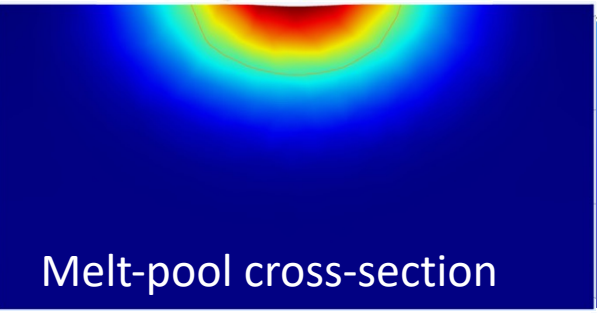
162um
50 um

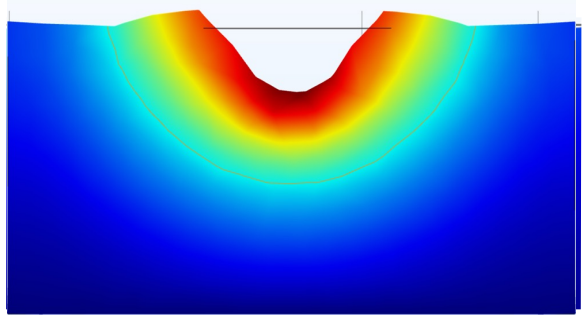


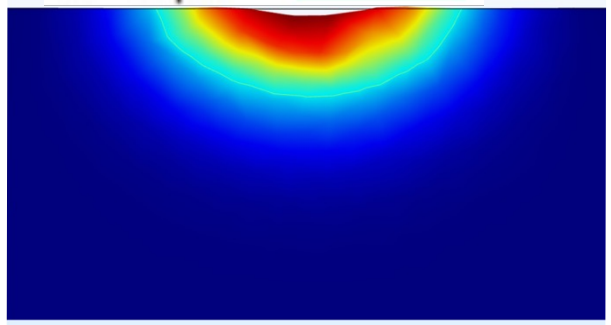
195W

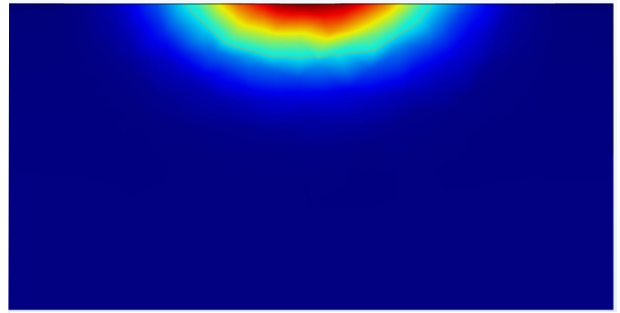
147um
40 um

Melt-pool cross-section

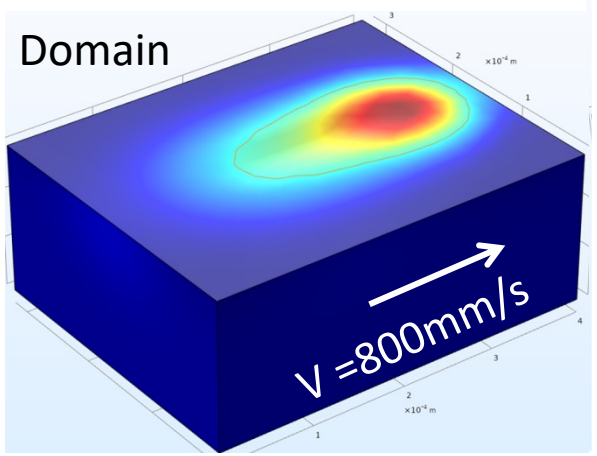


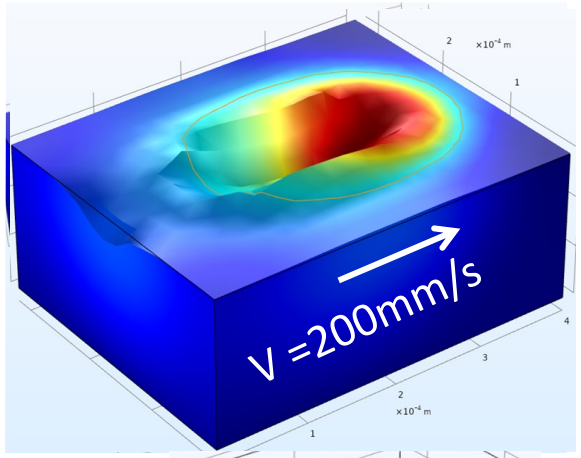


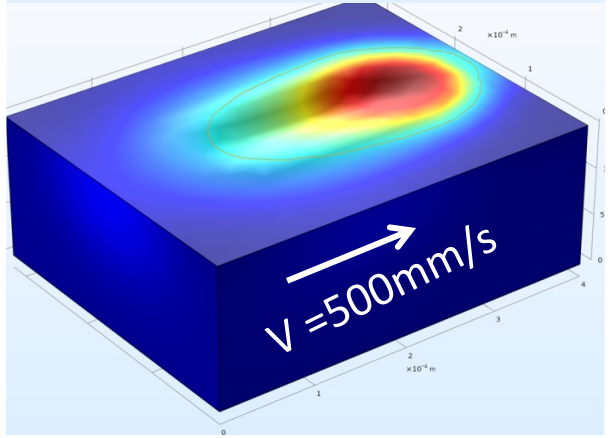


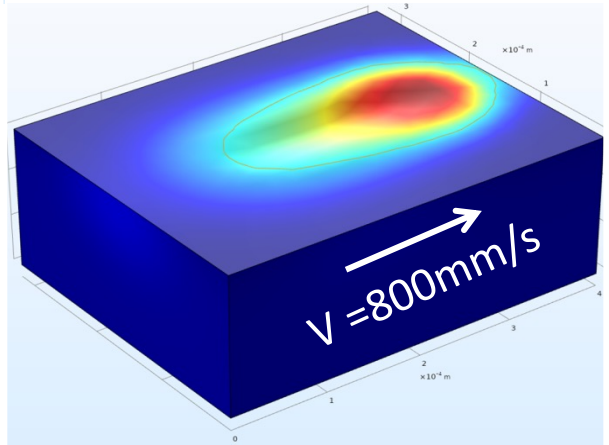


Domain

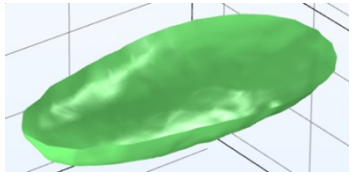


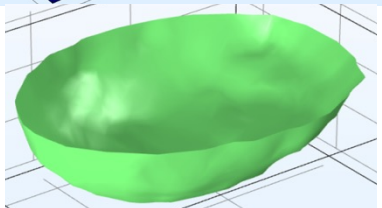


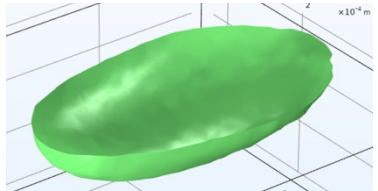


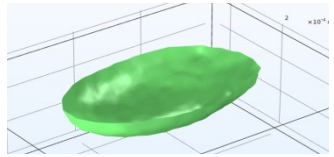


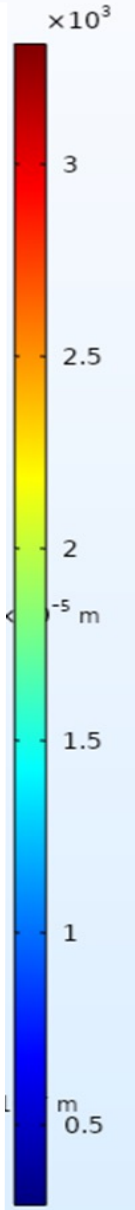
Melt pool shape

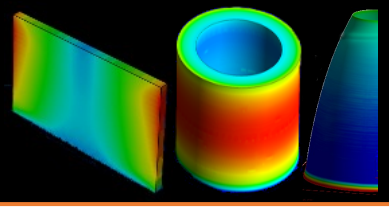




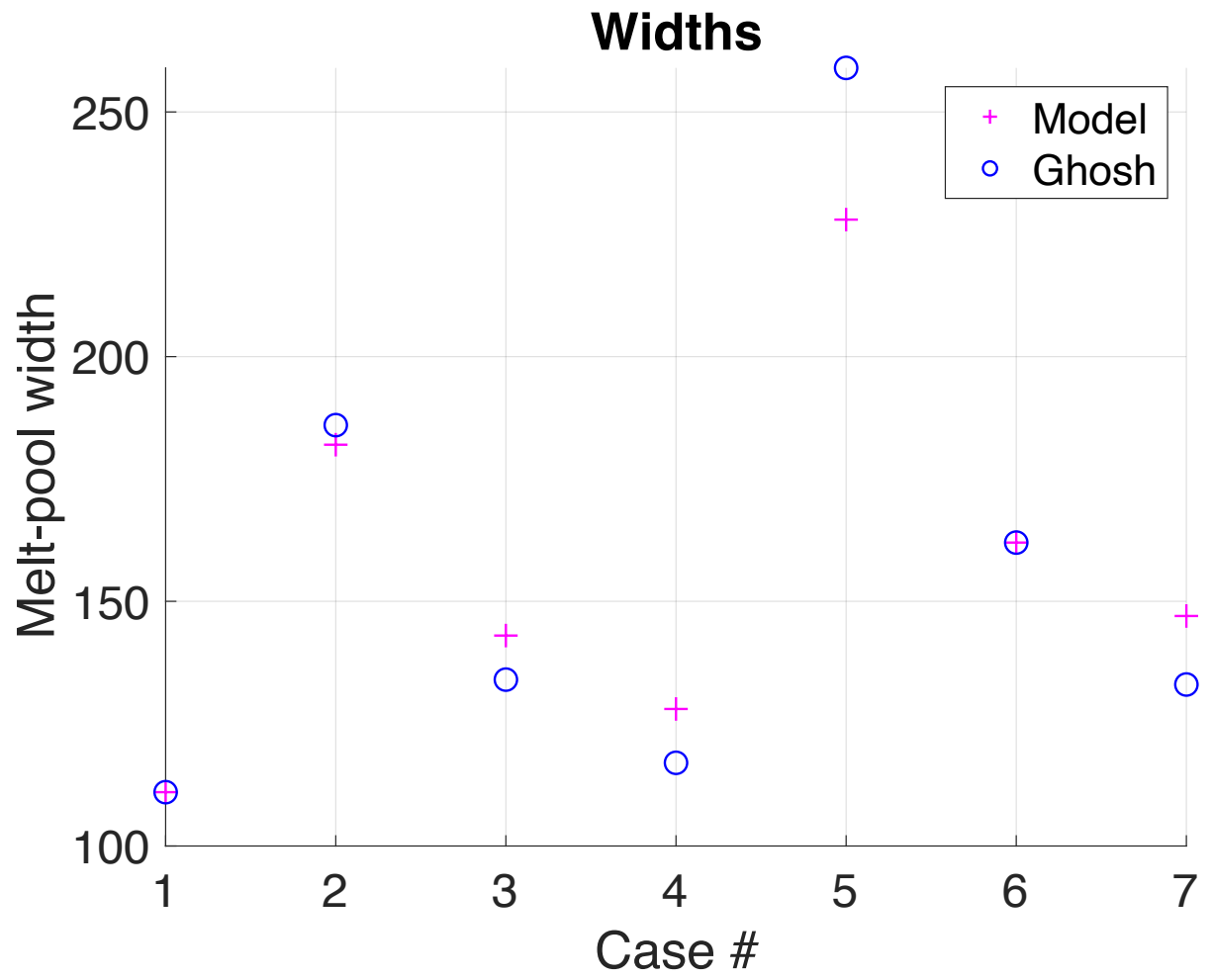


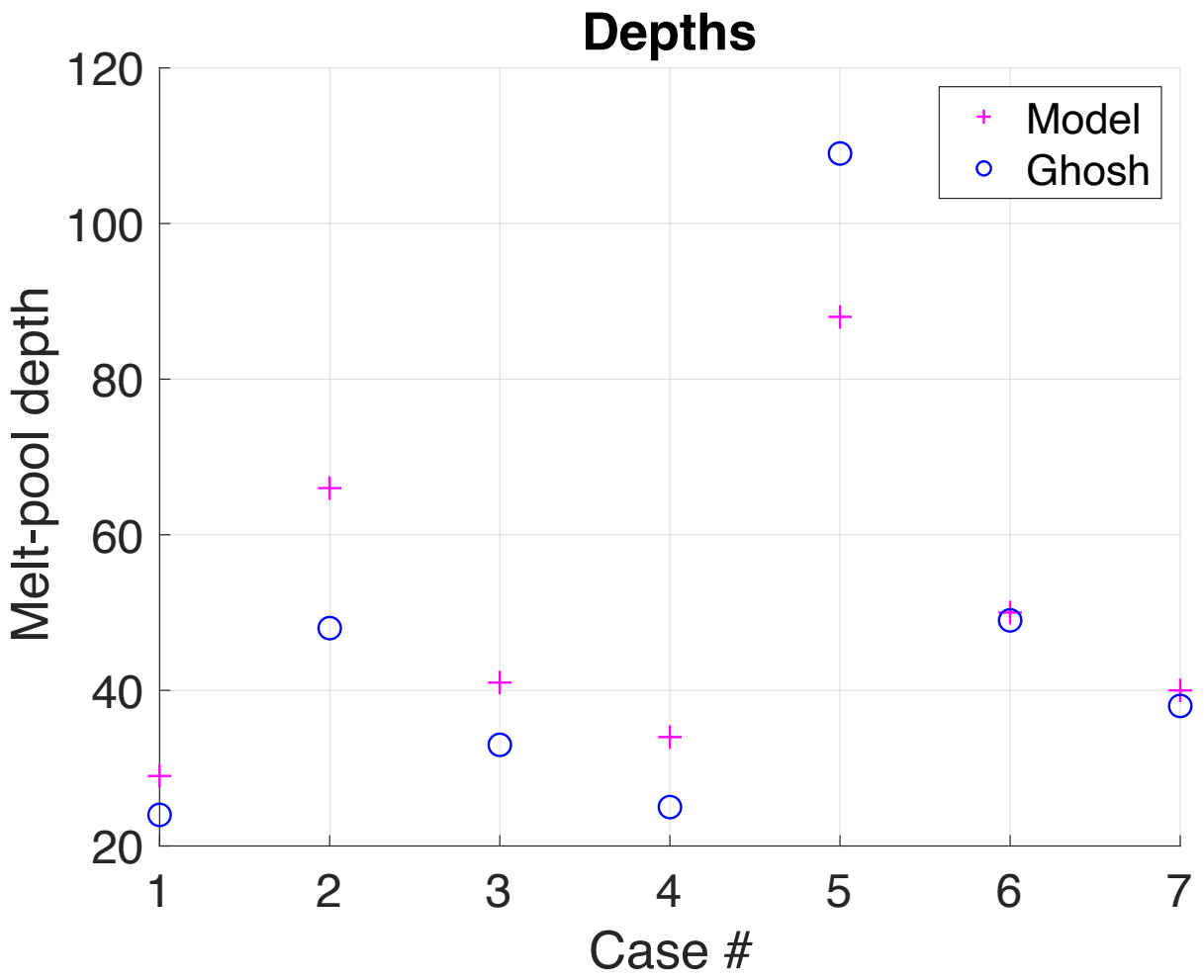


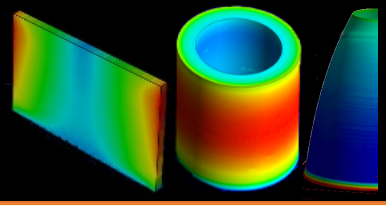




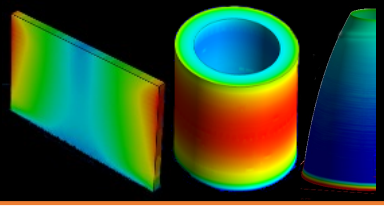
Melt-pool simulation comparison IN-625



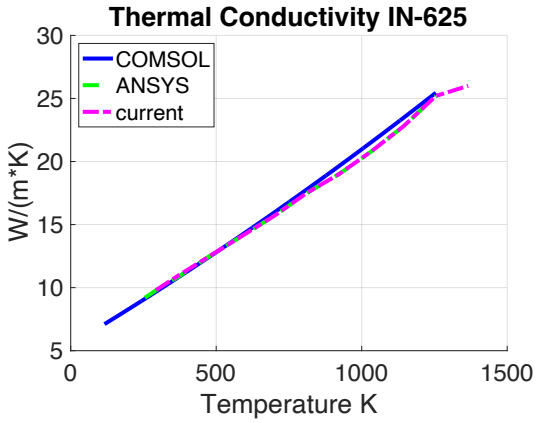


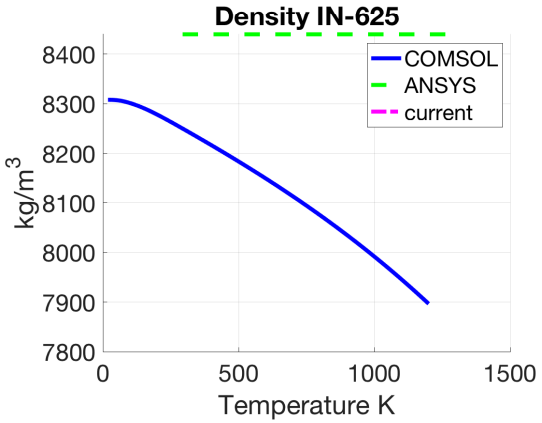


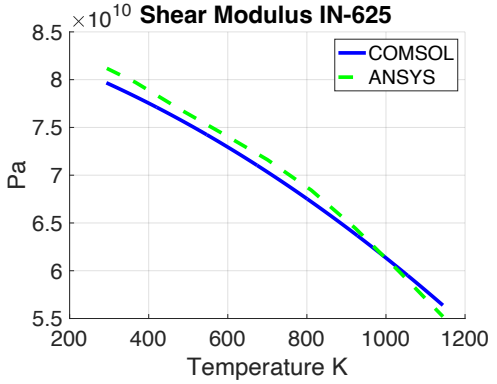
Material Characteristics

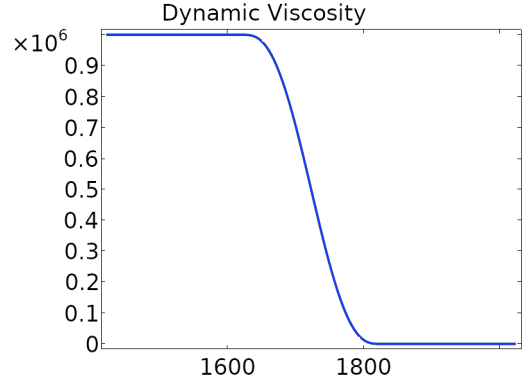


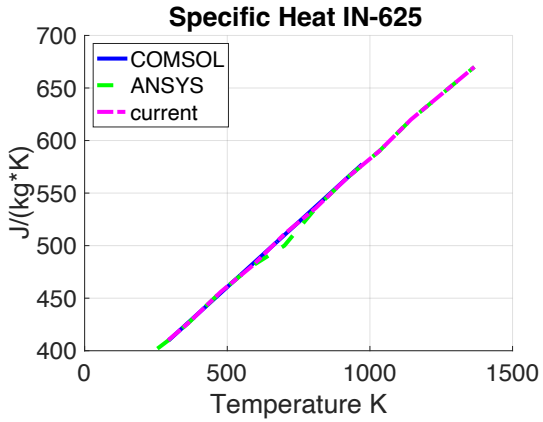
IN-625 Characteristics
Comparison of ANSYS, COMSOL & Literature

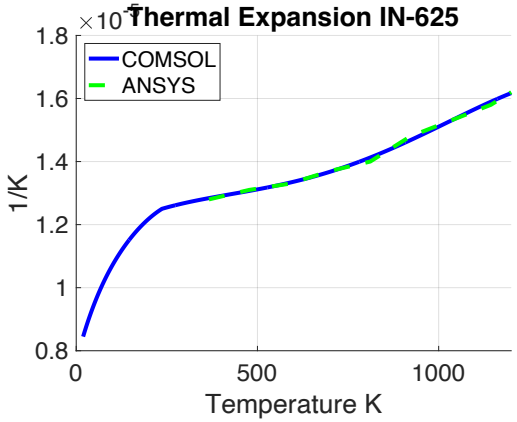


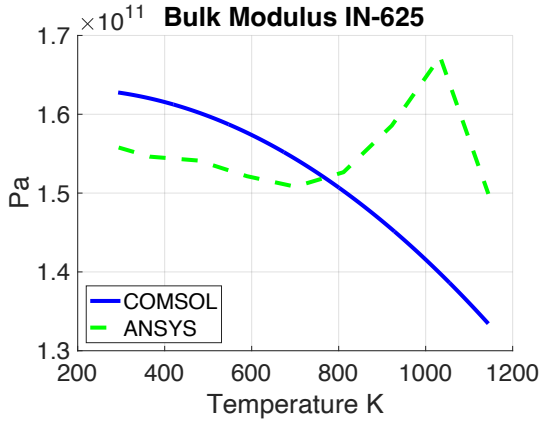


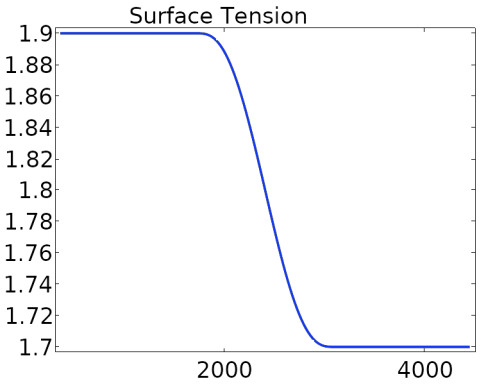




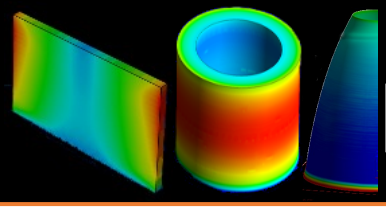








Thermal, mechanical and fluidic properties.

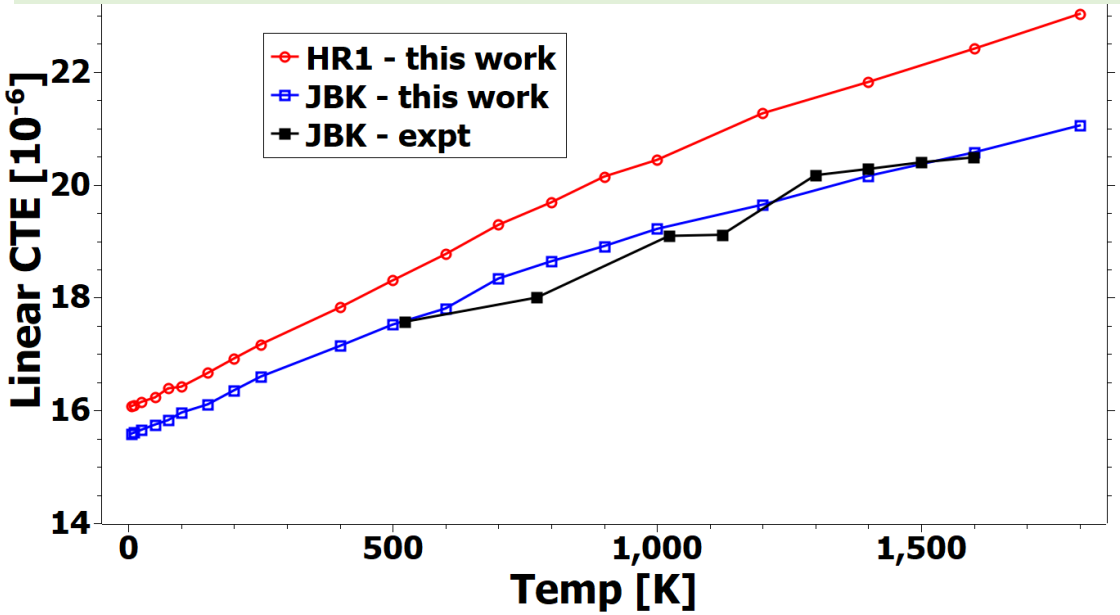


Material thermal characteristics modeling

Ab initio molecular dynamics:

- Computational materials method from first principles
- Atomic scale, quantum/electronic effects
- Uses a thermostat & barostat, evolves system of atoms forward in time, yields atomic positions, velocities, energetics
- Necessary inputs Force Fields and Atomic Structure. Well suited to austenitic Fe/Ni/Cr alloys.

Thermal expansion weighted by phase preferences



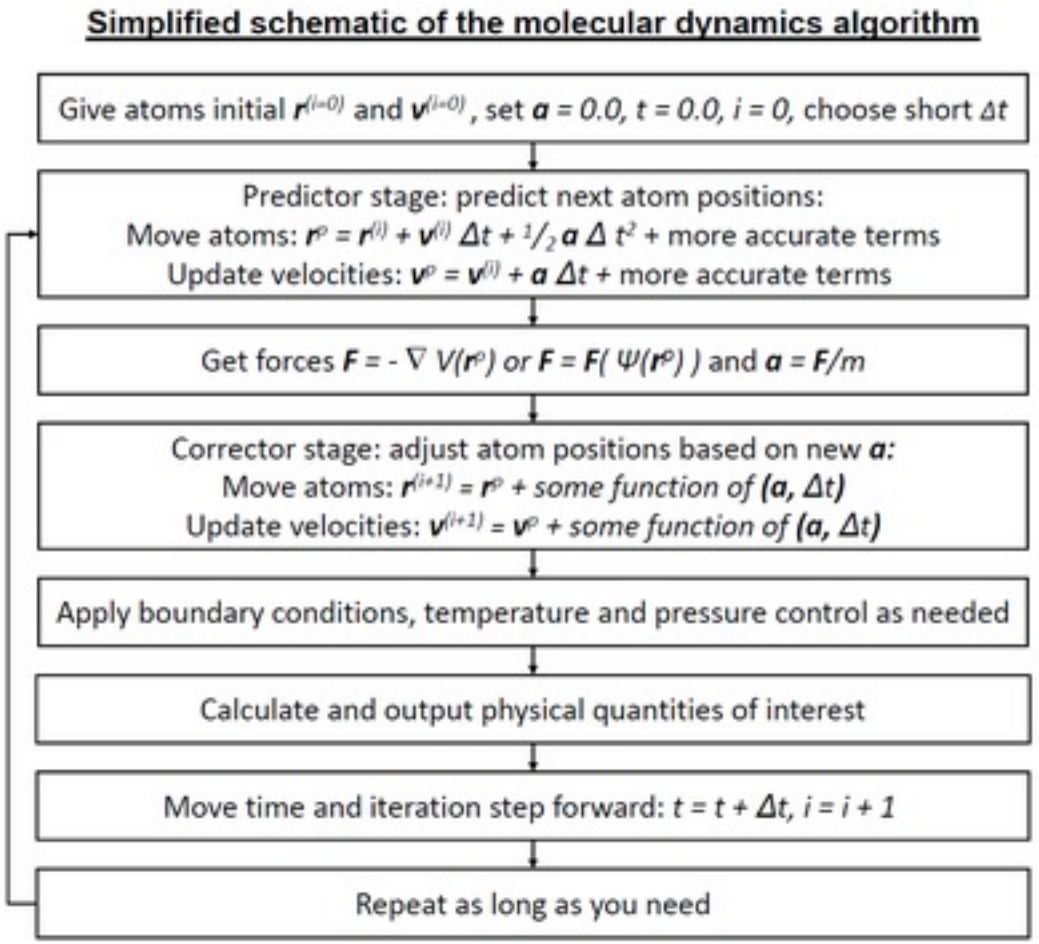
Atomistic simulation uses first principles to develop temperature dependent material curves such as CTE (coefficient of thermal expansion) as a function of temperature shown for JBK-75 and HR-1. JBK-75 used as validation with data, HR-1 new result.

For the simulated systems, the phase change is more gradual than in experiment, but the increased volumes associated with the alpha phase contribute significantly to the thermal expansion coefficient.

MD OVERVIEW

Molecular dynamics (MD):

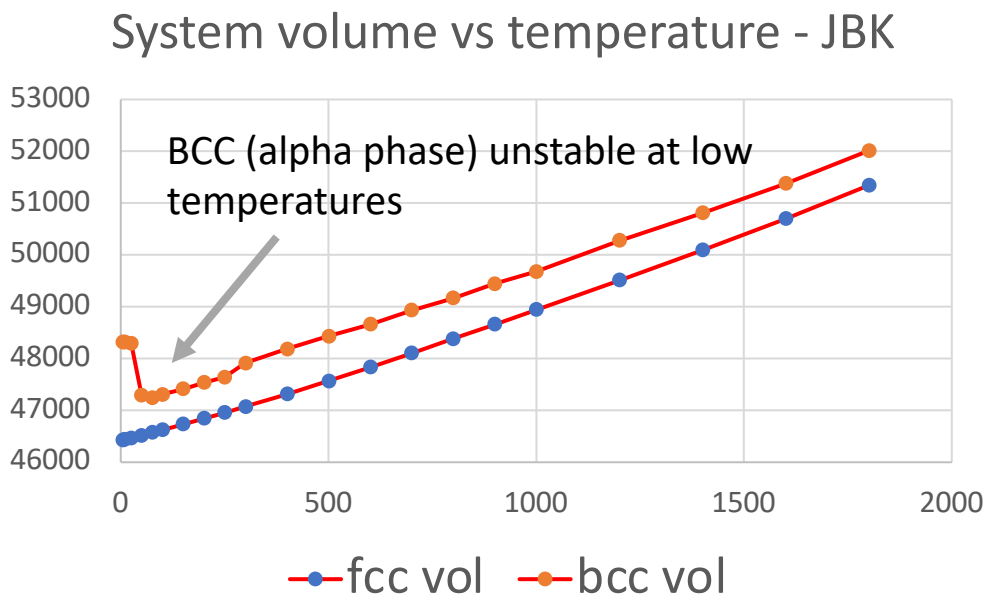
- Computational materials method
- Atomic scale, some electronic effects
- Using a thermostat and barostat, evolves system of atoms forward in time, yields atomic positions, velocities, energetics
- Necessary ingredients:
  - Force field
  - Atomic structure
- Force field used is well suited to studying austenitic Fe/Ni/Cr alloys in the solid phase. For details see https://doi.org/10.1002/jcc.25573



Wt% to at%, SQS, unit cells

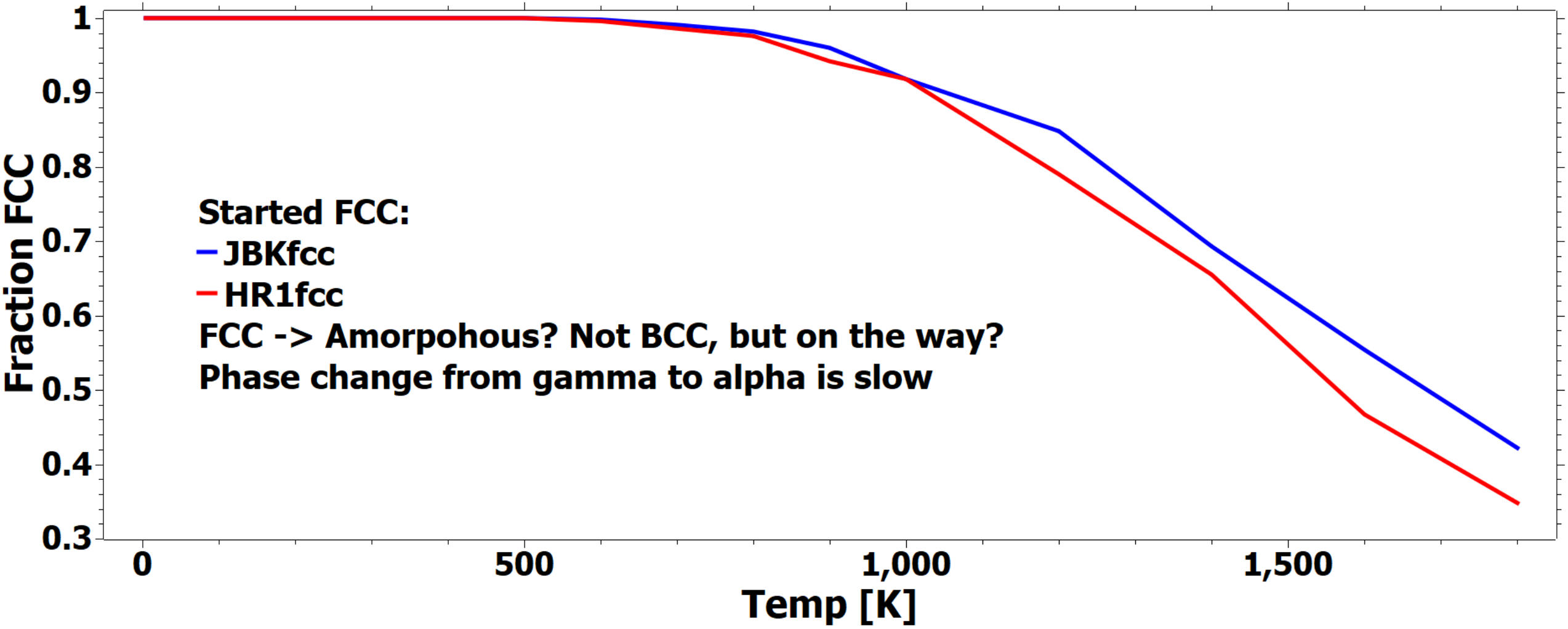
Two alloy systems, simplified to Fe-Ni-Cr.

- Disordered FCC alloys (at room temp) – for finite simulations we need to ensure that all of the "local" configurations of atoms are sampled
  - Pair, triple distribution functions
  - ATAT SQS toolkit – monte carlo creation of structures
- Unit cells of 4000 atoms created for both FCC and BCC (gamma and alpha phase)
- JBK75
  - By wt%: 53.3% Fe, 31.3% Ni, 15.4% Cr
    at%: 53.5% Fe, 29.9% Ni, 16.6% Cr
- HR1
  - By wt%: 45.4% Fe, 37.9% Ni, 16.7% Cr
    at%: 45.7% Fe, 36.2% Ni, 18.0% Cr



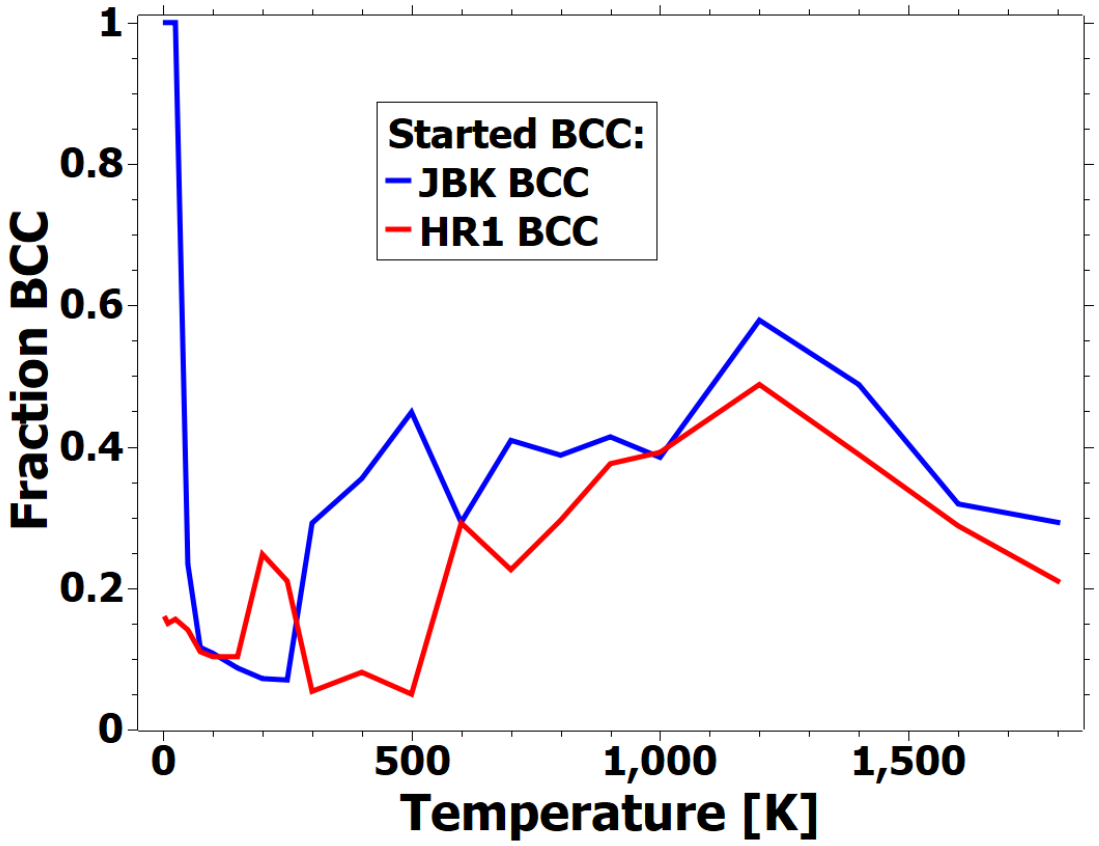


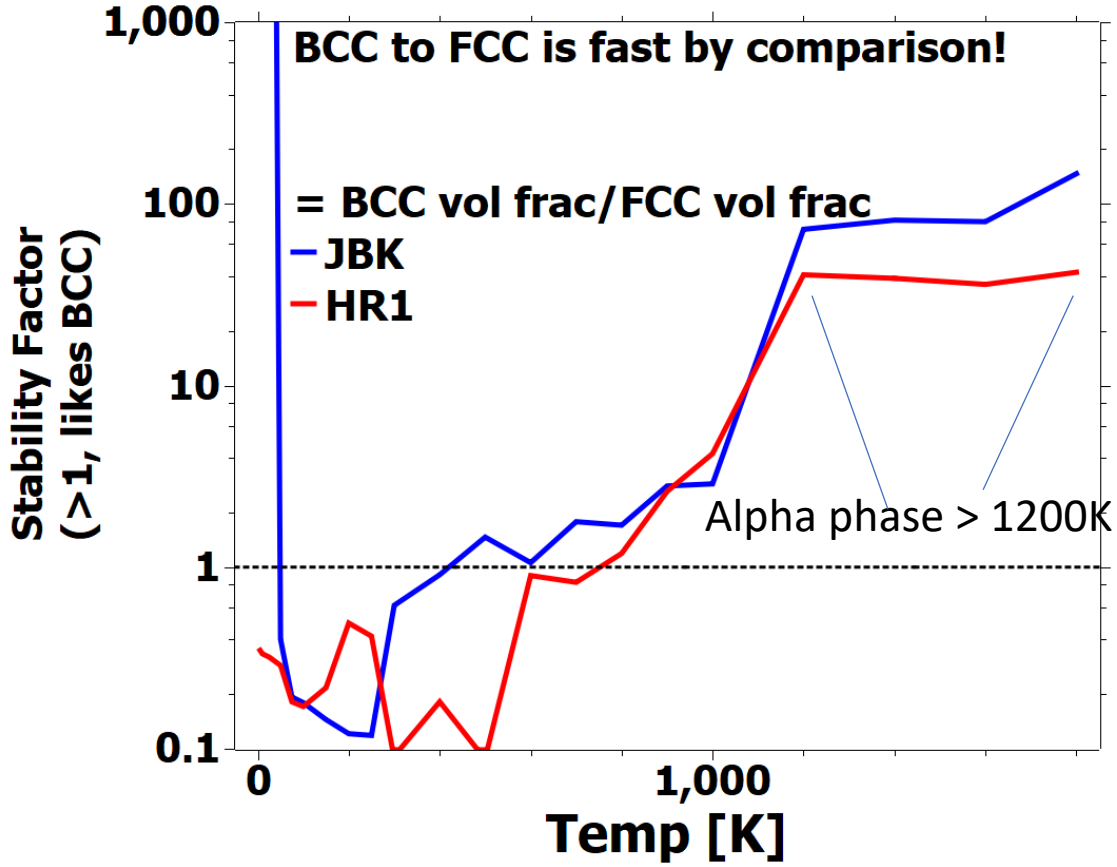
Gamma vs alpha phase stability



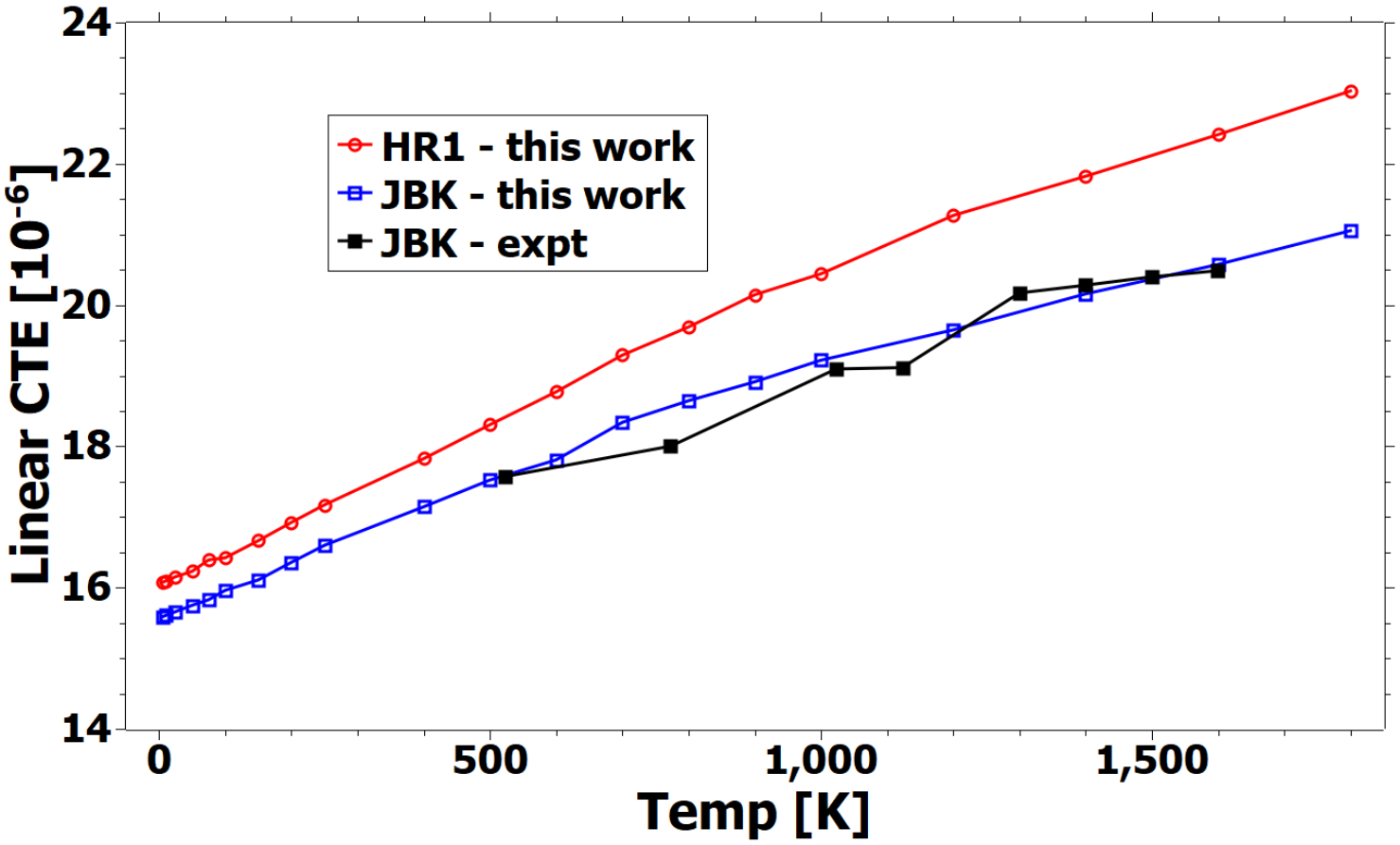
Gamma vs alpha phase stability

HR1's phase change will be less severe, but both alloys exhibit enhanced alpha phase formation at temps of 1200K and above

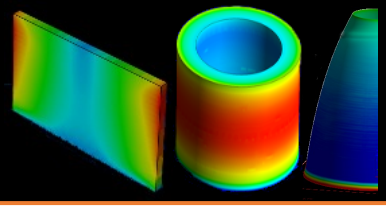




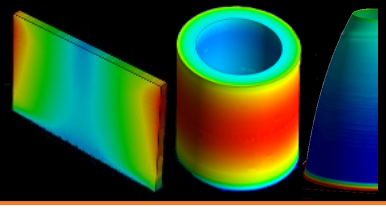
Thermal expansion, weighted by phase preferences



For the simulated systems, the phase change is more gradual than in the experiment but the increased volumes associated with the alpha phase contribute significantly to the thermal expansion coefficient



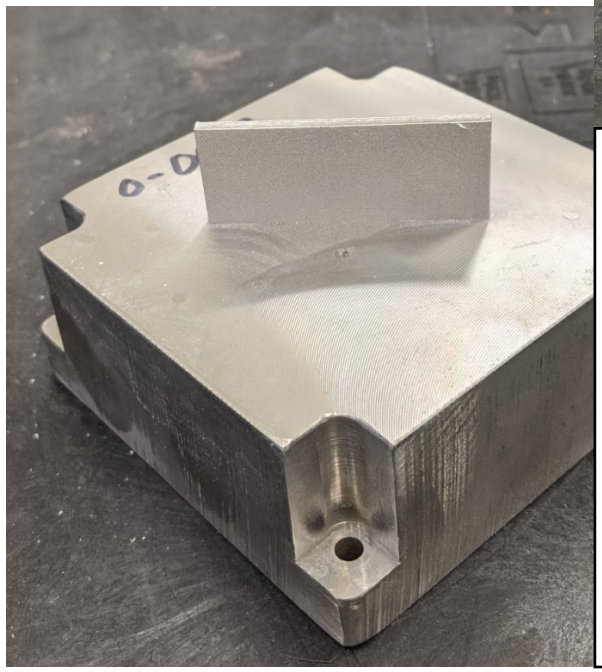
3 Coupons

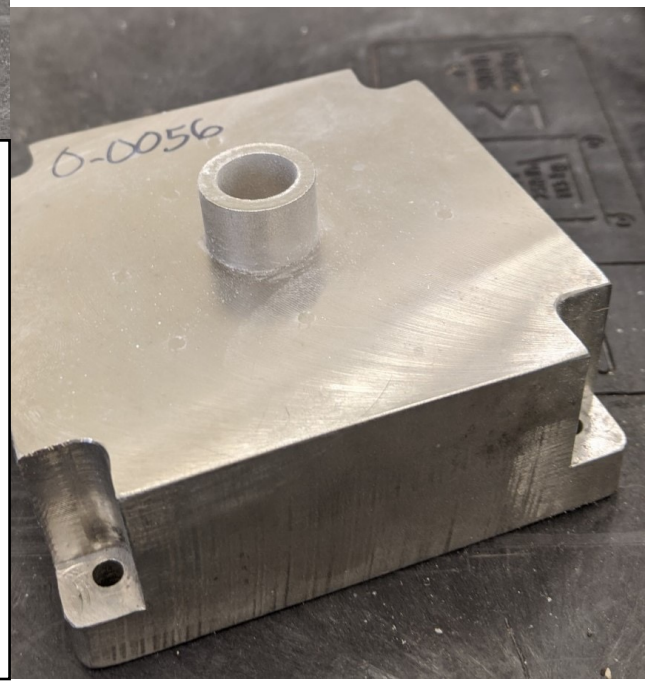


Validation Coupons

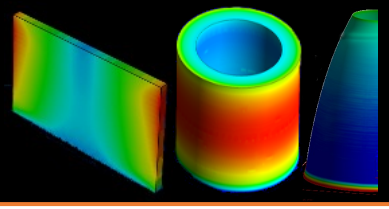
SLM IN625
Modeling Builds





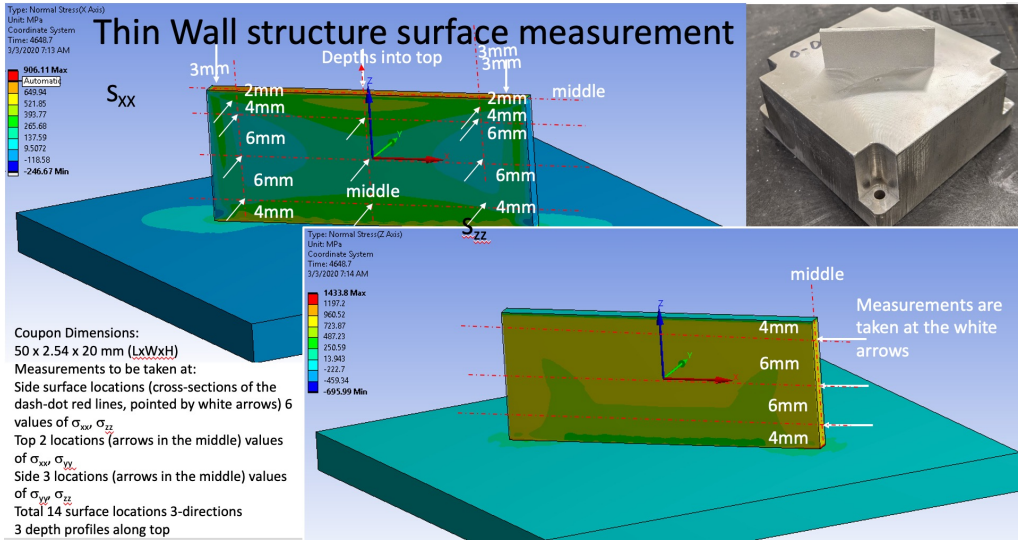


- Thin Wall
  - 50 x 2.54 x 20 mm (LxWxH)
- Cylinder
  - ID: 13 mm
  - OD: 19 mm
  - Height: 12 mm
- Twin Cantilever
  - Beam: 80 x 7.27 x 2.18 mm (LxWxH)
  - Main Pillar: 7.27 x 7.27 x 5.82 mm
  - Support pillars: 4.3 x 7.27 x 5.82 mm



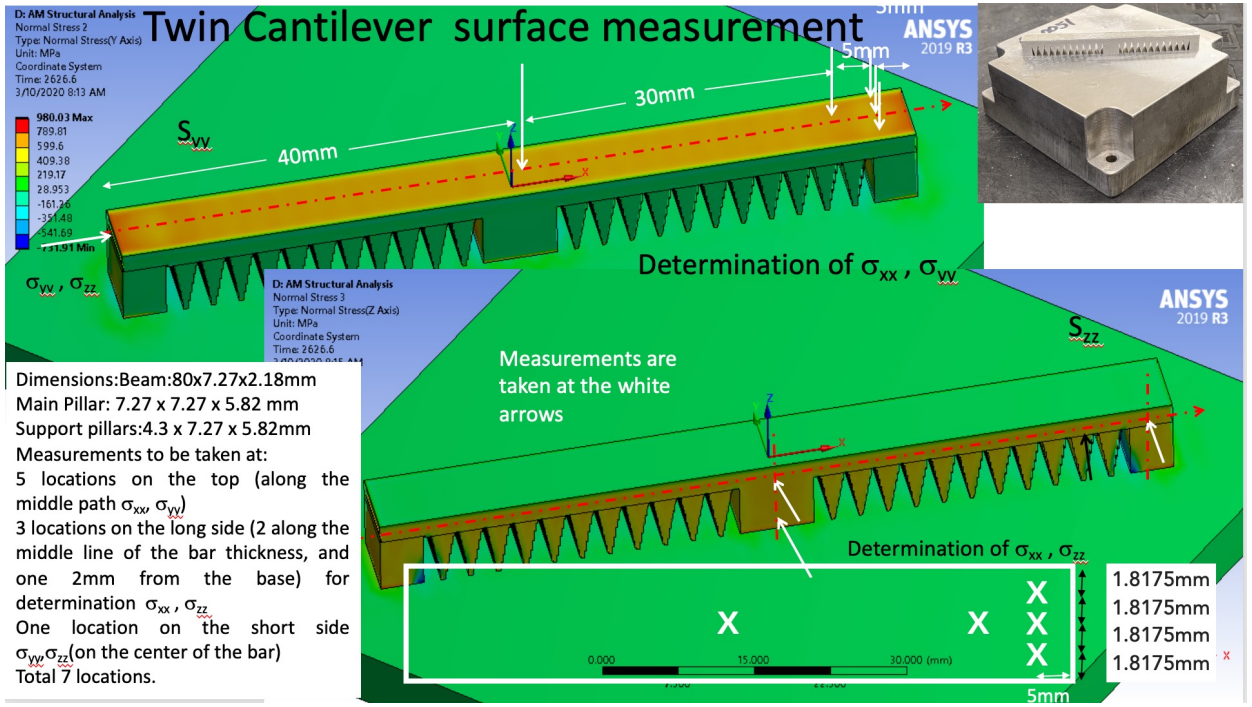
Measurement point selection

Modeling and Simulation



Coupon Dimensions:
50 x 2.54 x 20 mm (LxWxH)
Measurements to be taken at:
Side surface locations (cross-sections of the dash-dot red lines, pointed by white arrows) 6 values of σ_{xx}, σ_{zz}
Top 2 locations (arrows in the middle) values of σ_{xx}, σ_{yy}
Side 3 locations (arrows in the middle) values of σ_{yy}, σ_{zz}
Total 14 surface locations 3-directions
3 depth profiles along top

- Simulation studies were conducted using ANSYS Additive, ABAQUS and ALE-3D to understand stress fields in three coupons: thin wall, hollow cylinder and twin-cantilever.
- Locations for stress measurements using X-ray diffraction were chosen based upon simulations. Locations



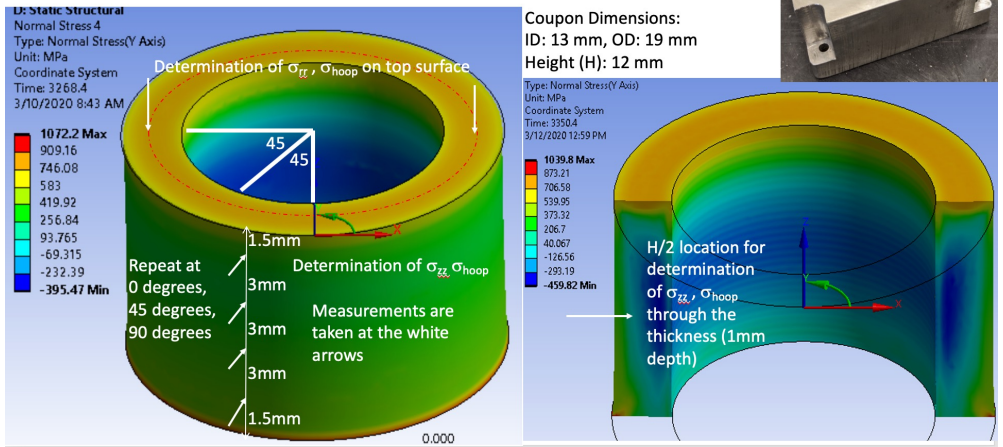
Dimensions:Beam:80x7.27x2.18mm
Main Pillar: 7.27 x 7.27 x 5.82 mm
Support pillars:4.3 x 7.27 x 5.82mm
Measurements to be taken at:
5 locations on the top (along the middle path σ_{xx}, σ_{yy})
3 locations on the long side (2 along the middle line of the bar thickness, and one 2mm from the base) for determination σ_{xx} , σ_{zz}
One location on the short side σ_{yy},σ_{zz}(on the center of the bar)
Total 7 locations.

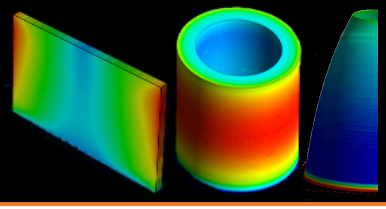
Cylinder Structure

Outer surface locations (arrows) 4 values of σ_{hoop}, σ_{zz}
Top 2 locations (in the middle of the wall) values of σ_{hoop}, σ_{rr}
One side location (in the middle=H/2) for determination values of σ_{hoop}, σ_{zz} through the thickness
One top place can also be considered for residual stress depth profiles. Total 5-6 surface locations and 1 or 2 depth profiles



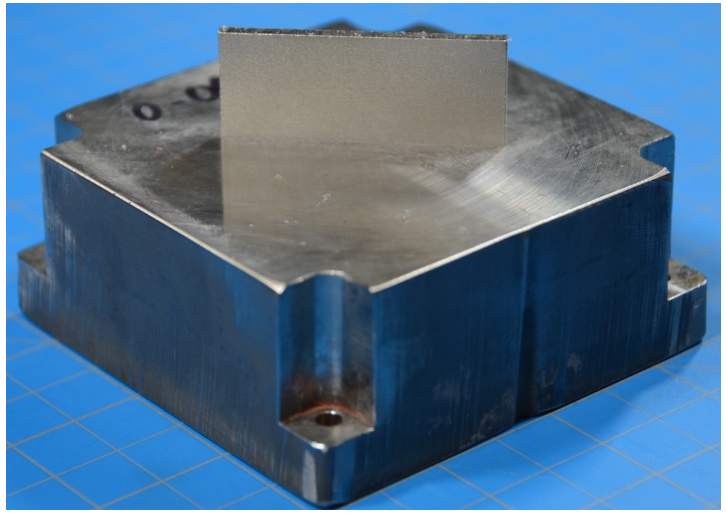
Coupon Dimensions:
ID: 13 mm, OD: 19 mm
Height (H): 12 mm

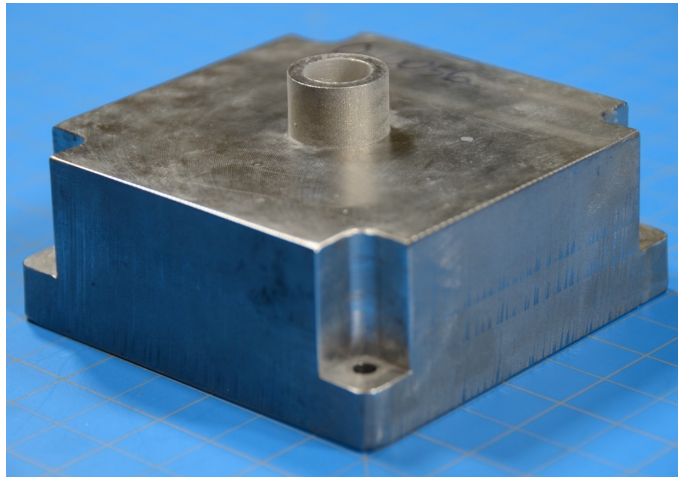


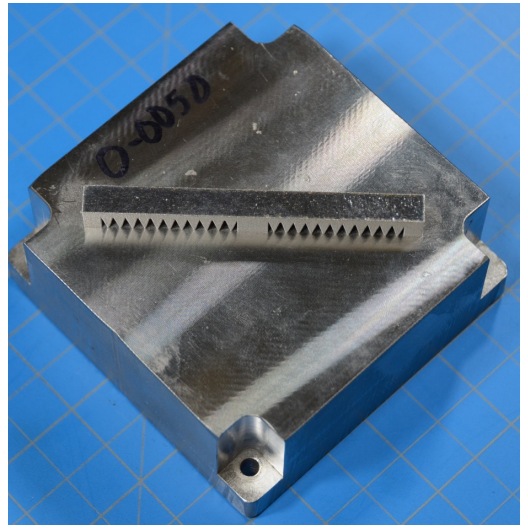


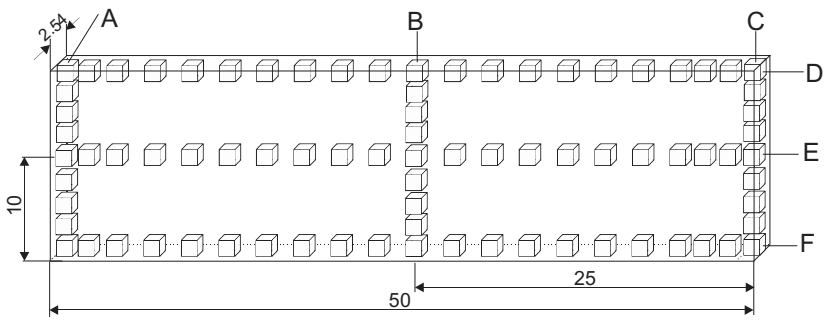
Residual stress coupons

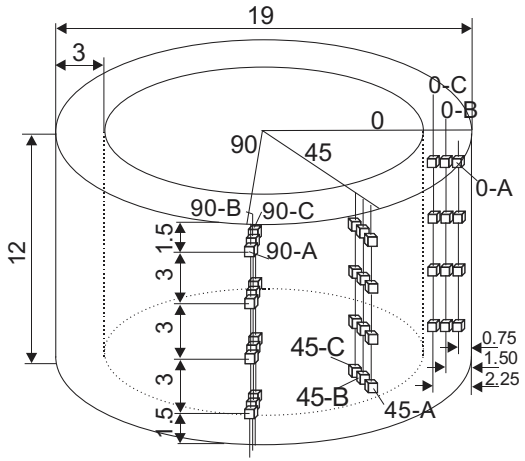
- Three coupons were designed and fabricated in LPBF IN-625.
- Computational models for the LPBF build process were developed in COMSOL Multiphysics, ABAQUS, ALE3D, ANSYS Additive.
- These models were used to predict residual stresses and deformation in the 3 coupons.
- NIST measured with neutron source.

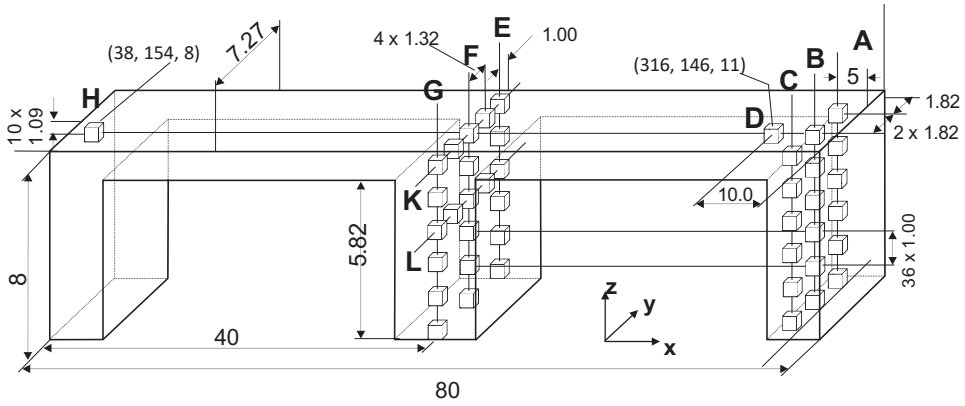


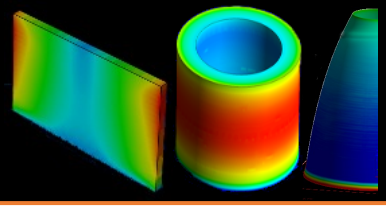




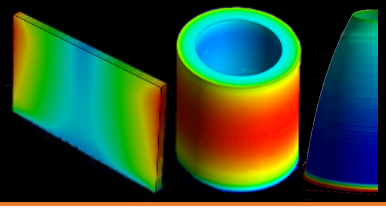






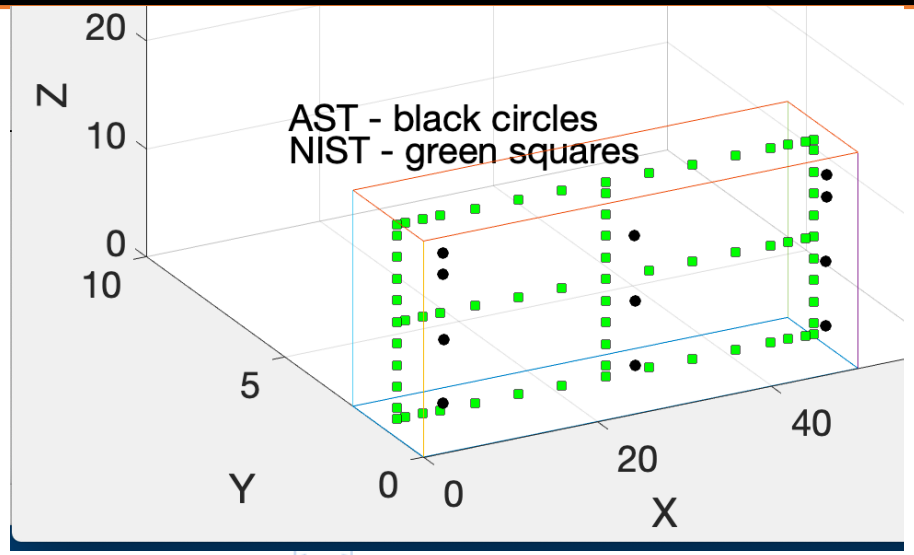


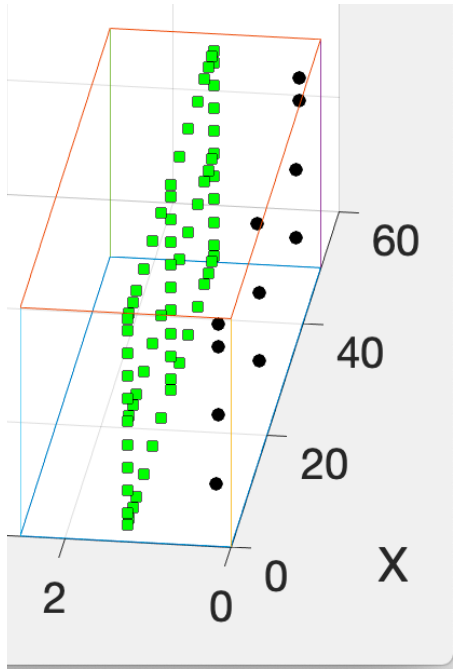
X-ray Diffraction vs. Neutron source for Residual stress measurements

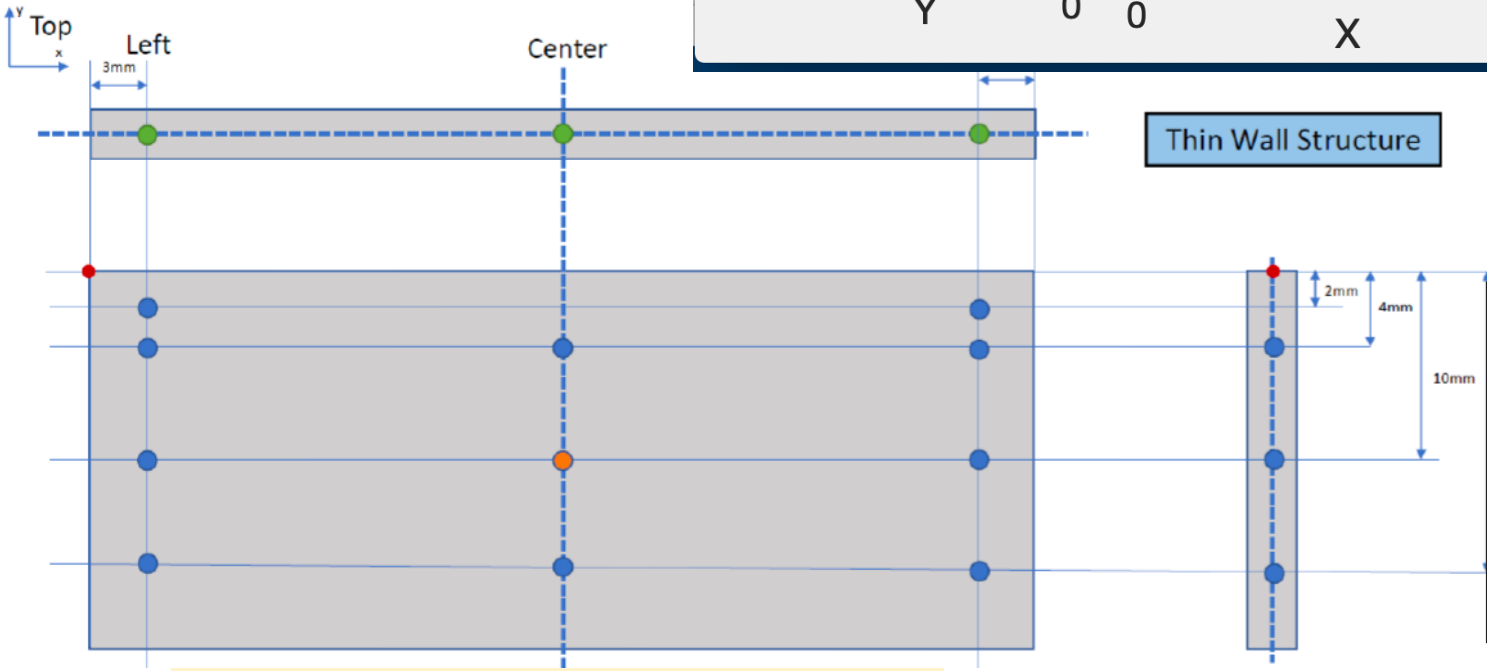


Thin Wall Measurements

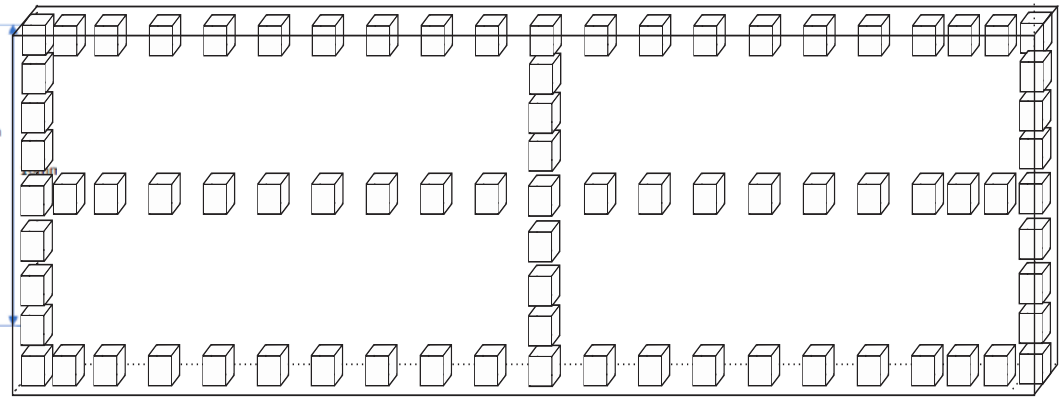
X-ray depth: 200µm
NIST depth: 750µm





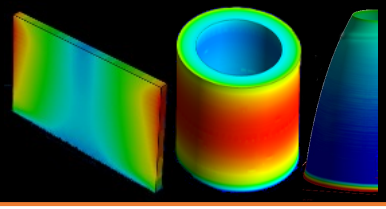


Thin Wall Structure



X-Ray

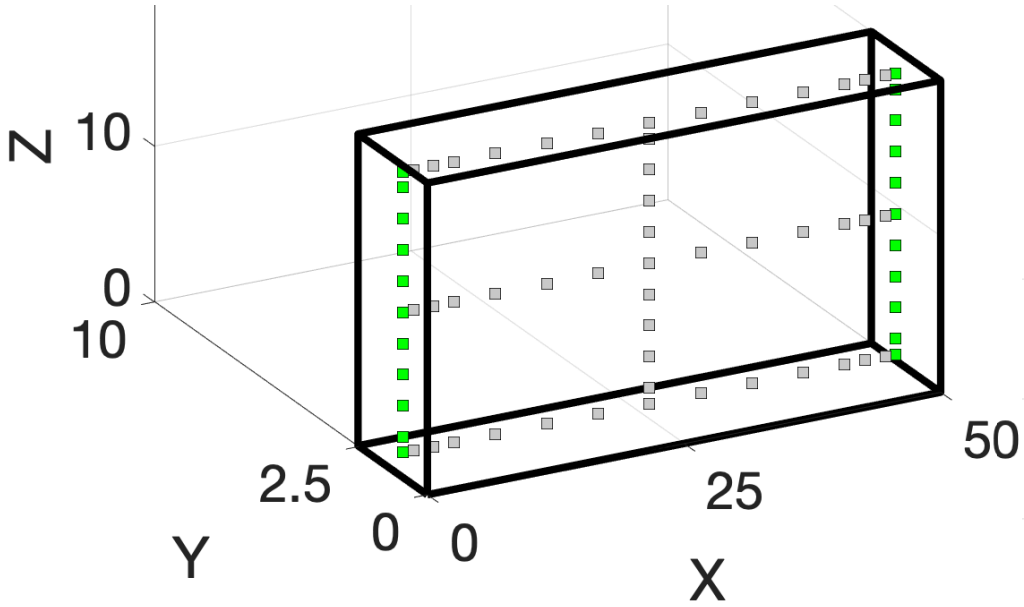
NIST Neutron

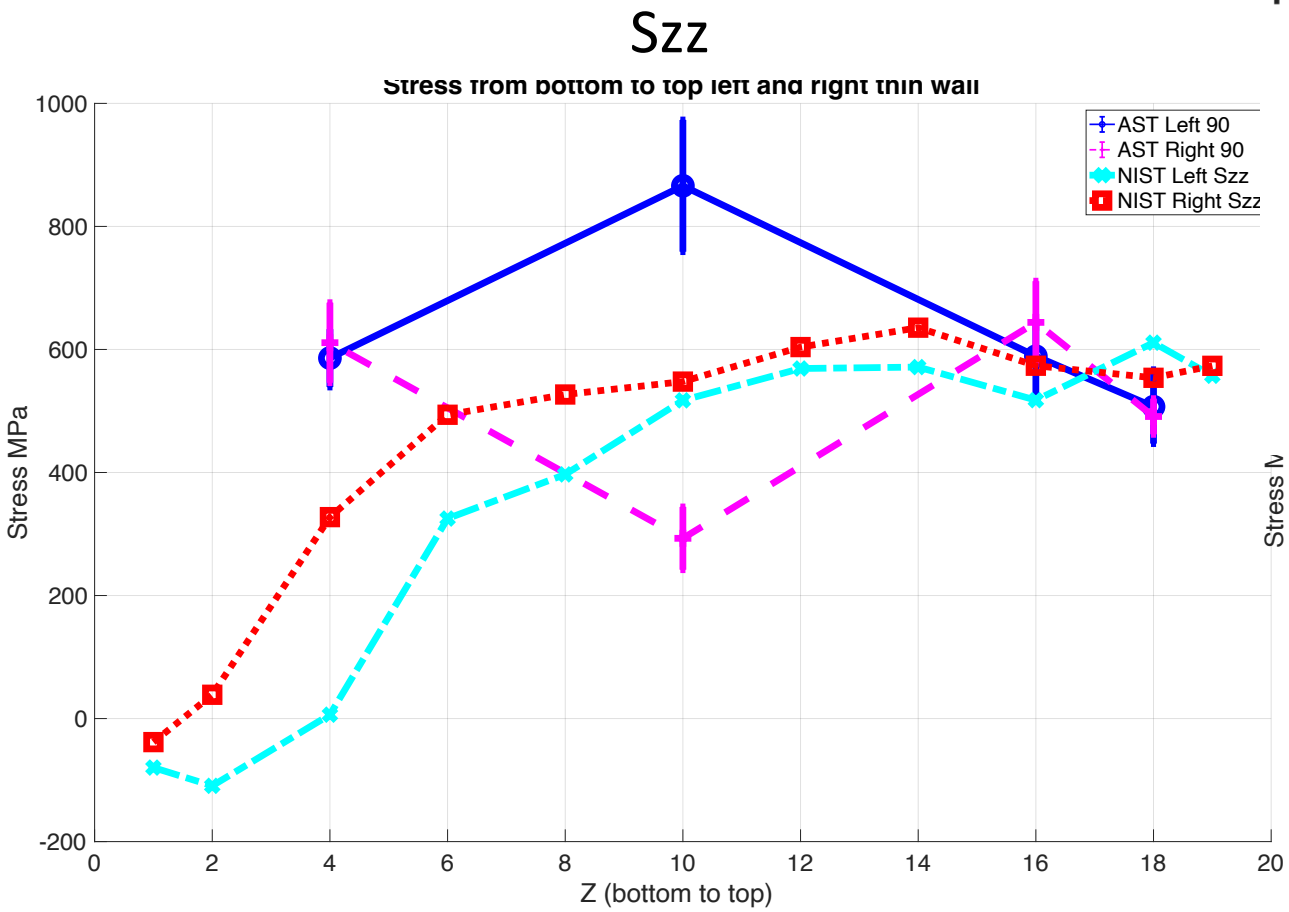


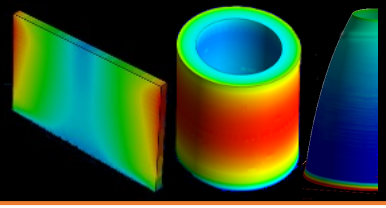
Thin wall Stress X-ray & Neutron

X-ray has greater variability
NIST Neutron aligns well
Greater variability near surface

Left and right vertical

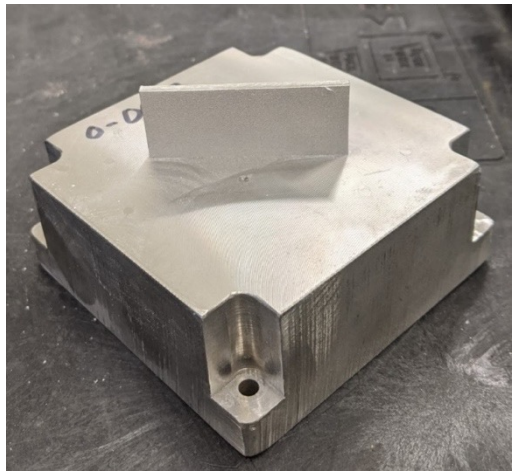


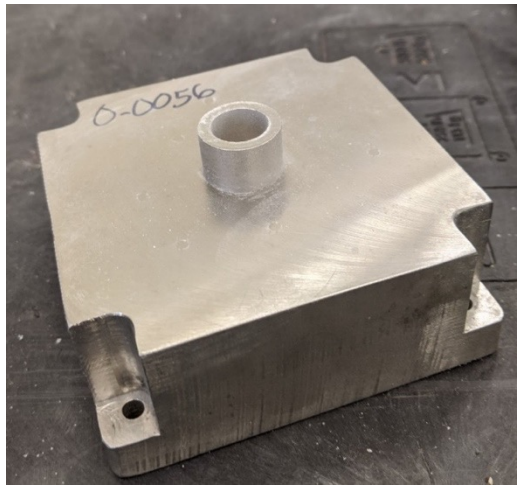


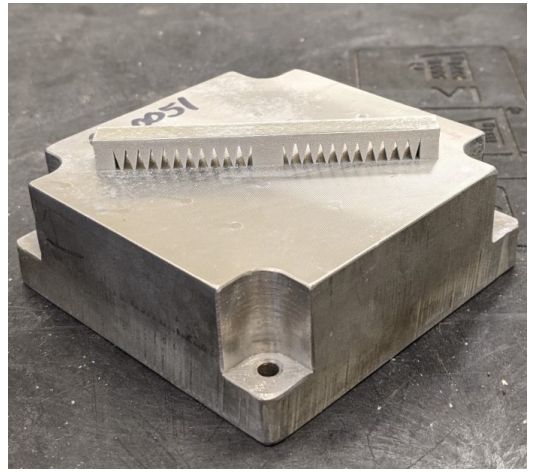


Coupon Measurements – Before & After

BEFORE Measurement:
- Thin wall,
- Hollow cylinder,
- Twin-cantilever





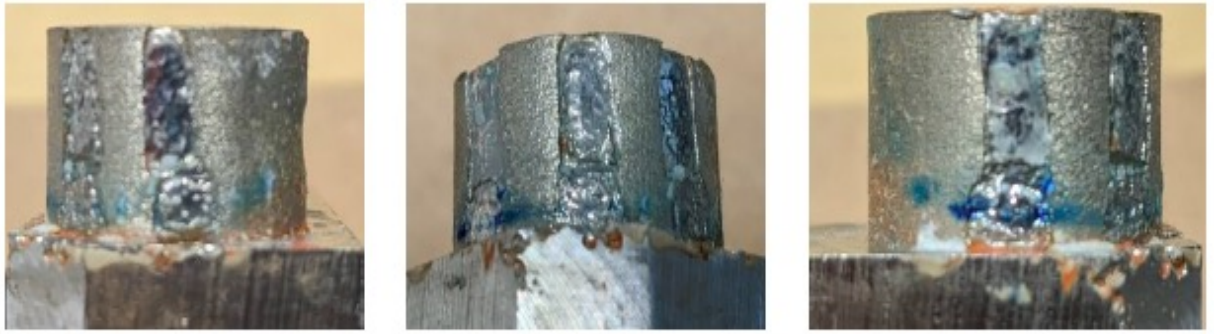


AFTER Measurement:
- Thin wall,
- Hollow cylinder

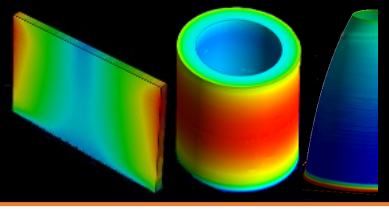




Photos of the Thin Wall Sample Top, Face, and Side after electropolishing. White is epoxy putty and orange is lacquer left from electropolishing.

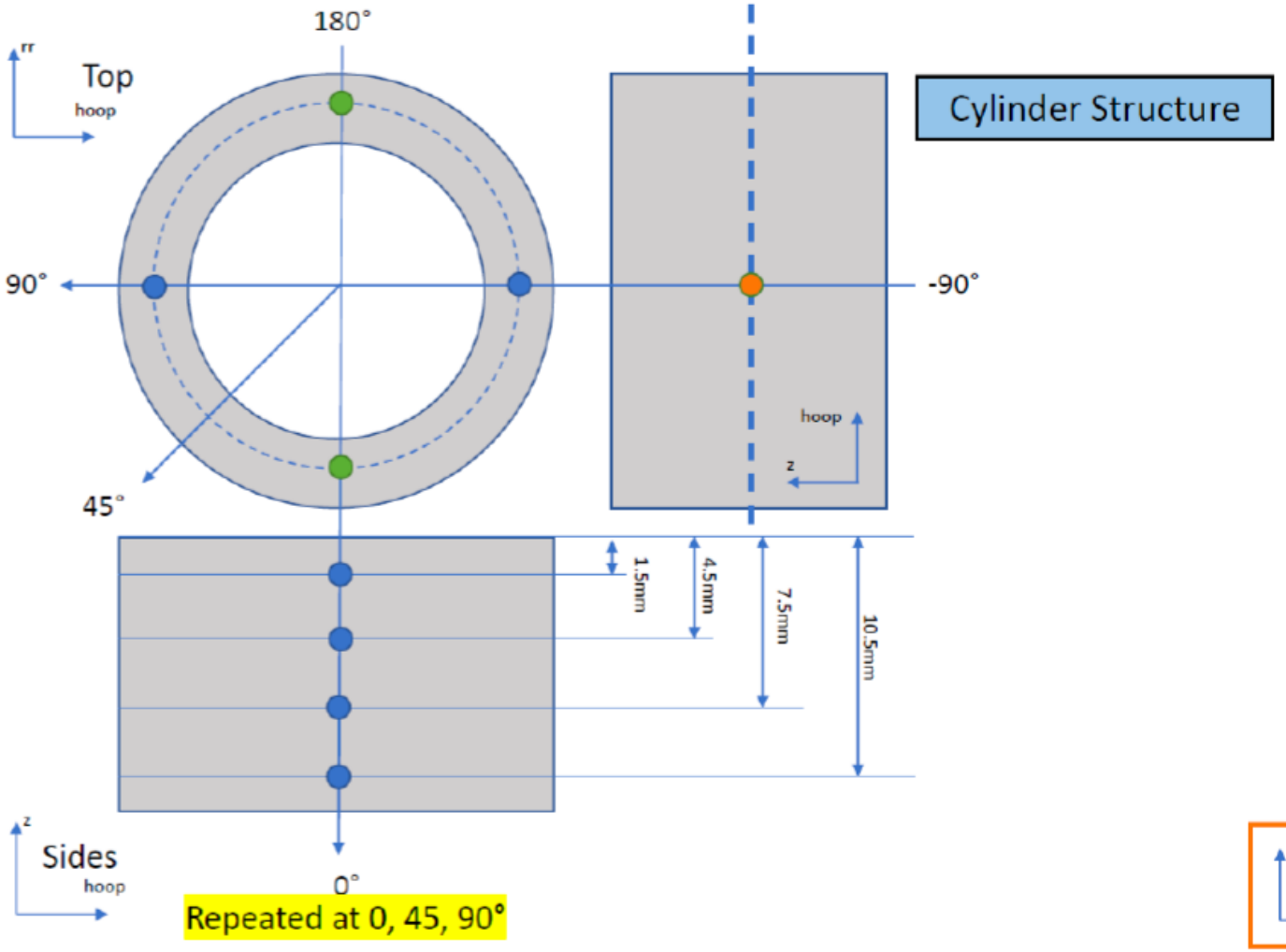


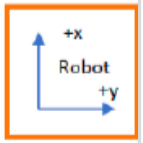
Photos of the sides of the cylinder from left to right 0, 45 and 90 degrees after electropolishing.



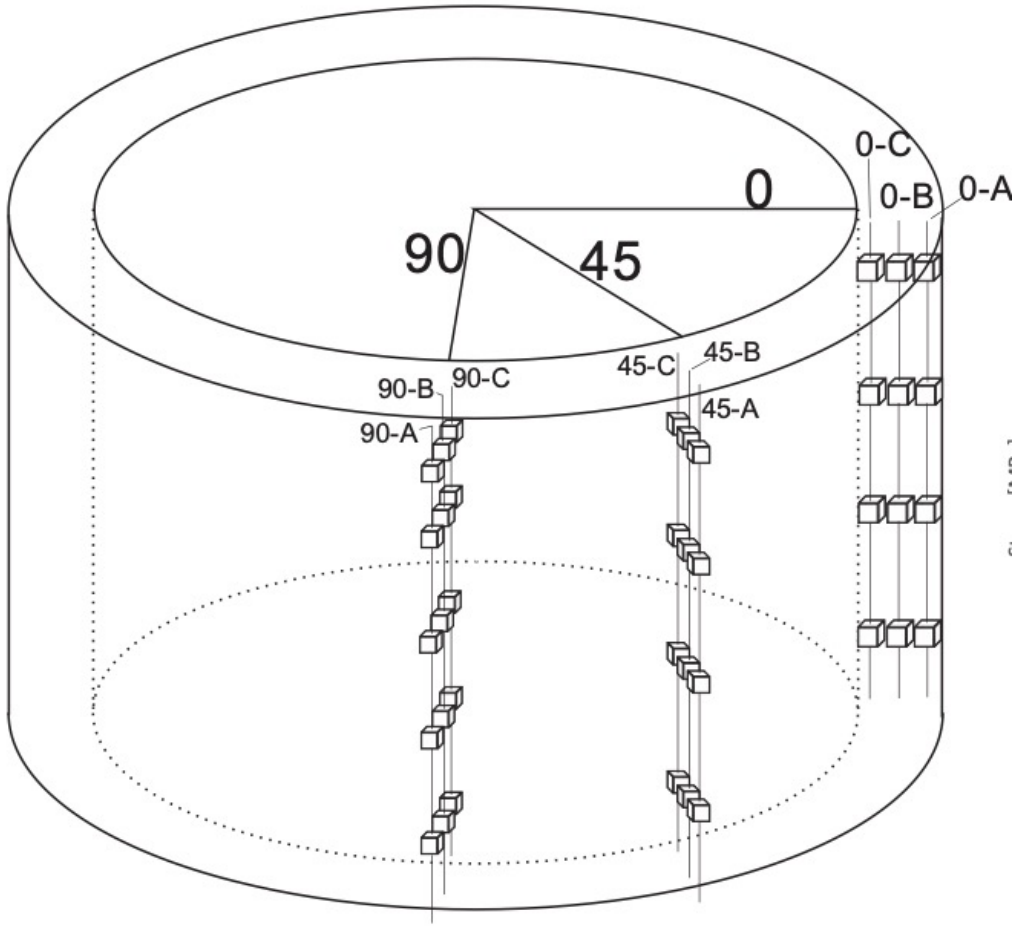
X-Ray and NIST Neutron Cylinder Measurements

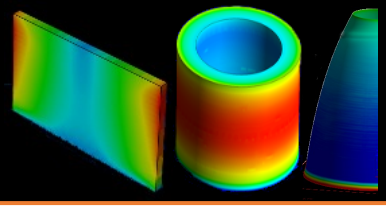
X-Ray



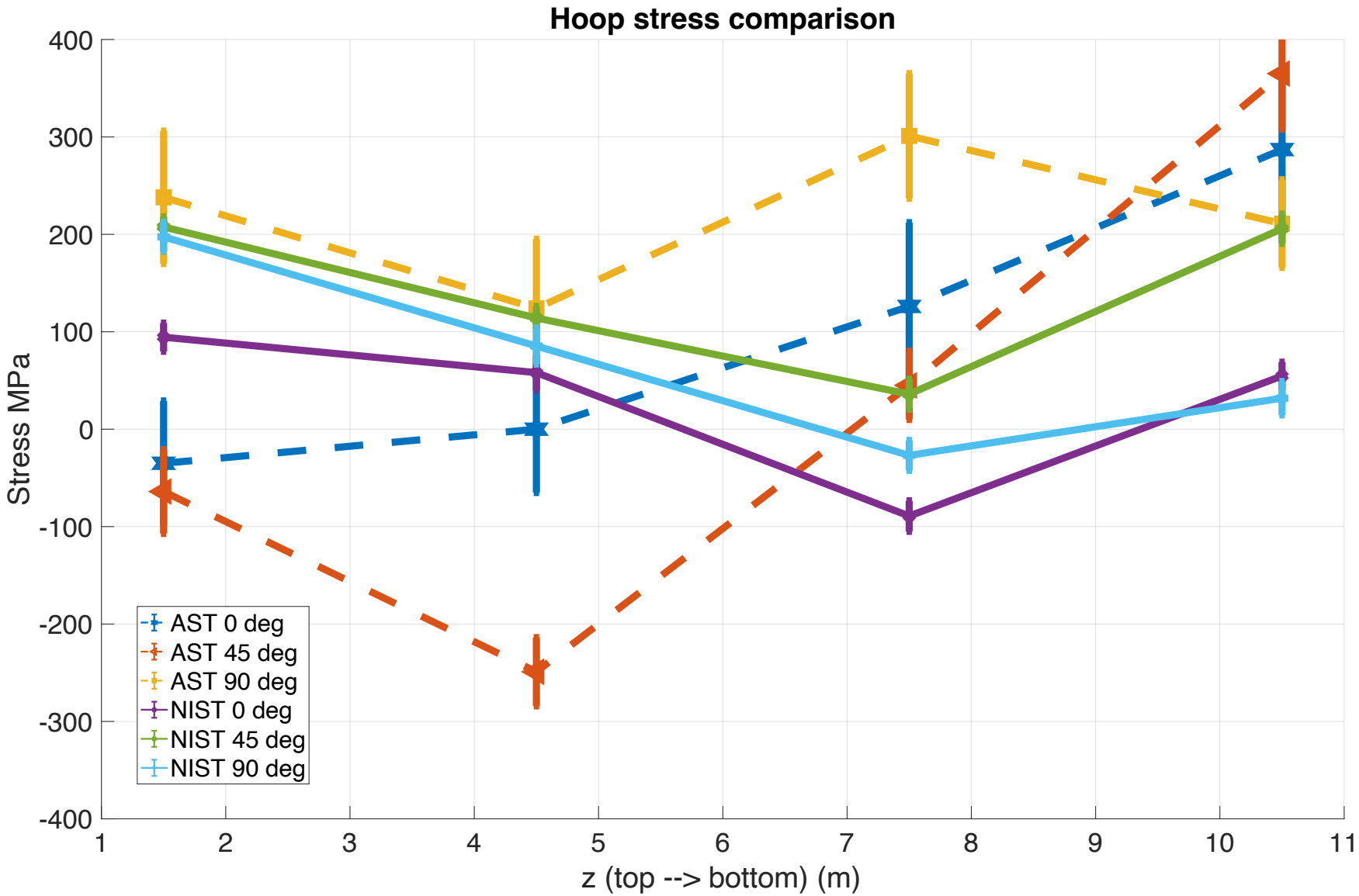


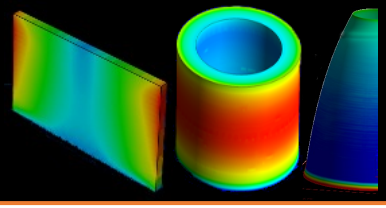
NIST Neutron



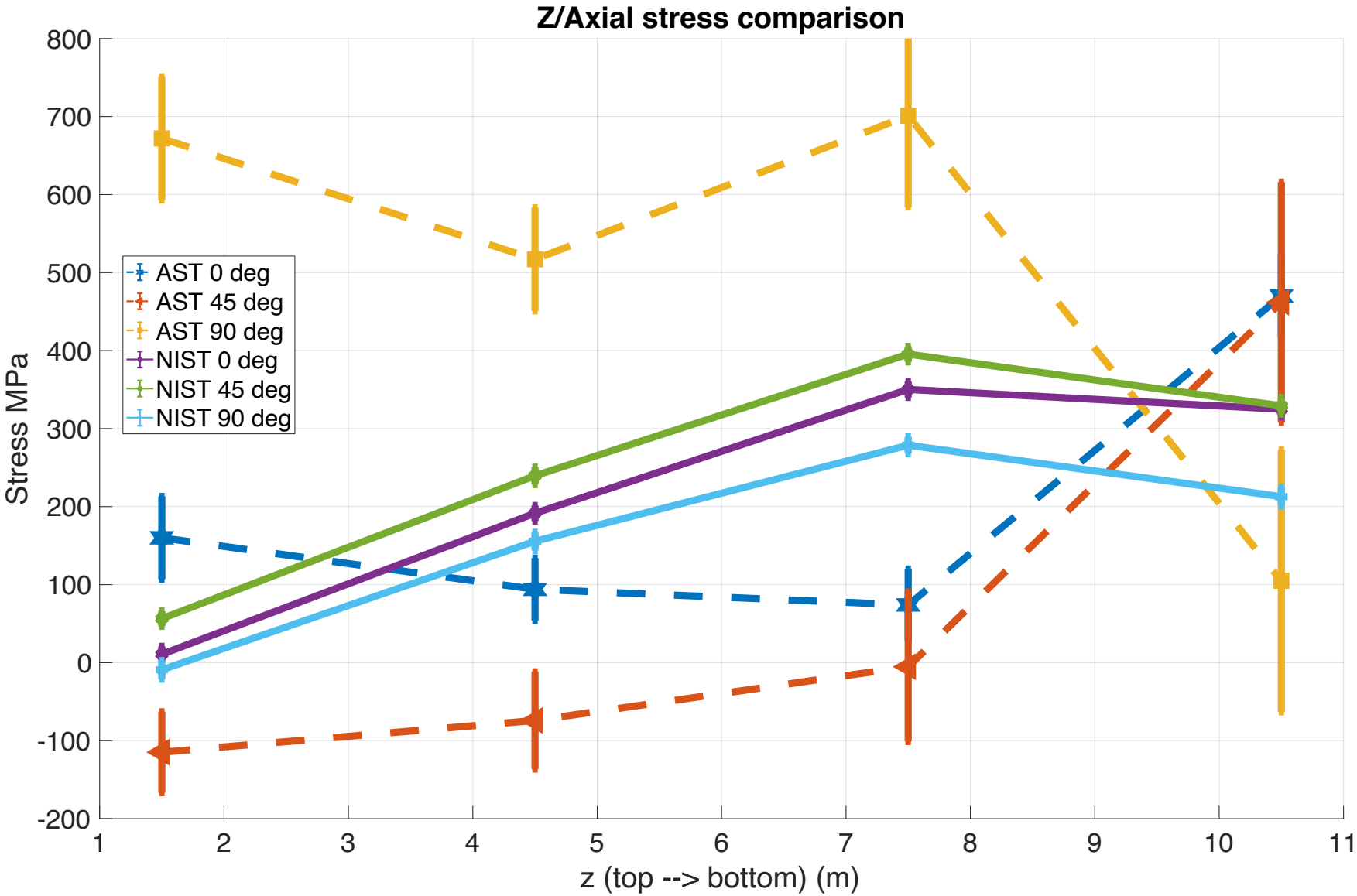


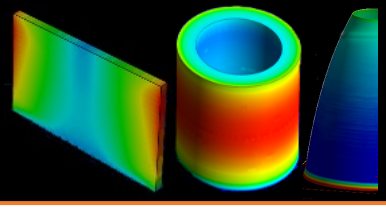
Hoop Stress
X-ray at 200μm and NIST at 750μm depth



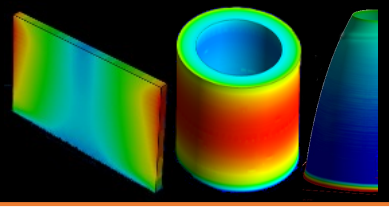


Axial Stress
X-ray at 200μm and NIST at 750μm depth

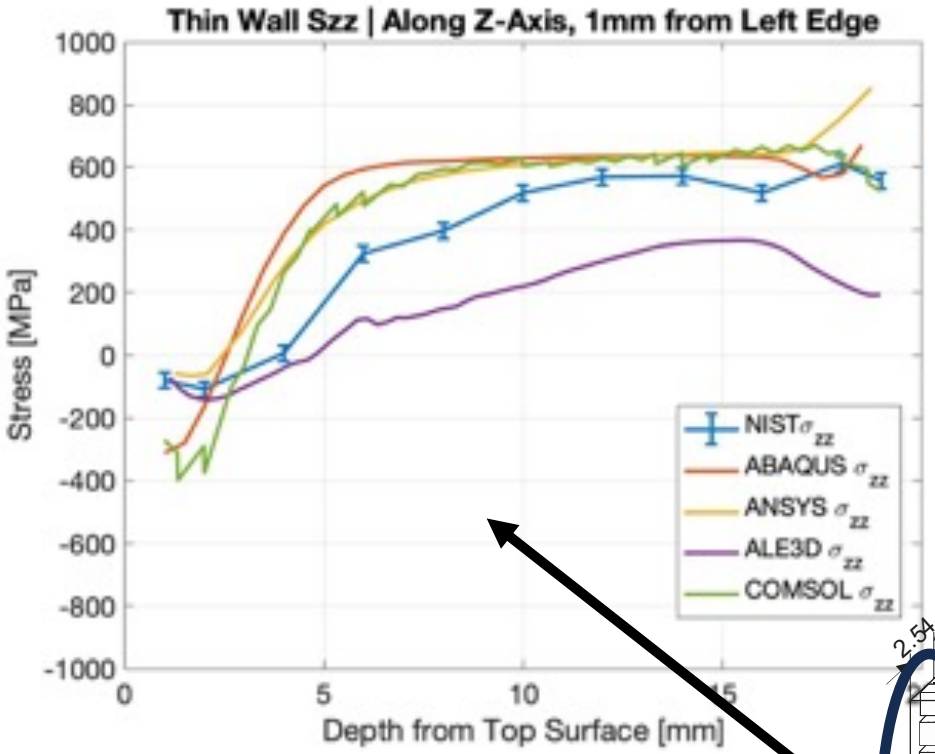


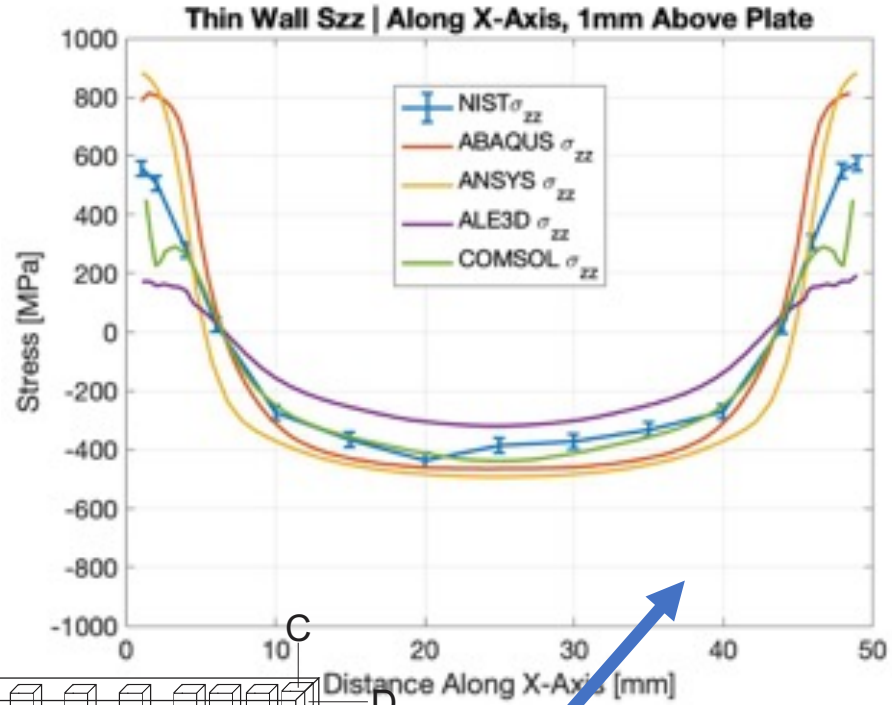


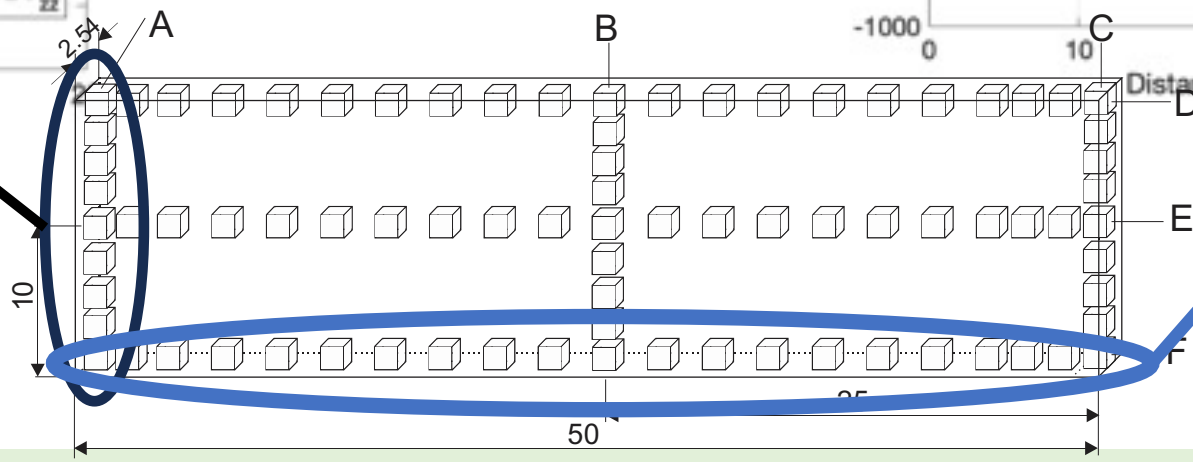
Comparison between Model Predictions and Measurements



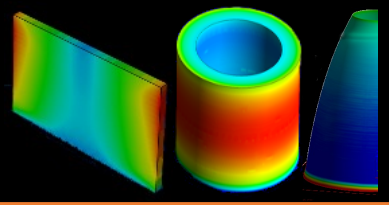
Residual stress thin wall



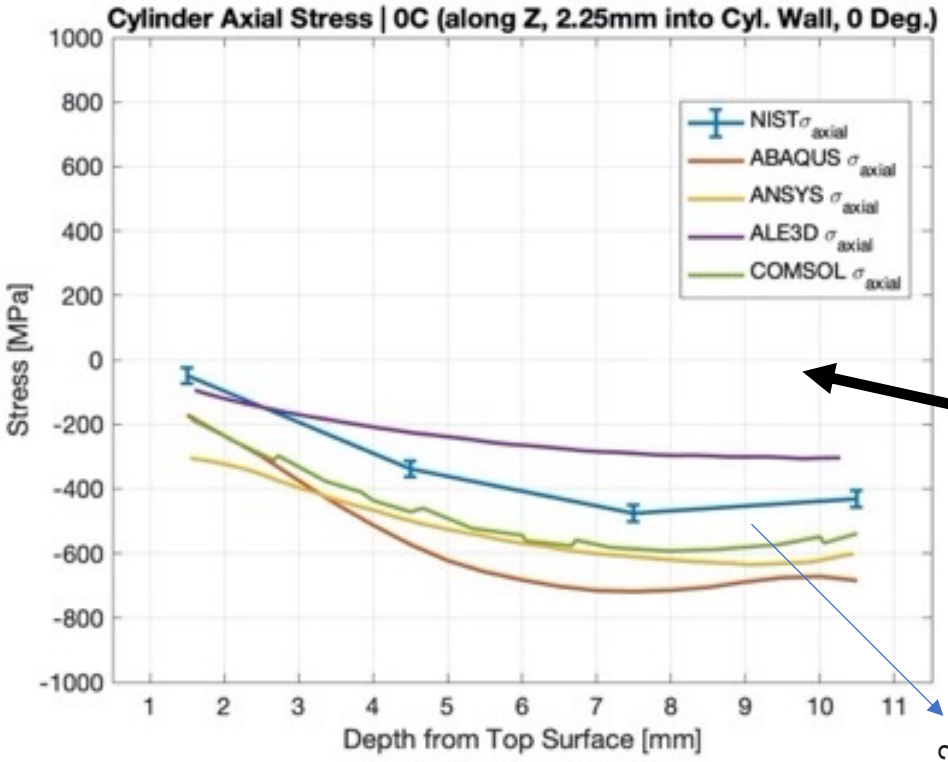


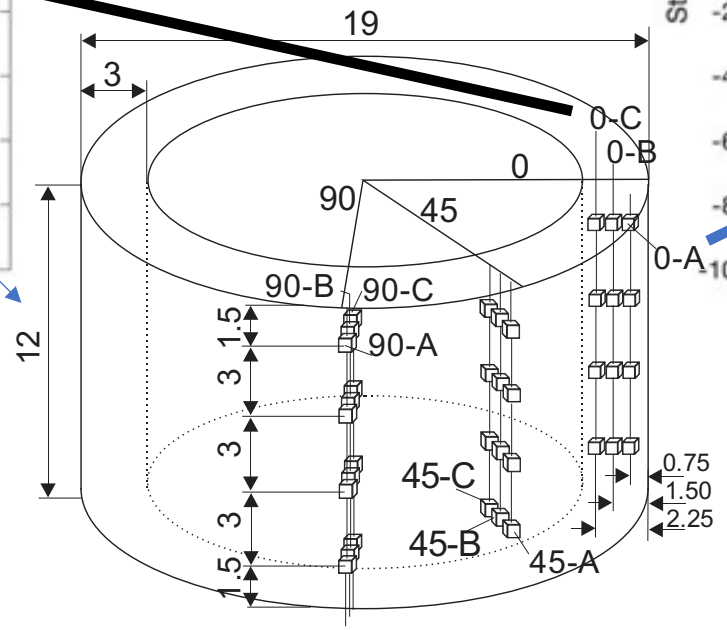


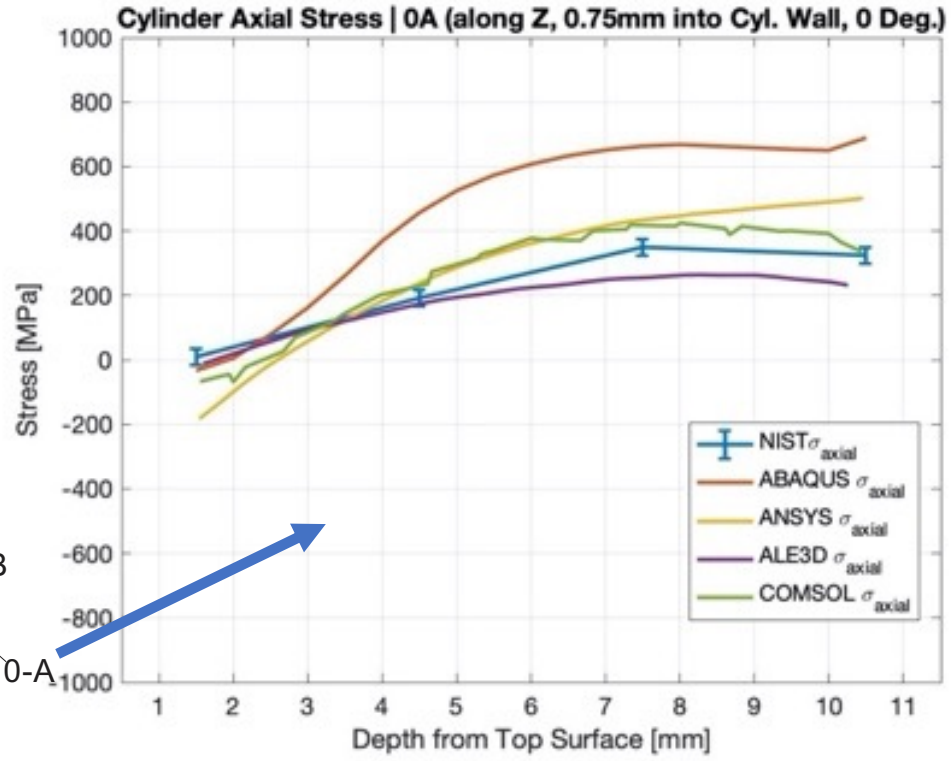
NIST measurements error bar is σ. Trend of all codes is similar. Codes seem to bound the measurements. Average of code results would be a reasonable predictor.



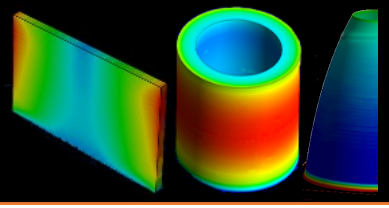
Residual stress hollow cylinder



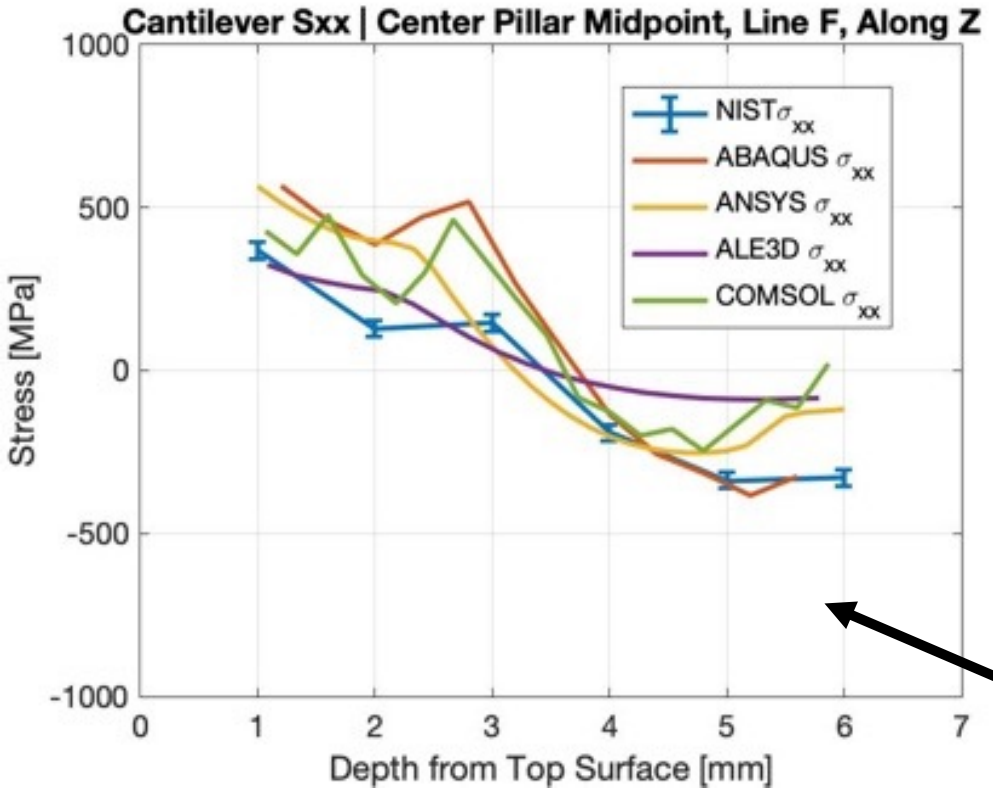


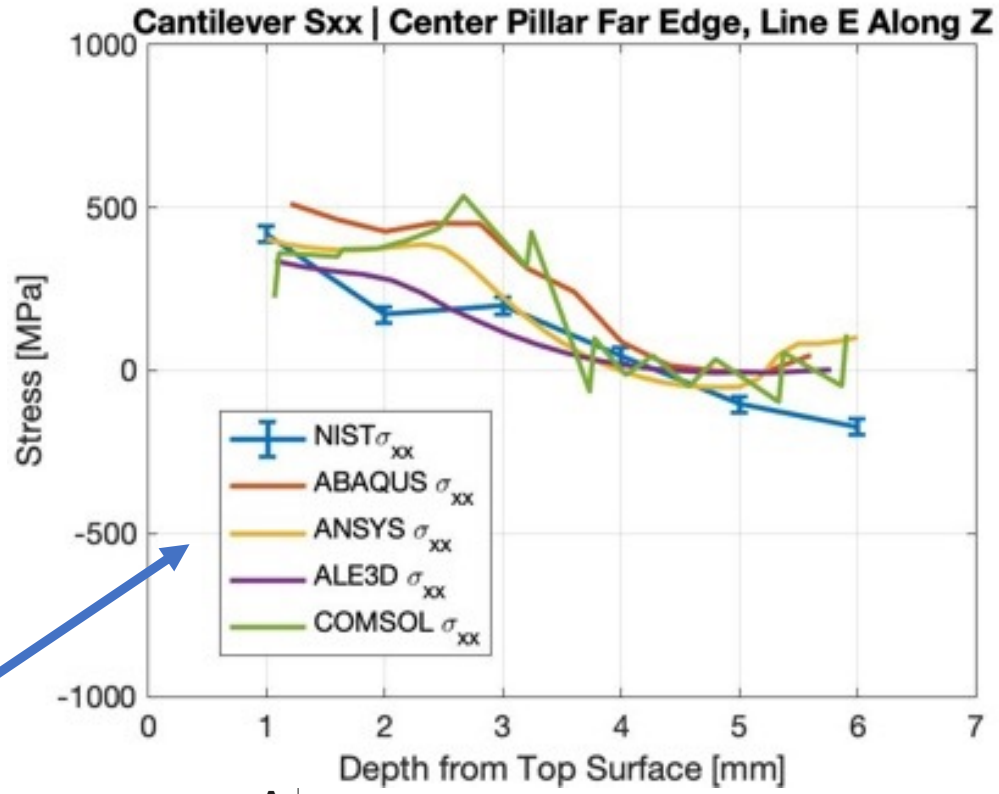


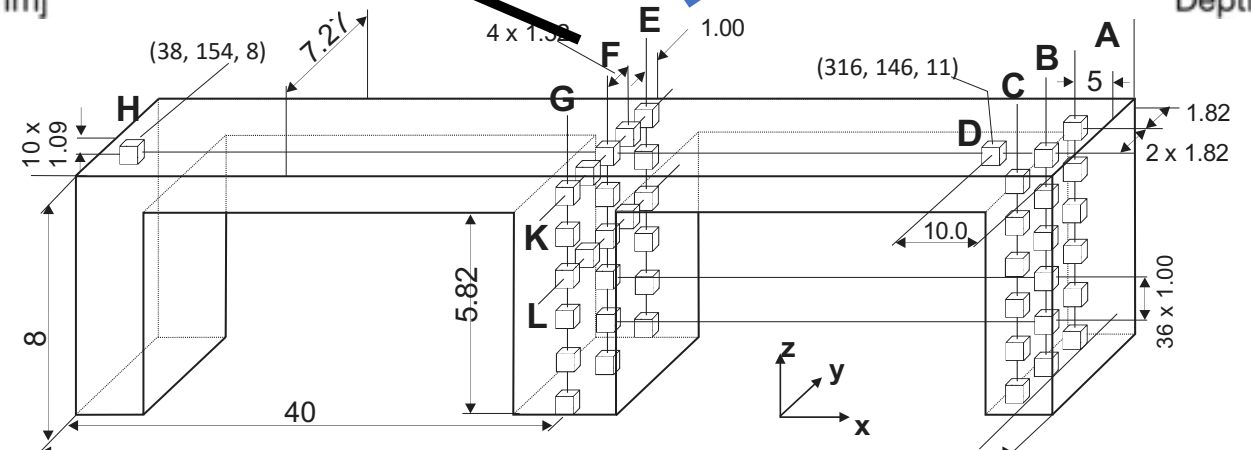
Trend of all codes is similar. Most codes are larger in magnitude than measurements. ALE3D and the other codes again bound the measurements.

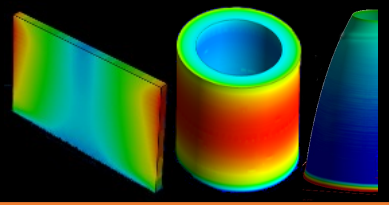


Residual stress cantilever

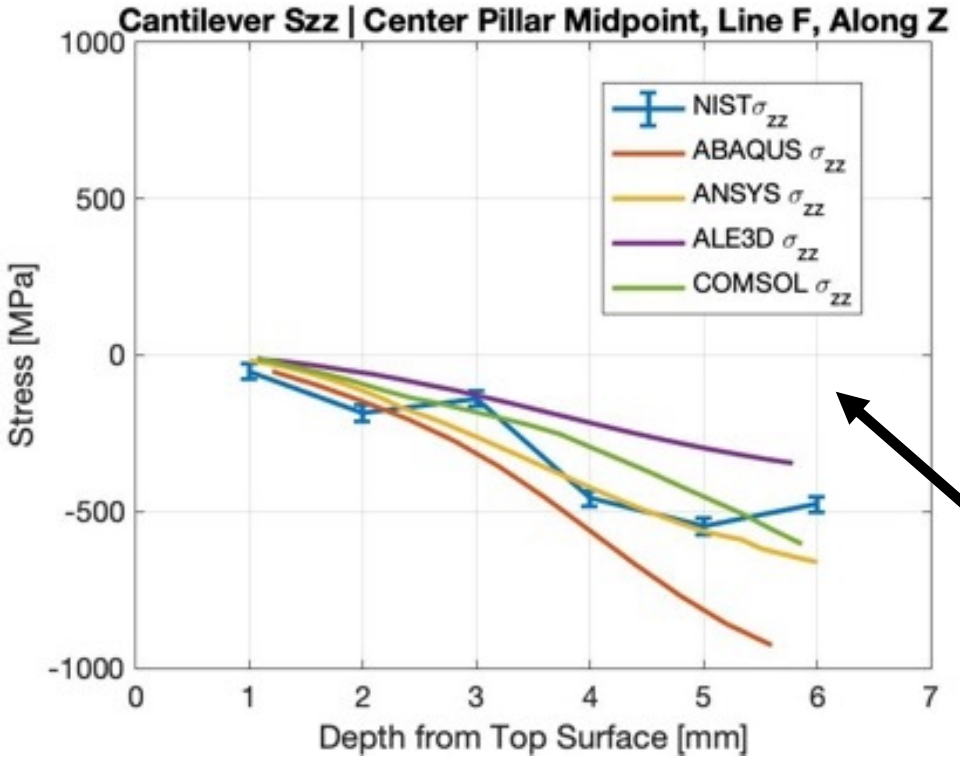


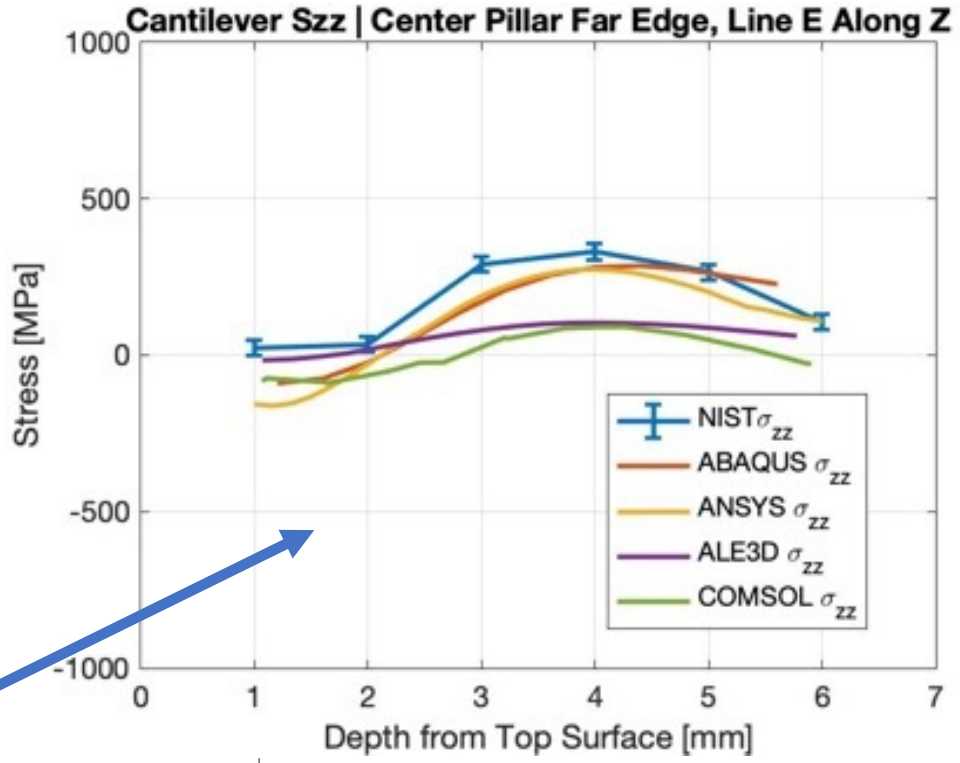


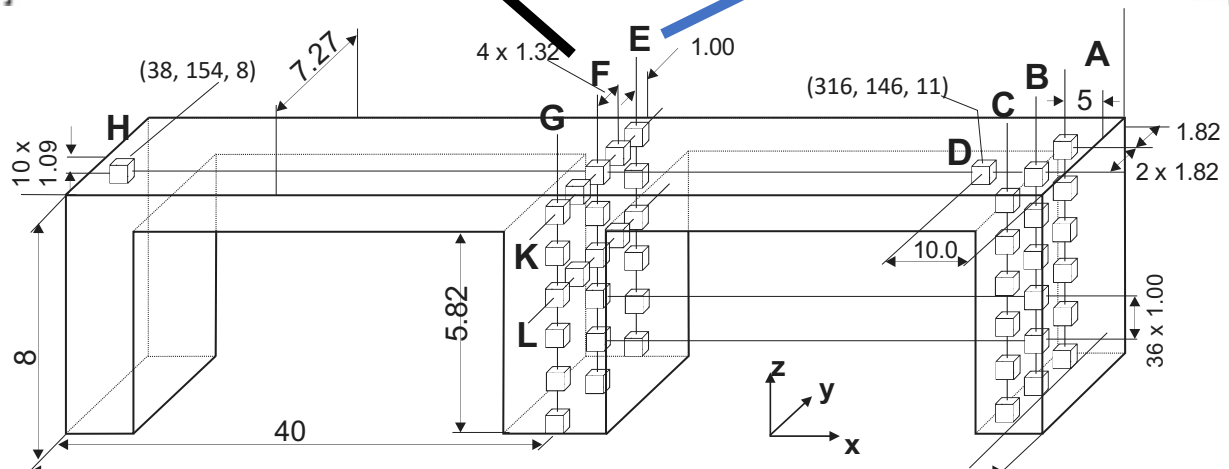


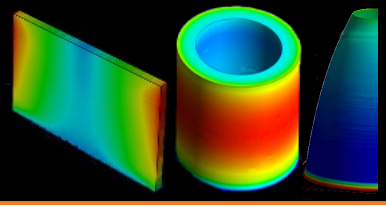


Residual stress cantilever

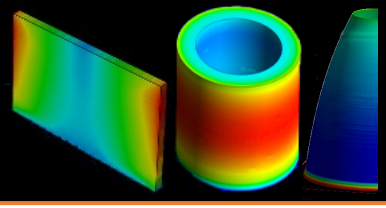








Scaling-up Modeling

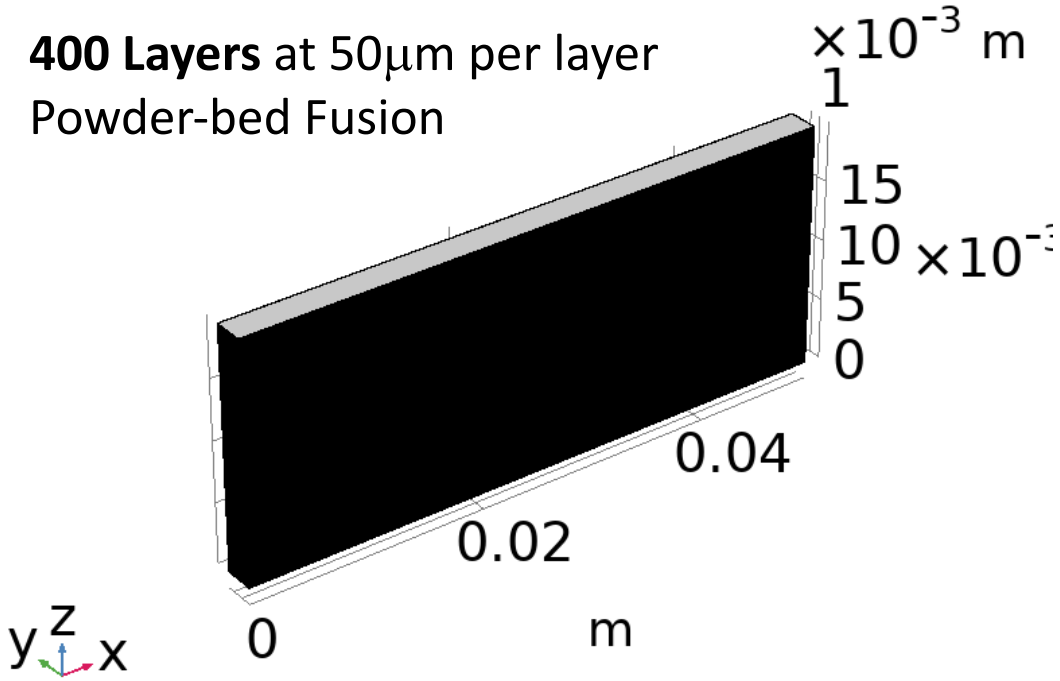


Pragmatic Method

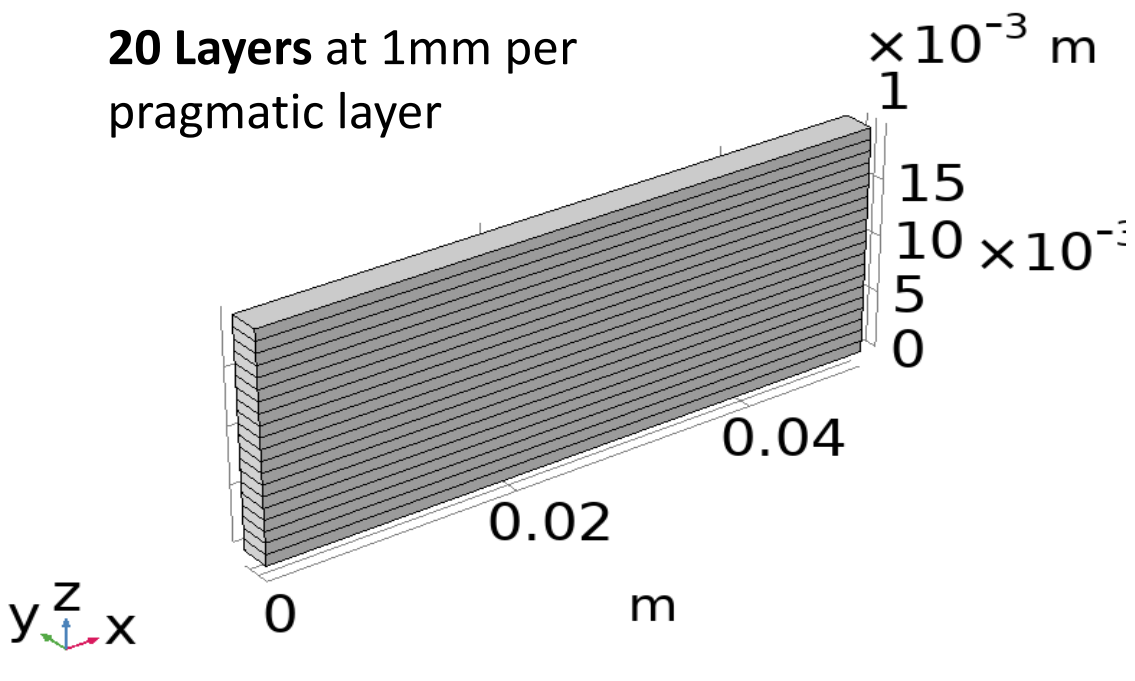
Pragmatic Approximation Method

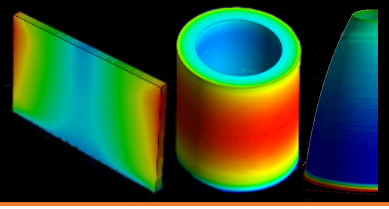
- Small thin wall coupon consists of over 400 layers, too many to individually model.
- To scale computations up to coupon scale, need to lump many layers together.
- Heat whole lumped layer, then feed thermal gradients to stress calculations.
- Only do stress calculations for 20 layers instead of 400.

400 Layers at 50μm per layer
Powder-bed Fusion

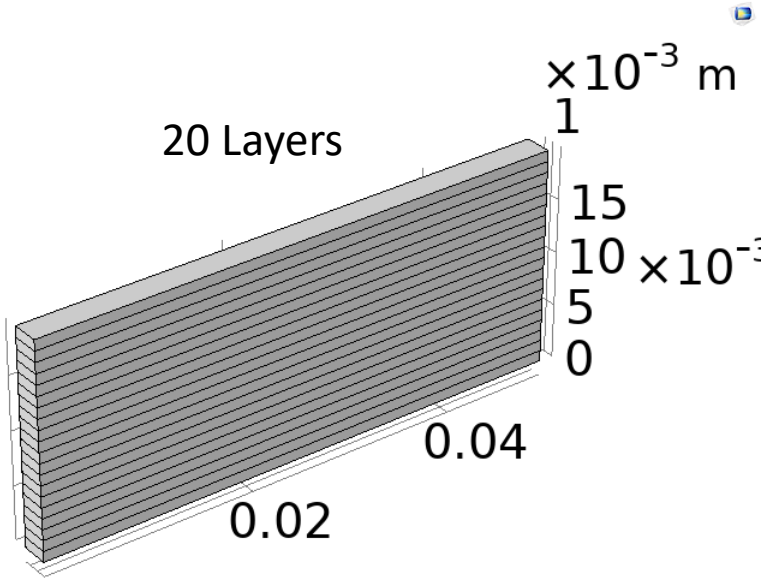


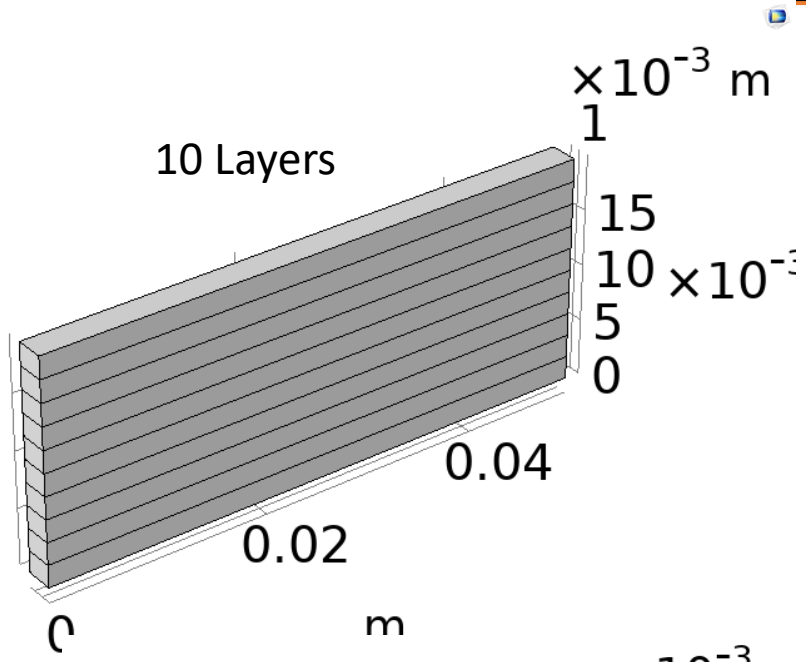
20 Layers at 1mm per
pragmatic layer

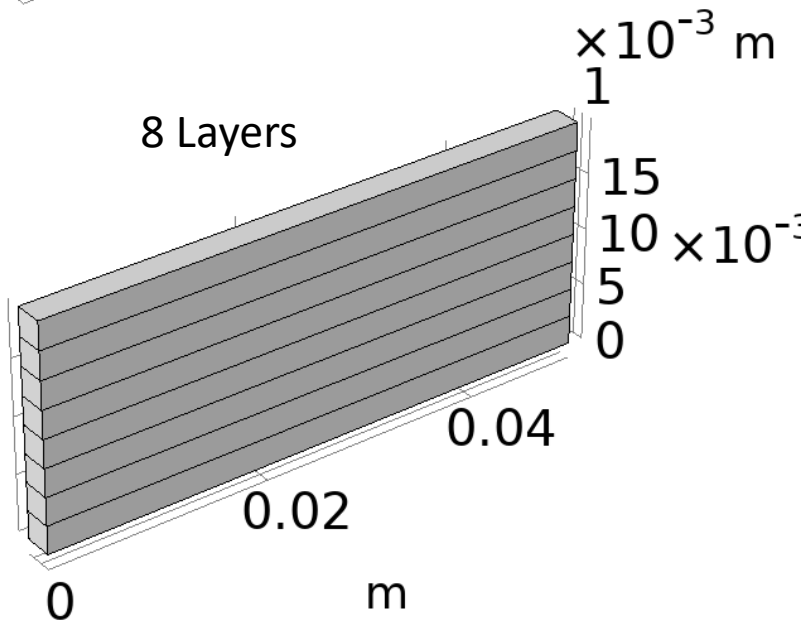


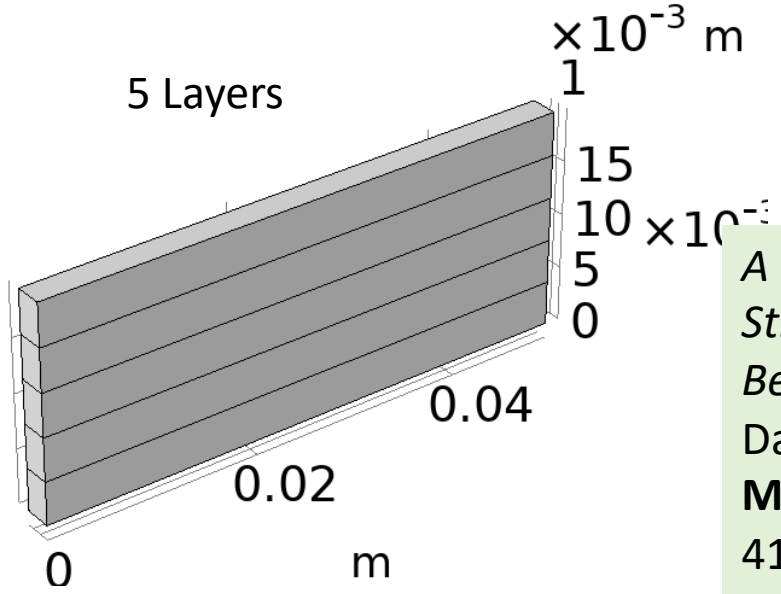


Pragmatic Approximation





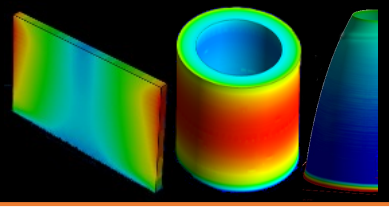




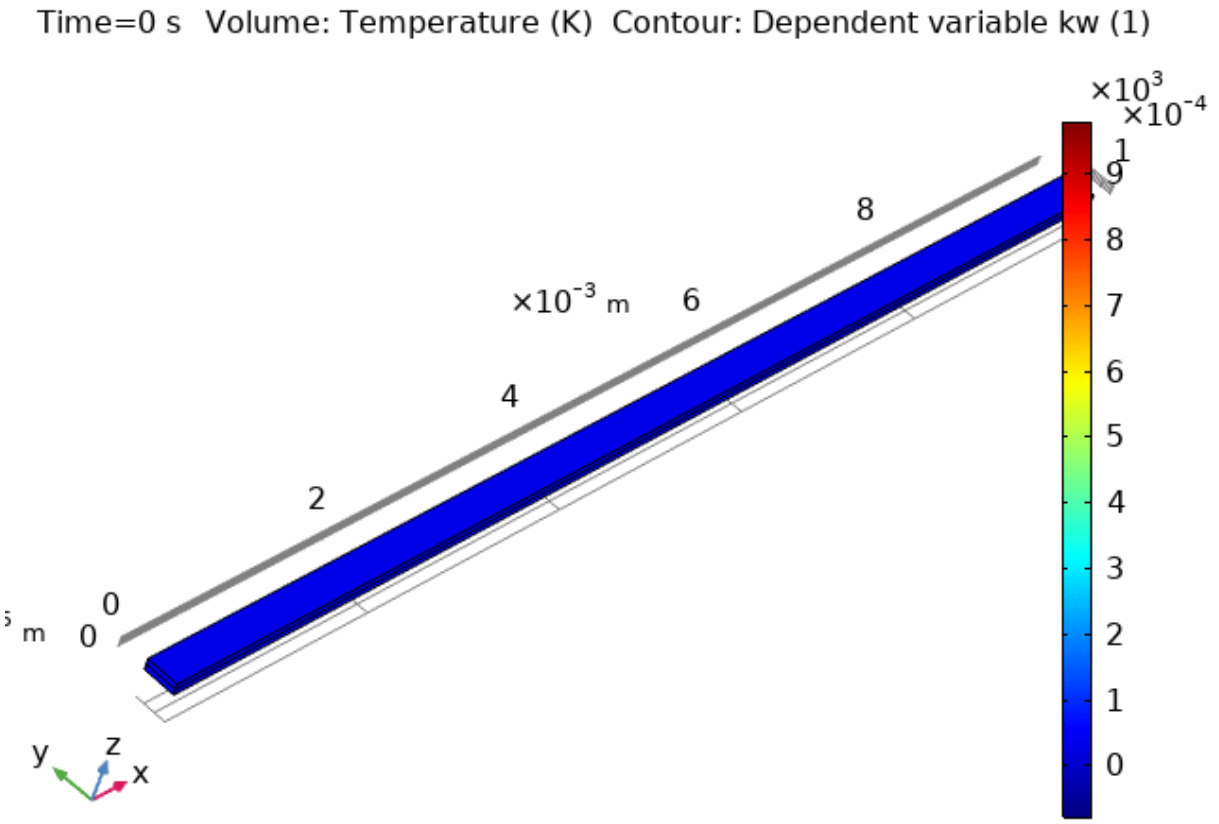
Lumped temperature layers are heated and cooled for several real layers at a time.

20mm tall part with 50um layers has at least **400** real layers.

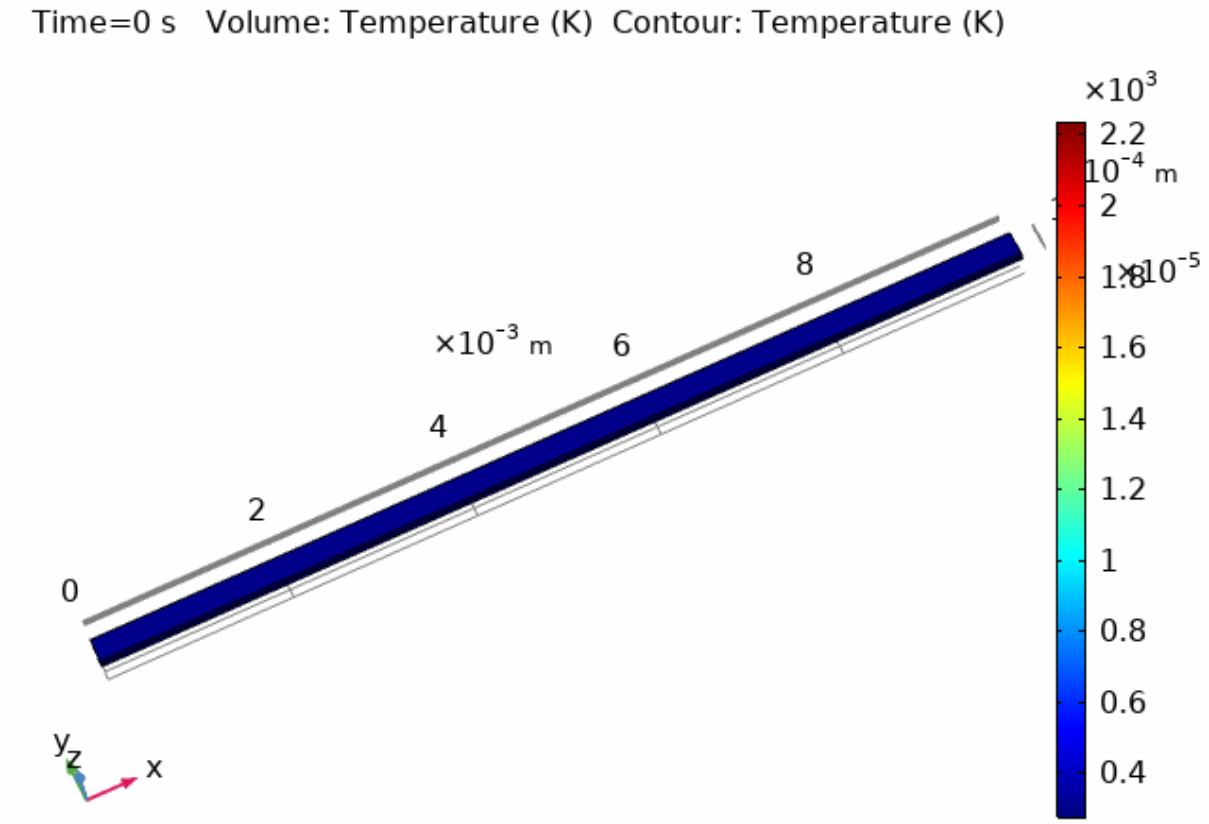
A Pragmatic Part Scale Model for Residual Stress and Distortion Prediction in Powder Bed Fusion, Richard J. Williams, Catrin M. Davies, Paul A. Hooper, **Additive Manufacturing**, Vol. 22, August 2018, pp. 416-425.



Thermal analyses – scans vs. bulk

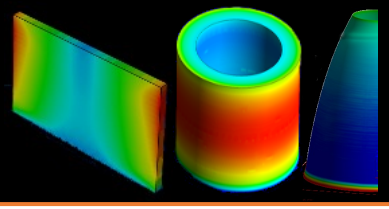


Thermal scan takes 1 hour on 54 cores per centimeter.



Bulk thermal profile takes 9 minutes resulting in same stresses.

Order of magnitude reduction per cm.
Typically applied for multiple layers simultaneously.



Thermal & Structural Physics for Pragmatic Method

Segregated solutions used for pragmatic approach.

Heat Equation:

$$\rho C_p \frac{\partial T}{\partial t} + \rho C_p \mathbf{u} \cdot \nabla T + \nabla \cdot \mathbf{q} = Q + Q_{ted}$$

$$\mathbf{q} = -k \nabla T$$

- Mechanics uses temperature field history as input
- Large plastic strain model
- Yield function is von Mises
- Linear isotropic hardening
- Layer by layer activation
- Powder surfaces free of stress
- Symmetry boundary conditions when possible

Structural Mechanics:

Linear elasticity:

$$0 = \nabla \cdot (FS)^T + \mathbf{F}_V, \quad F = I + \nabla \mathbf{u}$$

$$S = S_{ad} + J_i F_{inel}^{-1} \left(\mathbf{C} : \epsilon_{el} \right) F_{inel}^{-T}, \quad \epsilon_{el} = \frac{1}{2}\left(F_{el}^T F_{el} - I \right), \quad F_{el} = F F_{inel}^{-1}$$

$$S_{ad} = S_0 + S_{ext} + S_q$$

$$\epsilon = \frac{1}{2}\left[(\nabla \mathbf{u})^T + \nabla \mathbf{u} + (\nabla \mathbf{u})^T \nabla \mathbf{u} \right]$$

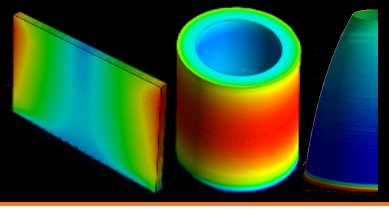
$$\mathbf{C} = \mathbf{C}(E, \nu)$$

Plasticity:

$$F_{inel}^{-1} \rightarrow F_{pl}^{-1} F_{inel}^{-1}$$

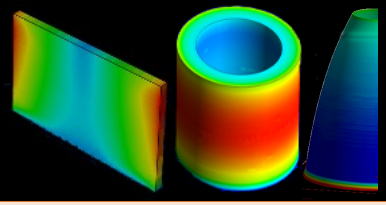
$$J F \left(\dot{M} M + M \dot{M} \right) = -2\lambda \frac{\partial Q}{\partial \sigma} F M^2, \quad M = F_{pl}^{-1}$$

$$\lambda \geq 0, \quad F(\sigma, \sigma_{ys}) \leq 0, \quad \lambda F = 0$$



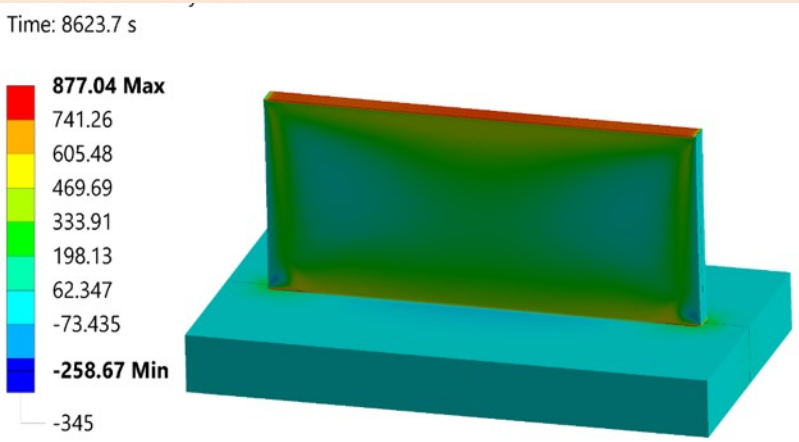
Inherent Strain Method in ANSYS

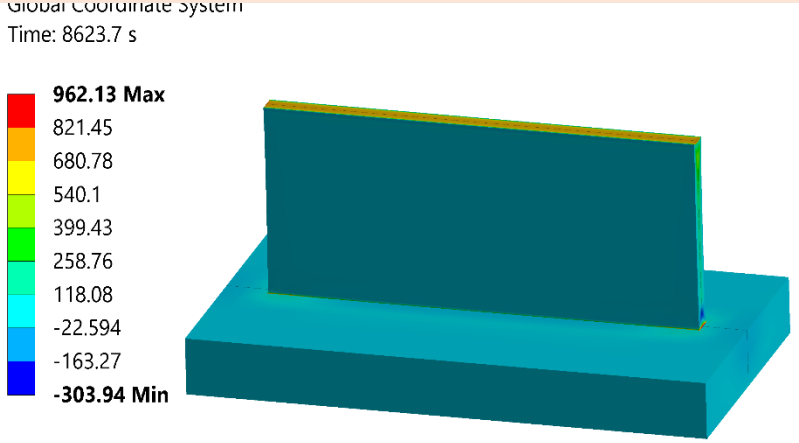
- Inherent strain method in ANSYS Additive has been compared with lumped thermal model for 3 coupons.
- Inherent strain method is much faster but requires a scaling parameter that must be obtained with calibration experiment.
- With the Inherent Strain method, strains are calculated not from material properties and thermal loads but from the use of a Strain Scaling Factor. The strain is equal to the Strain Scaling Factor multiplied by yield strength and divided by elastic modulus. Strain Scaling Factors are tabulated by Ansys depending on the manufacturing parameters deposition layer, scanning speed , etc.
- This approach does not need temperature history and is about 5-10 times faster than standard AM simulation approach.
- If large model like a full-scale nozzle is simulated preliminary residual stresses might be obtained by inherent strain method. If experimental data are available residual parameters can be tunned by calibrations of the isotropic Strain Scaling Factor (SSF).
- Current inherent strain approach will not support bi-metallics.

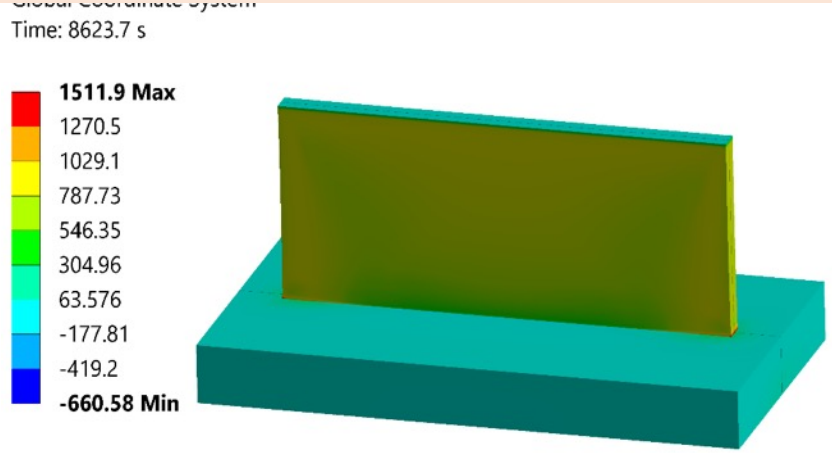


Residual stress wall coupon

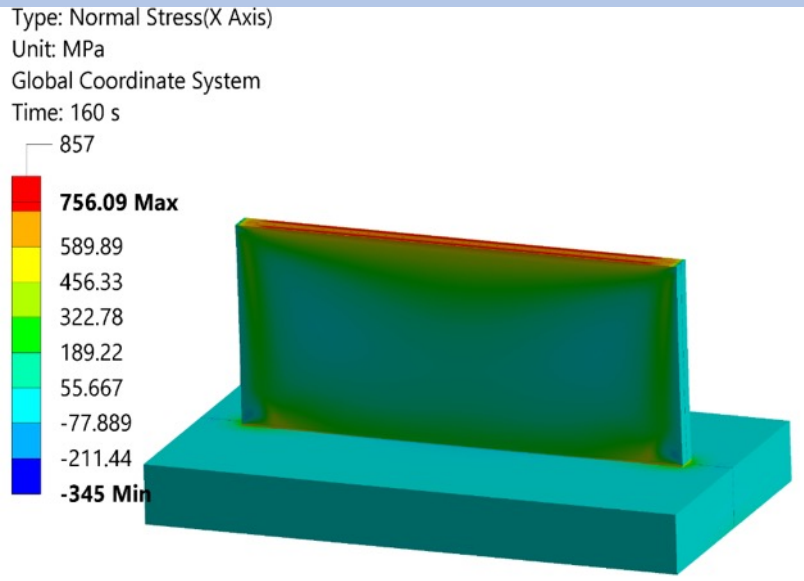
Simulation based on the temperature history – 30 hours on 12 cores

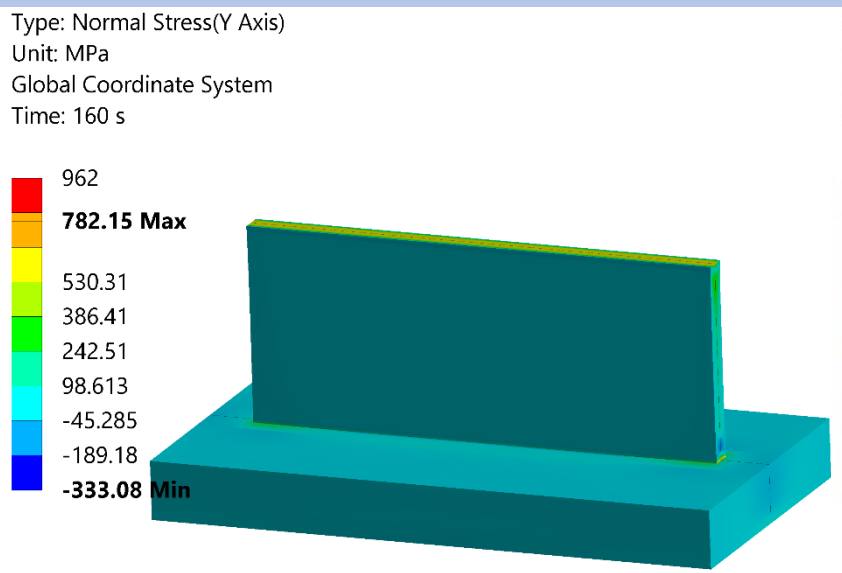


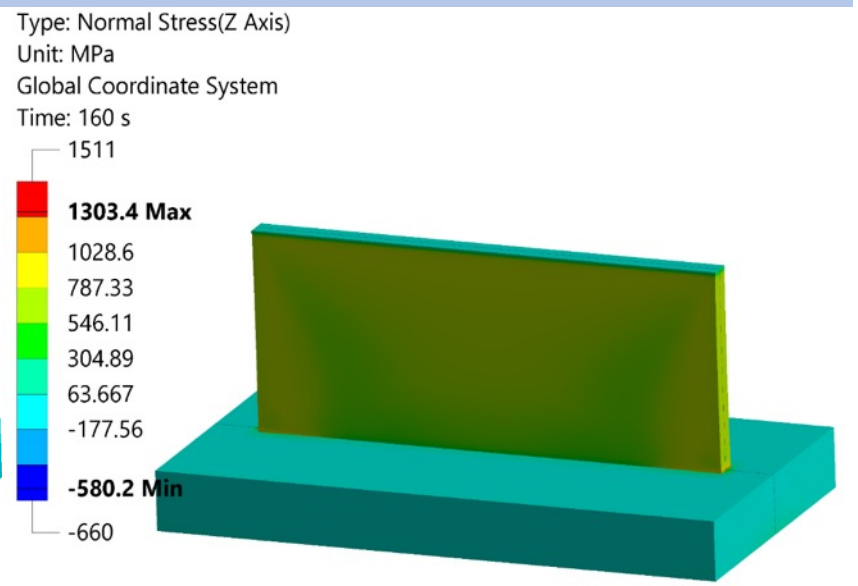


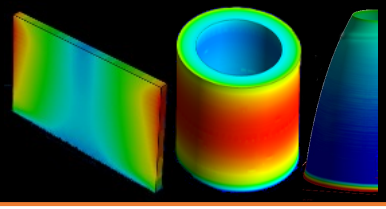


Inherent strain approach - 5 hours on 12 cores



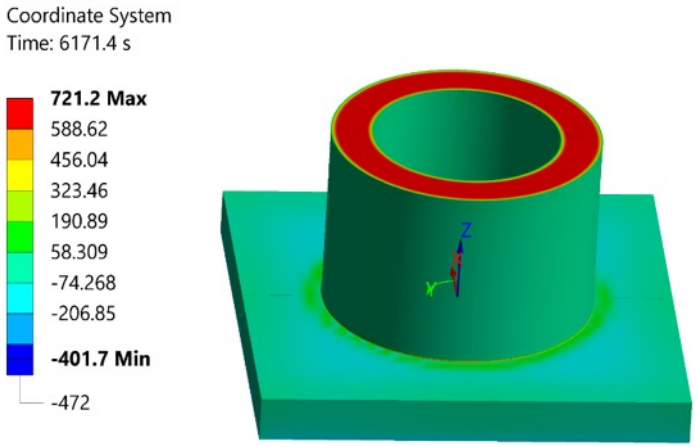


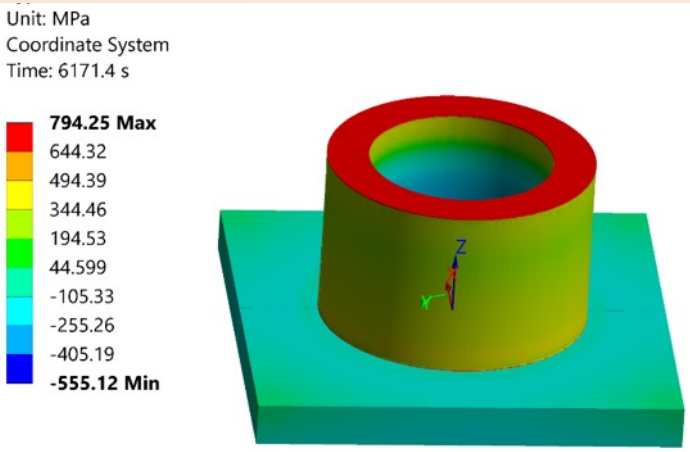


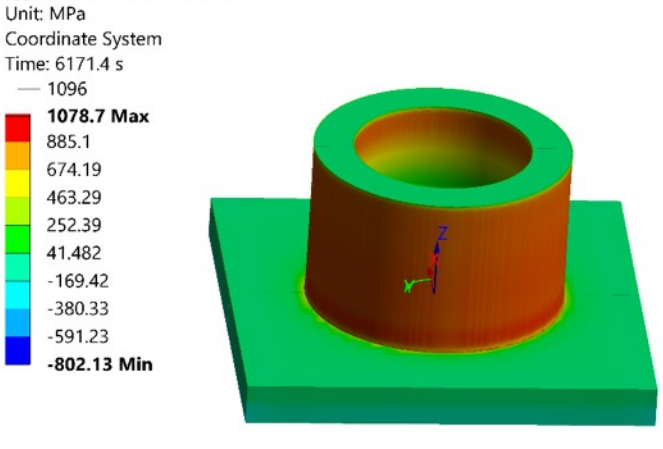


Residual stress cylinder coupon

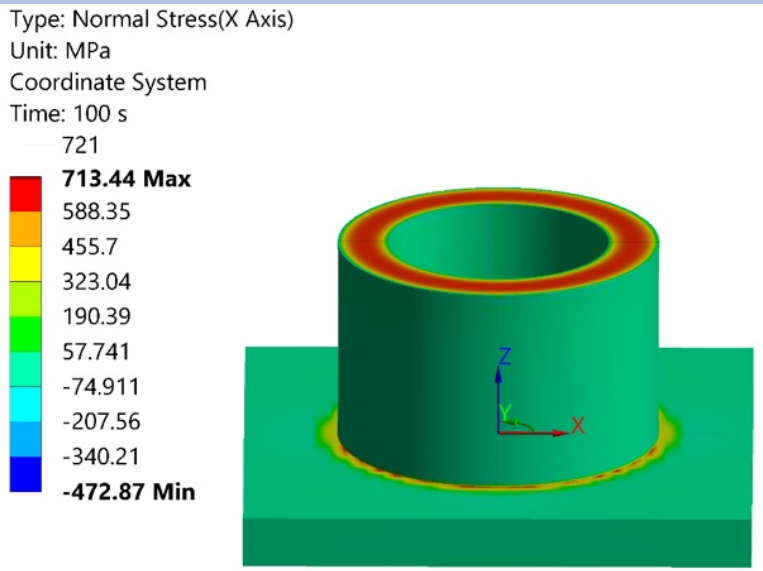
Simulation based on the temperature history – 7 hours

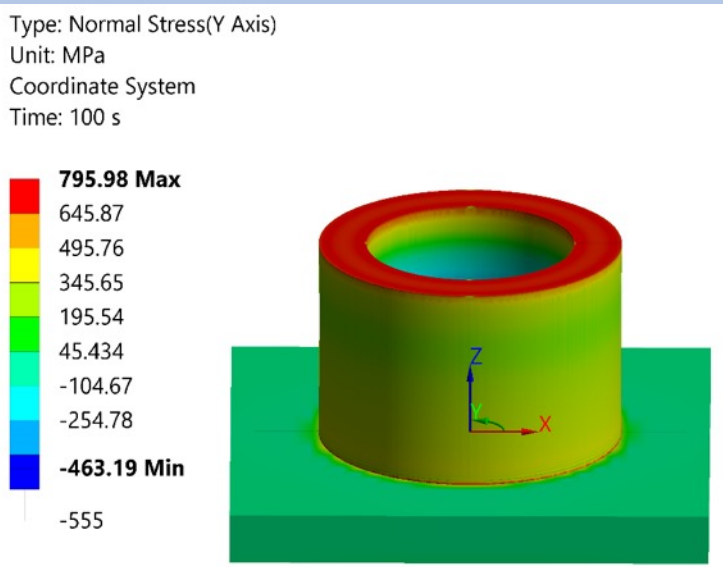


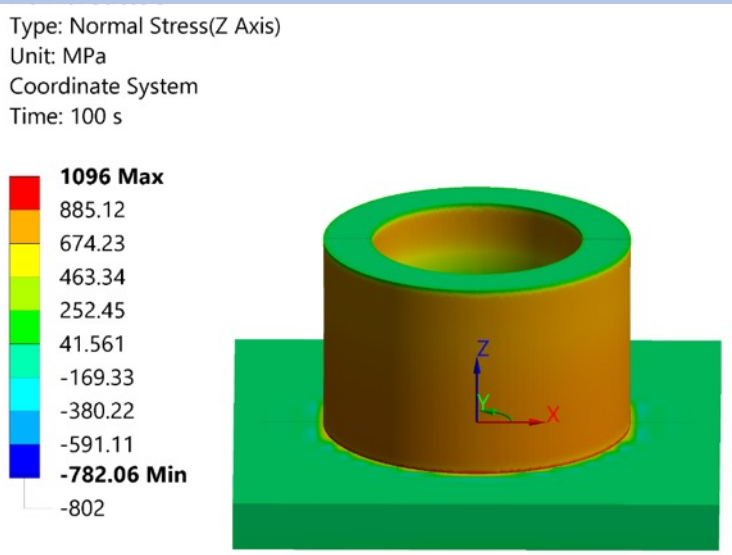


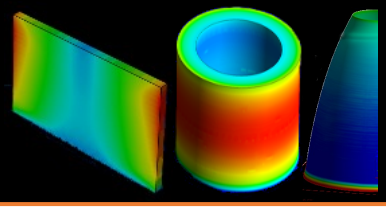


Residual Stresses for Cylinder Coupon - Inherent strain approach – 1.5 hours



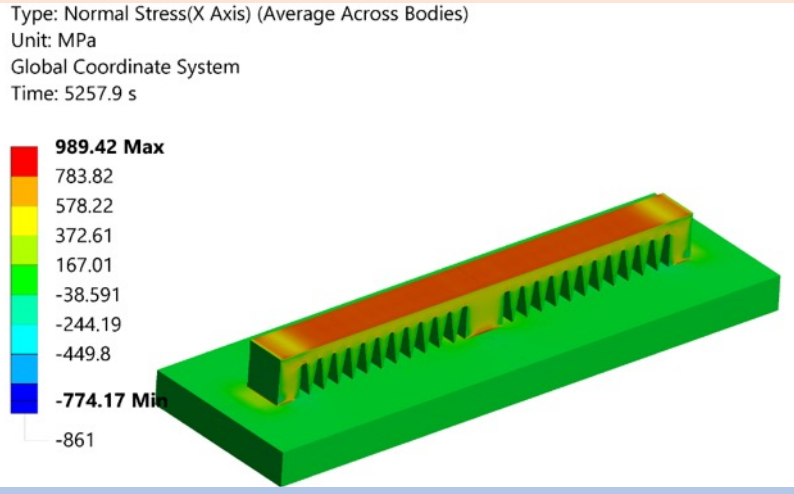


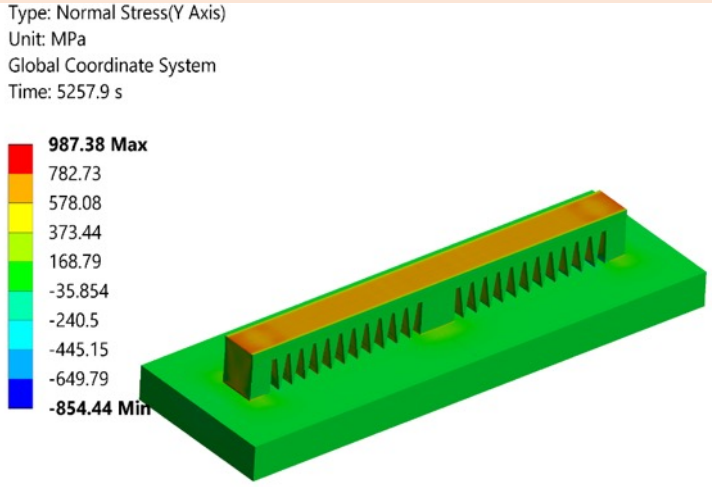


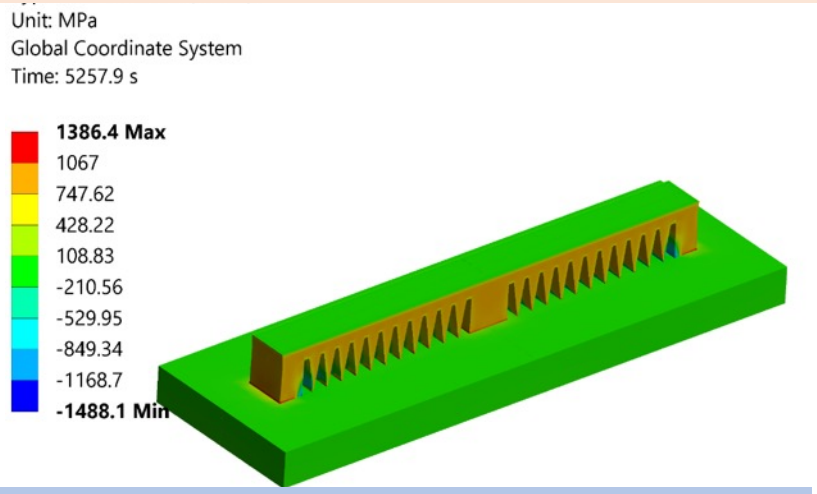


Residual stress wall coupon

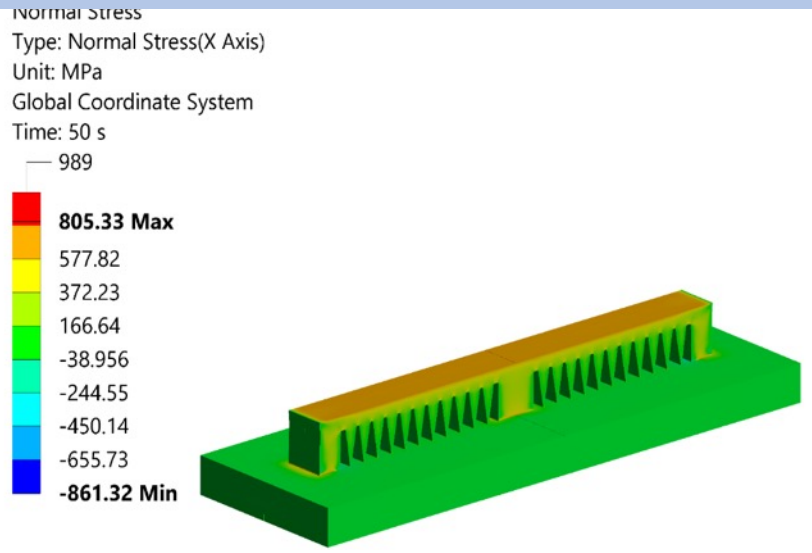
Simulation based on the temperature history – 2.5 hours

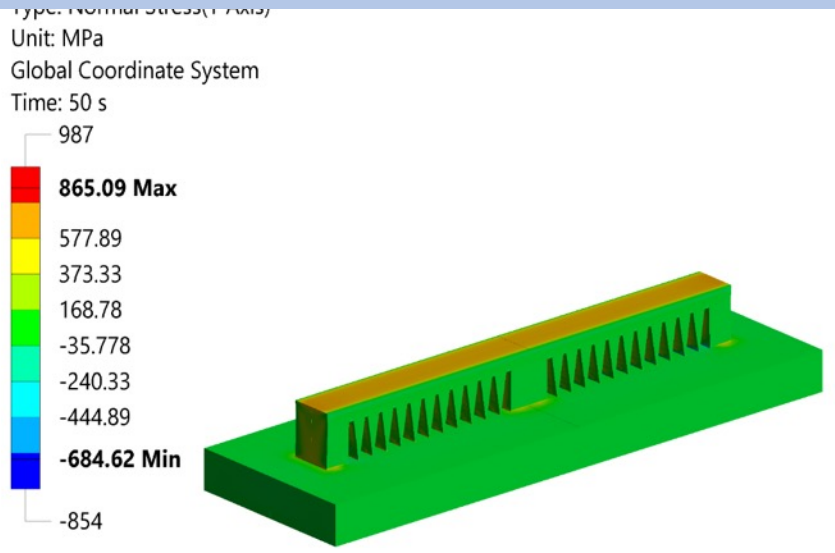


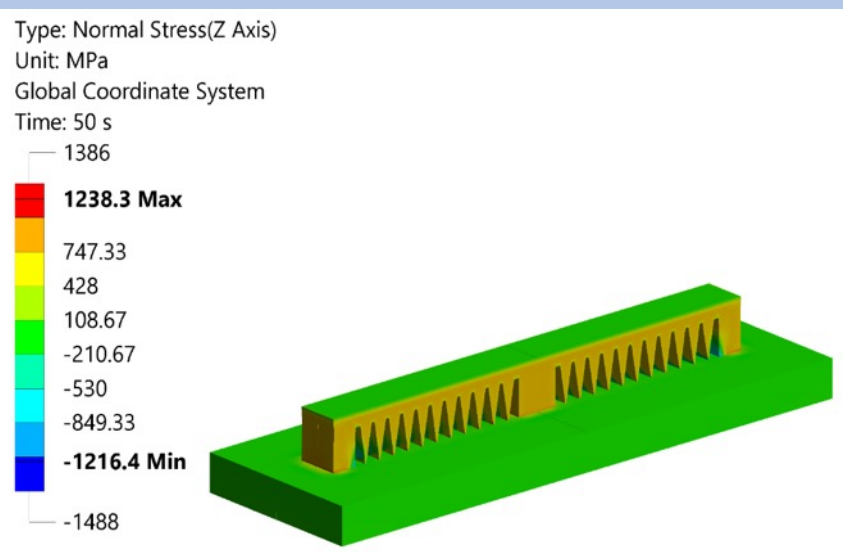


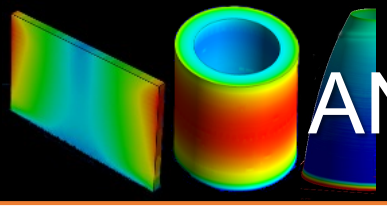


Residual Stresses for Wall Coupon - Inherent strain approach – 0.25 hours



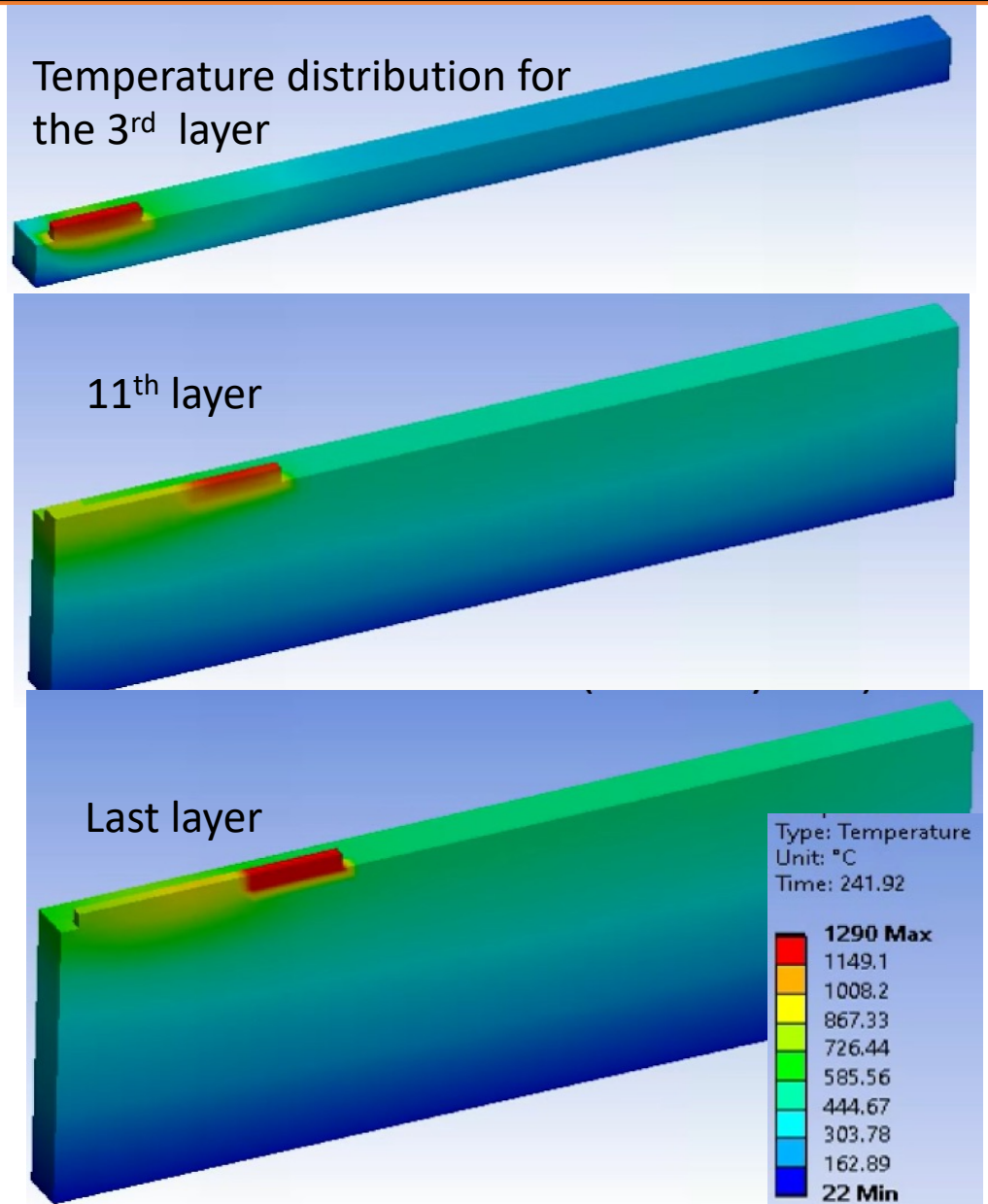


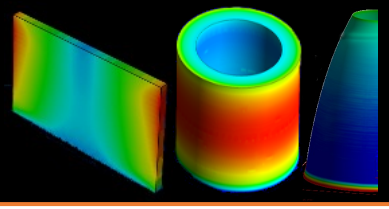




ANSYS DED Process Simulation

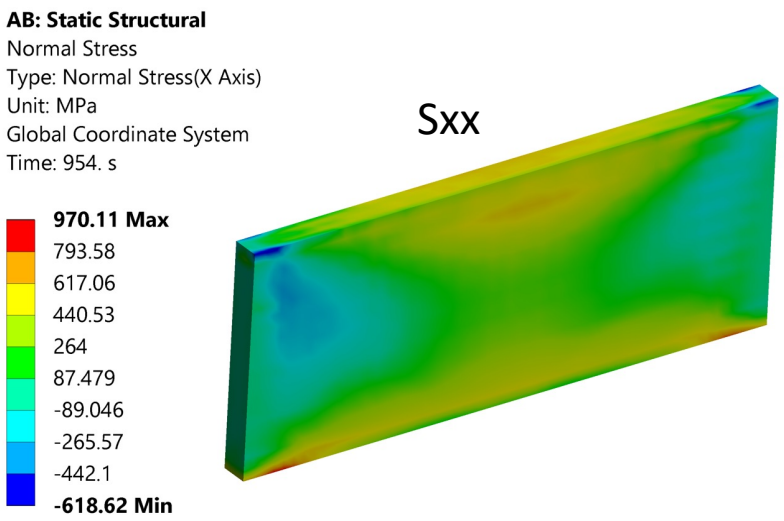
- Thin wall coupon was used for DED simulation and results were compared with the results obtained earlier for residual stress in the part
- The DED Process Simulation in Workbench Additive was performed to predict the macro-level temperature distribution by implementing tool path modeling approach (as an example snapshots of the simulations are presented in the right-hand side plot).
- G-Code, as a most commonly programming language for computer numerical controlled (CNC) machines, is used to form a tool paths during DED manufacturing.
- Clustering of the mesh elements is used to form mesh "clusters" that are exposed to one temperature in a time step. In the thin wall coupon example (on the right-hand side plot) 5 mesh elements are integrated in one cluster having initial melting temperature during simulation.
- The temperature time history of the DED process was used to predict residual stresses and distortions in the wall coupon.



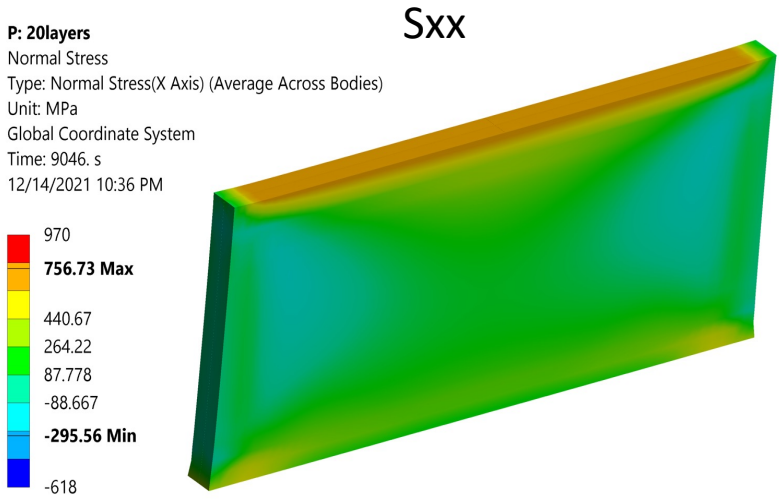


Residual stress comparison for DED simulation using G-code and standard ANSYS

Tool path temperature history using G-code

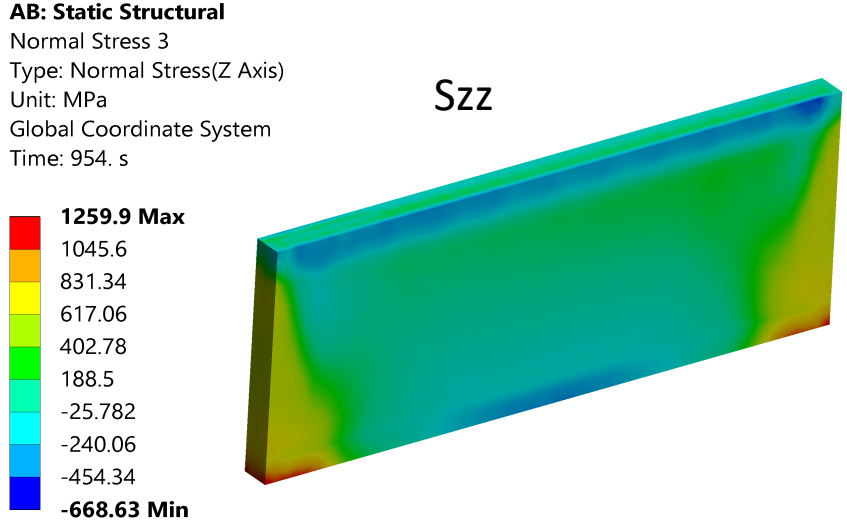


Melting temperature applied for each layer

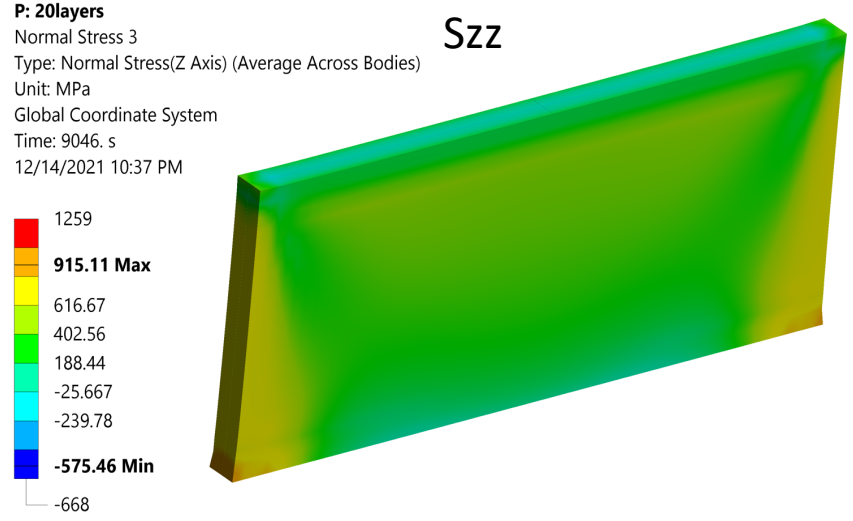


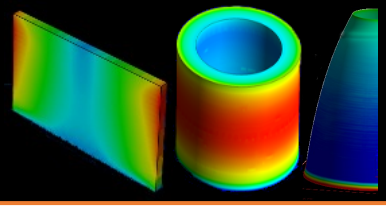
- DED simulation was performed in Ansys Workbench using G-code for thin wall structure.
- Havin a G-code of the real process we used it to obtain temperature distribution dynamics.
- All stress components and distortions were determined this based on temperature history.
- The results were compared for the standard approach while the whole layer initial temperature is prescribed to melting temperature.
- The results show comparable stresses for these two simulation approaches (results for Sxx residual stresses –left-hand plot and Szz –right hand side plot).
- Residual stresses for DED manufac-turing are a little bit larger in a certain area (like at the base junction).

Tool path temperature history using G-code

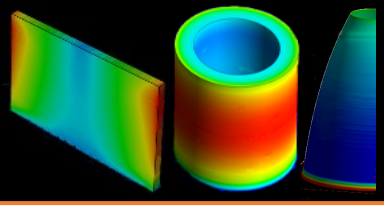


Melting temperature applied for each layer





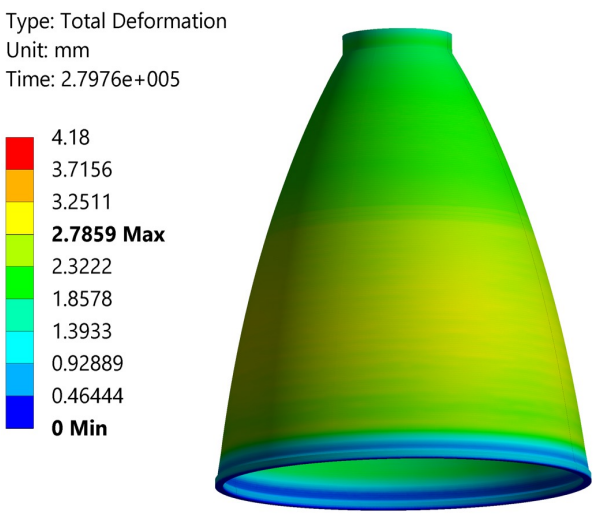
Nozzle scale

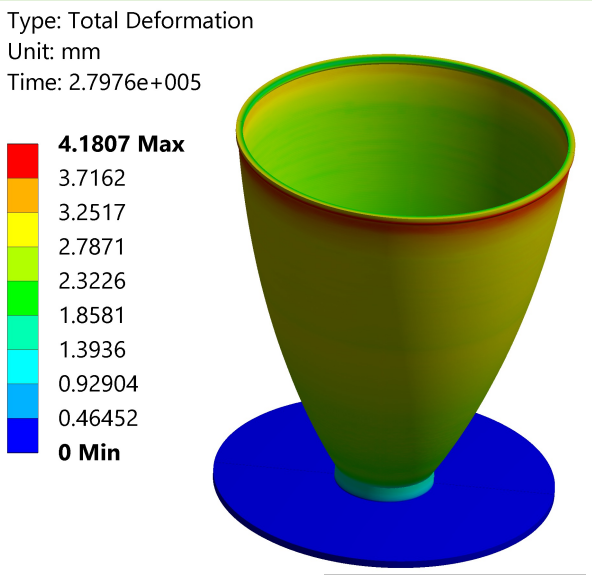


Nozzle Build Orientation

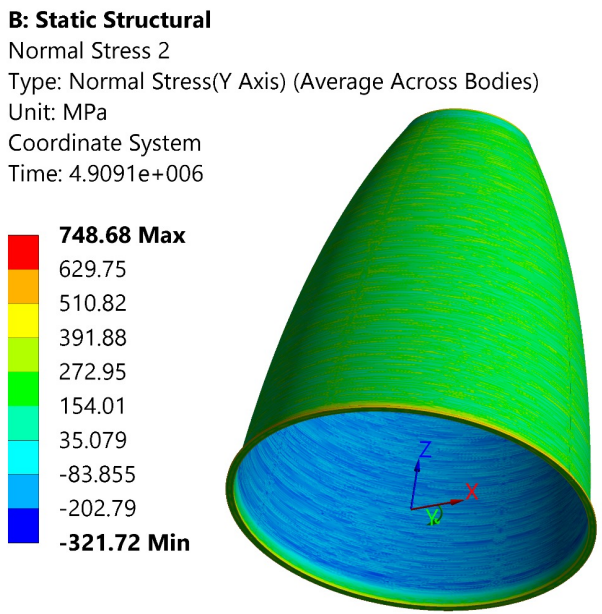
Questions: 1. Which build orientation, top to bottom or bottom to top would mitigate distortion? 2. How does dual-head deposition affect residual stress?
Simulation-based answers: 1. Half-scale and Full scaled RS-25 nozzle liner best to build large end down on base-plate. 2. Diameter is large enough that dual-head should be fine.
Outcome: DM3D Technologies built large end down with dual-head deposition.

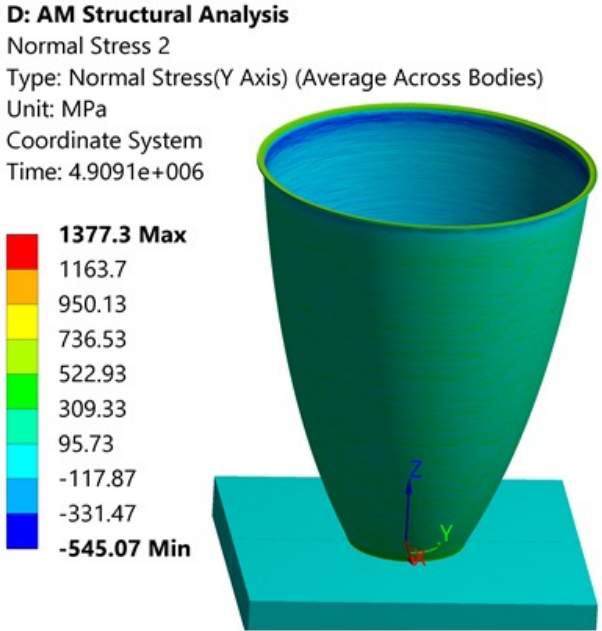
Half scaled RS25 nozzle simulation: Predicted deformation for wide dimeter down is much less then the wide end up (2.8 mm vs. 4.2 mm). Total deformation is mainly radial compression.

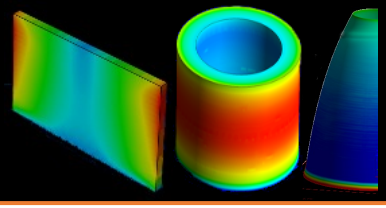




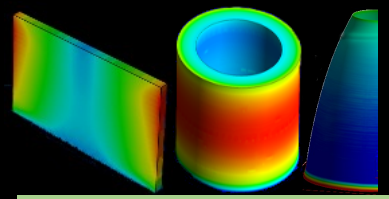
Full scale nozzle RS25 simulation: Predicted hoop stress lower big end down.







Bi-metallic/Tri-metallic



Computational Modeling

Computational modeling & validation to predict residual stresses and distortion in bi-metallic additive parts from process parameters. Accomplishments: 1. Coupons built, 2. Developed and utilized tri-metallic pragmatic method.

Addresses Goal #2 & Objective #4

Goal #2 - Identify and optimize additive manufacturing design and fabrication processes that lead to reduced production lead times and analysis life cycle for large scale thrust chamber assemblies.

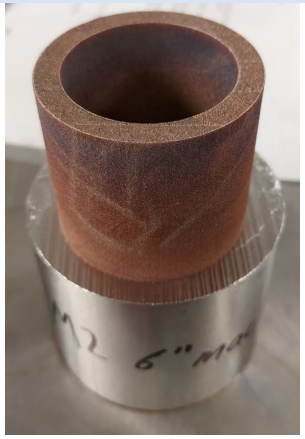
Objective #4 - Advance modeling and simulations of large-scale deposition techniques to obtain optimal property predictions, material designs, and develop "smart" tool-paths to reduce distortion and provide acceptable components.

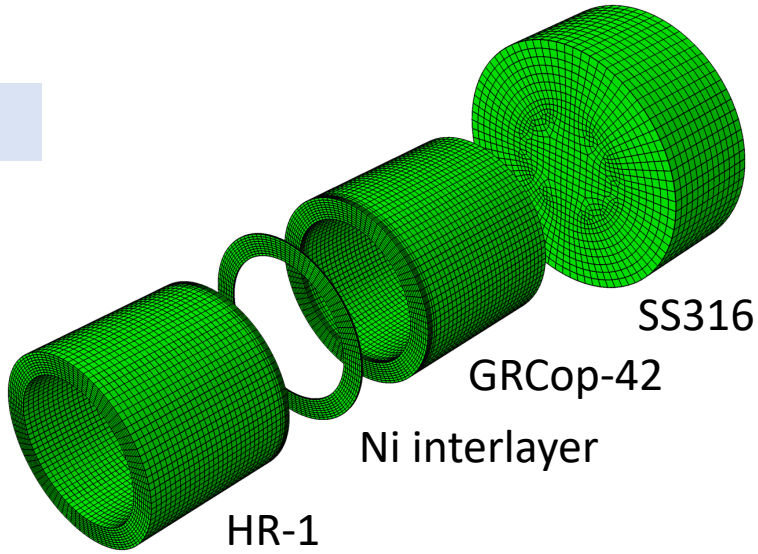
ID: 44.704 mm
OD: 34.704 mm
Height:
GRCop-42: 38.1 mm
Nickel: 0.3 mm
HR-1: 38.1 mm

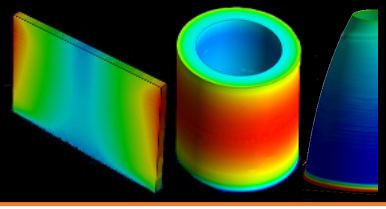
Approach:

1. Built analysis coupons: LPBF GRCop-42, cold spray nickel, DED HR-1.
2. Predict stresses & distortion with multiple simulation codes using tri-metallic **Pragmatic Method**.
3. Compare results between codes.
4. Compare with measurements at NIST.

GRCop-42 cylinder on base





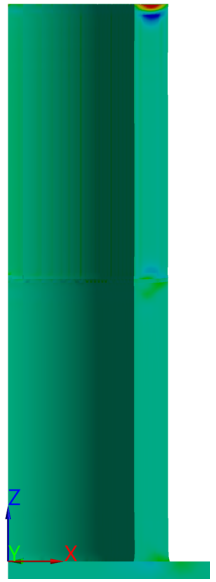


Predicted tri-metallic stresses

T: Static Structural
Normal Stress
Type: Normal Stress(X Axis)
Unit: MPa
Coordinate System
Time: 33625 s

846.44 Max
698.75
551.05
403.35
255.65
107.95
-39.743
-187.44
-335.14
-482.84 Min

Radial stress



T: Static Structural
Normal Stress 2
Type: Normal Stress(Y Axis)
Unit: MPa
Coordinate System
Time: 33625 s

1018.7 Max
850.07
681.41
512.75
344.1
175.44
6.7773
-161.88
-330.54
-499.2 Min

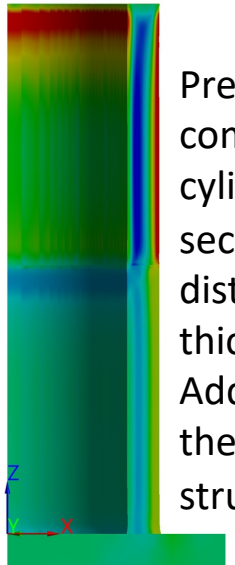
Hoop stress



T: Static Structural
Normal Stress 3
Type: Normal Stress(Z Axis)
Unit: MPa
Coordinate System
Time: 33625 s

1057.7 Max
857.42
657.19
456.96
256.73
56.502
-143.73
-343.96
-544.19
-744.42 Min

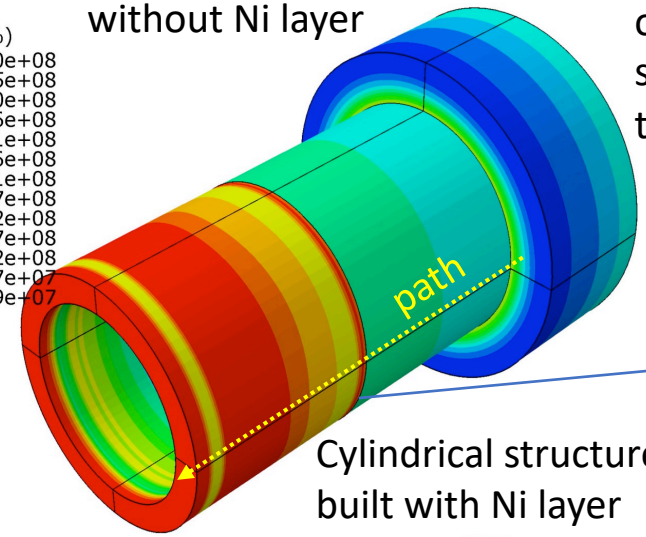
Axial stress



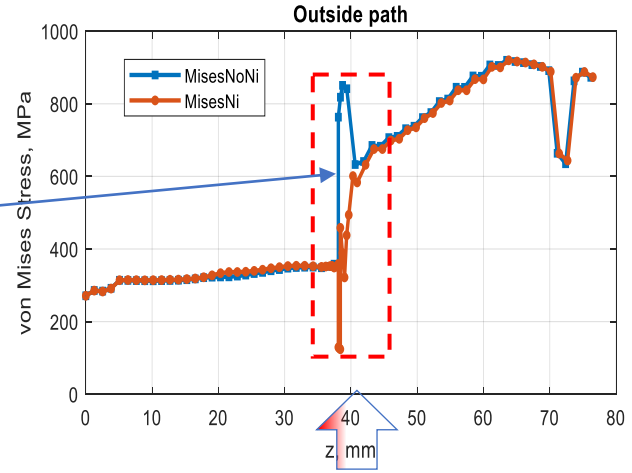
Predicted residual stress components for tri-metallic cylindrical coupon. Vertical cross-section shows residual stress distribution through the thickness of the wall. (Ansys Additive simulation for quarter of the tri-metallic cylinder structure).

Cylindrical structure built without Ni layer

S, Mises
(Avg: 75%)
+9.20e+08
+8.45e+08
+7.70e+08
+6.96e+08
+6.21e+08
+5.46e+08
+4.71e+08
+3.97e+08
+3.22e+08
+2.47e+08
+1.72e+08
+9.77e+07
+2.29e+07

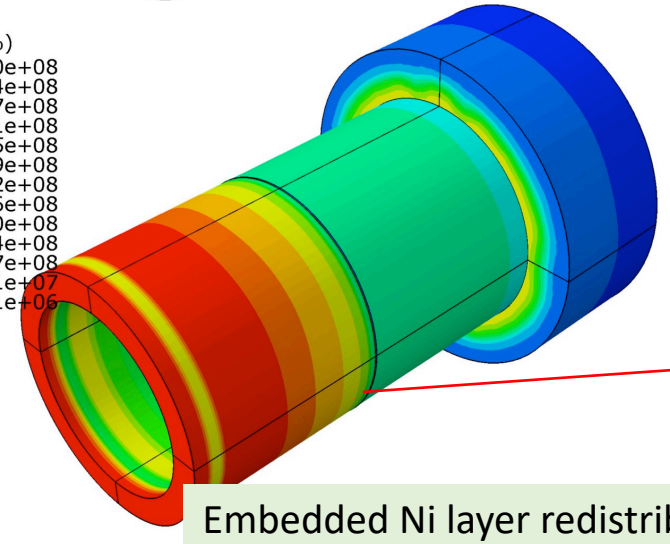


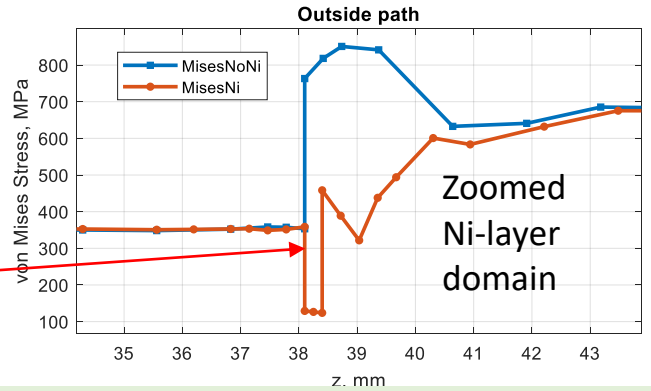
Von Mises residual stresses along a path on the outer wall surface have about the same stresses except the small vicinity of the Ni layer in HR1



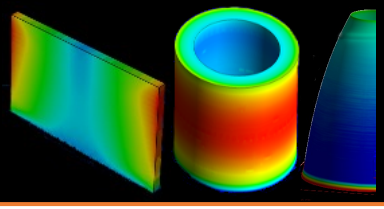
Cylindrical structure built with Ni layer

S, Mises
(Avg: 75%)
+9.20e+08
+8.44e+08
+7.67e+08
+6.91e+08
+6.15e+08
+5.39e+08
+4.62e+08
+3.86e+08
+3.10e+08
+2.34e+08
+1.57e+08
+8.11e+07
+4.91e+06





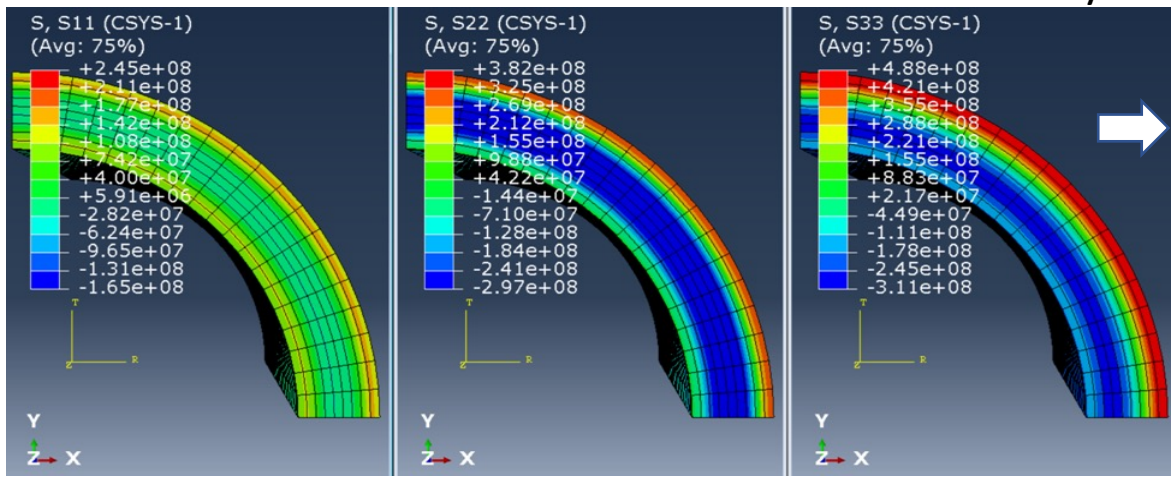
Embedded Ni layer redistributes residual stress components having much smother transition from GRCop-42 to HR1



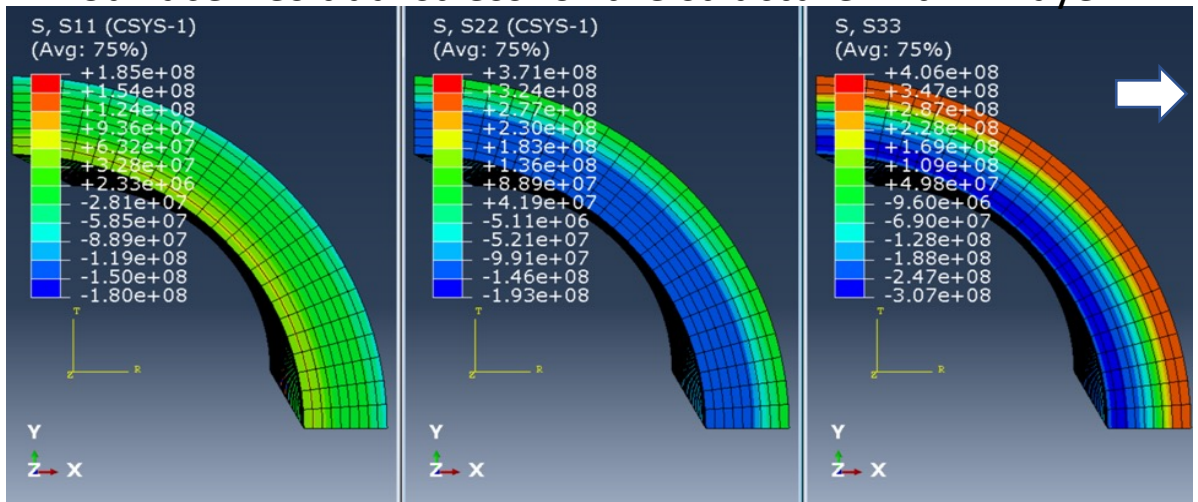
Effects of cold spray nickel layer

Nickel layer between GRCop-42 & HR-1 reduces hoop stress

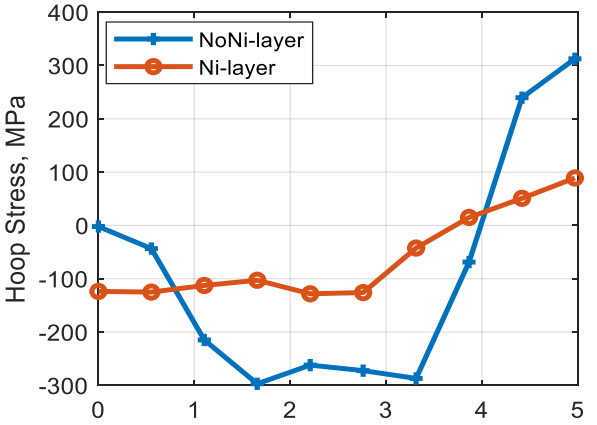
Surface residual stress for the structure without Ni layer



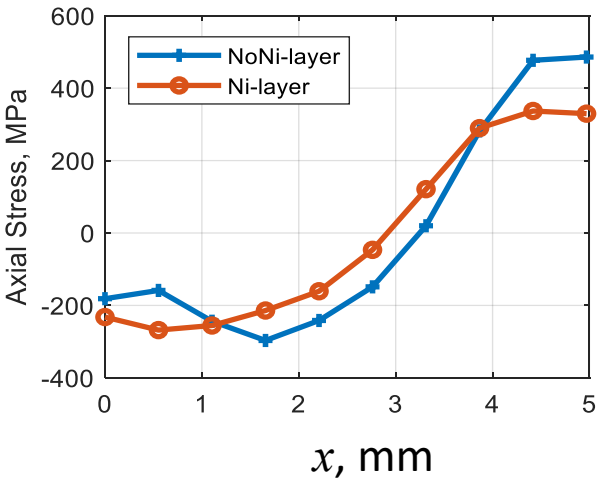
Surface residual stress for the structure with Ni layer

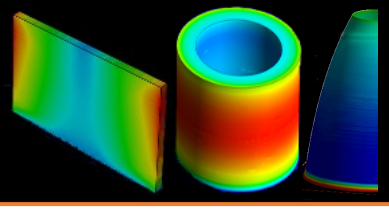


Hoop stress along the radius



Axial stress along the radius



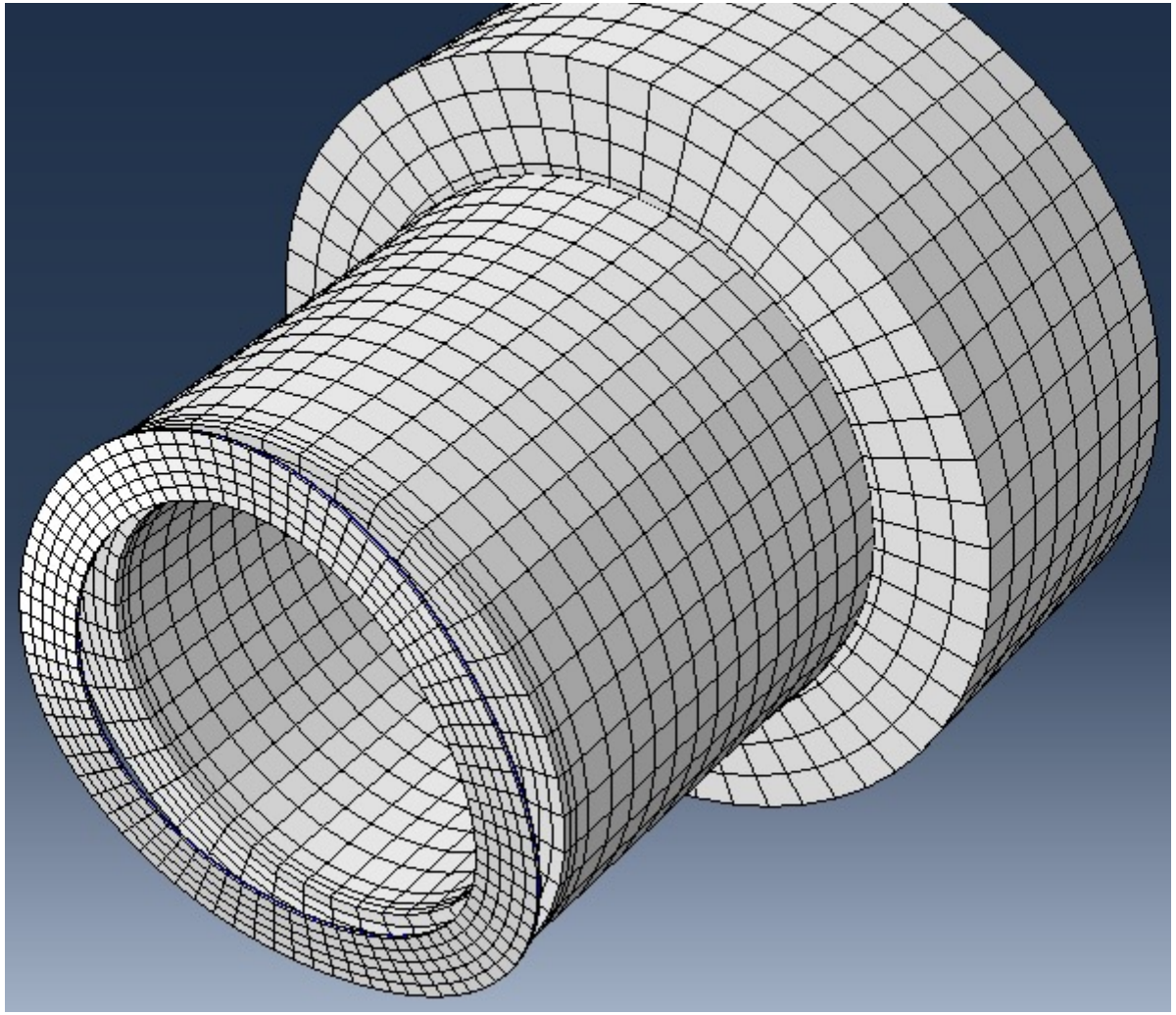


Failure from Ni layer delamination

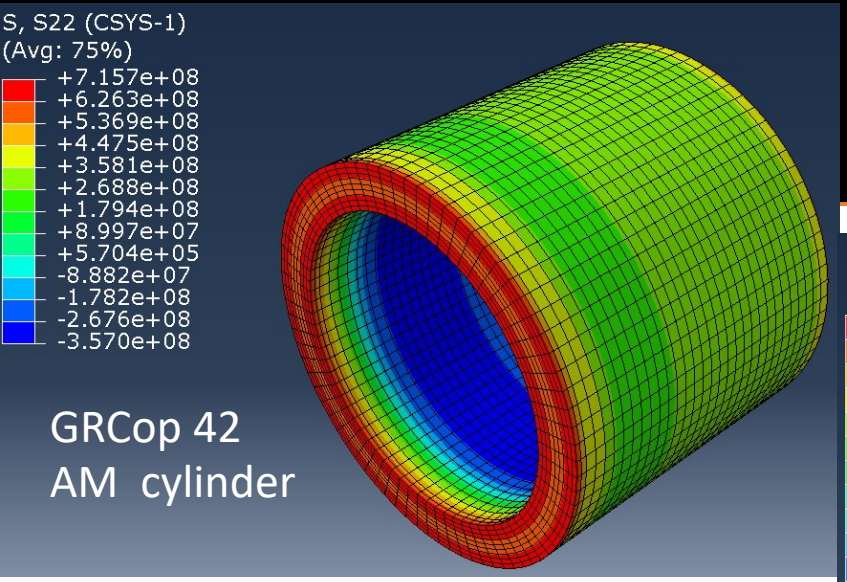
Deposition of HR-1 onto cold sprayed Ni failed due to delamination of nickel.

Suspected causes:

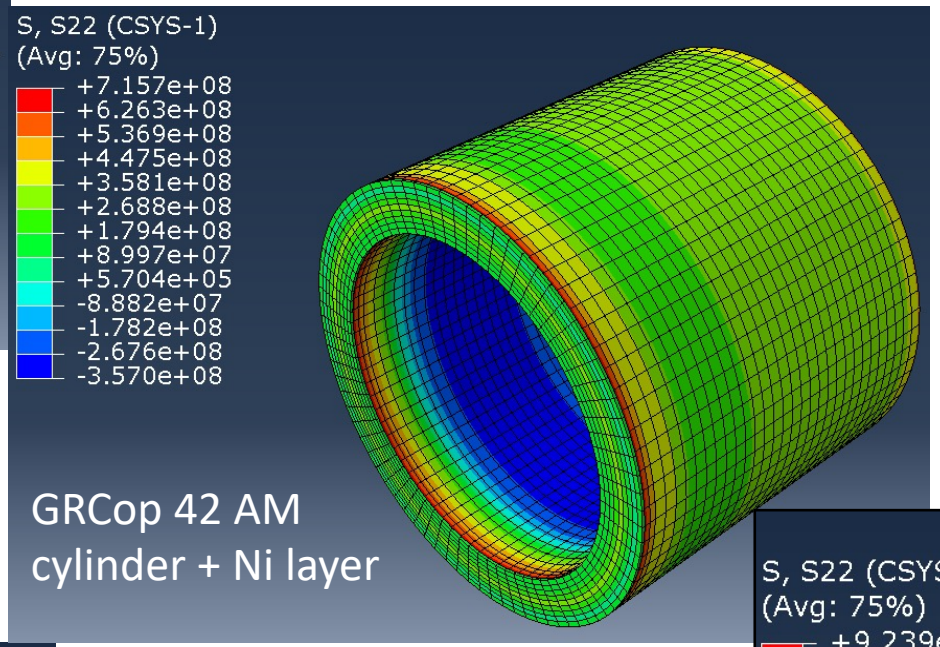
1. DED of HR-1 was too hot/deep and thus the melt-pool went through the diffusion layer of Ni.
2. The Ni diffusion layer was too shallow from an unknown changed in the cold spray process.



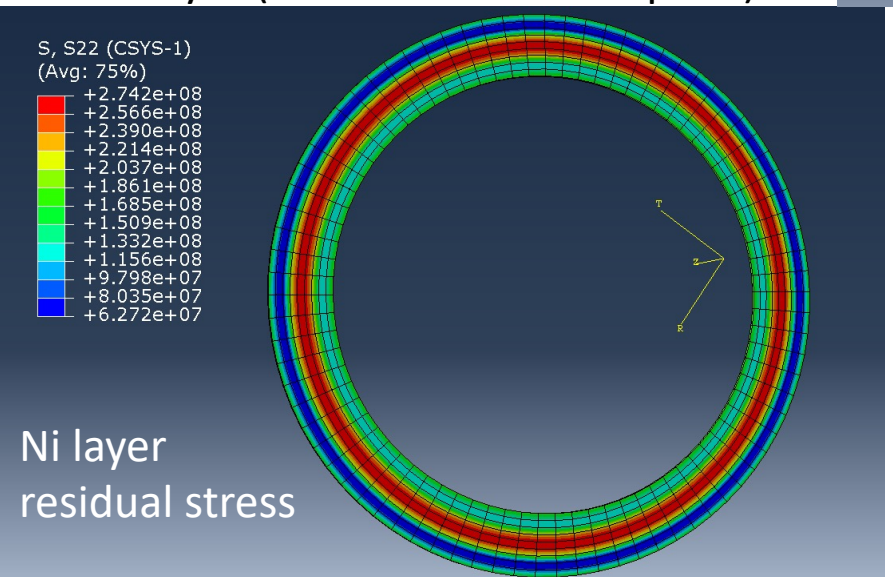
Hoop residual stress



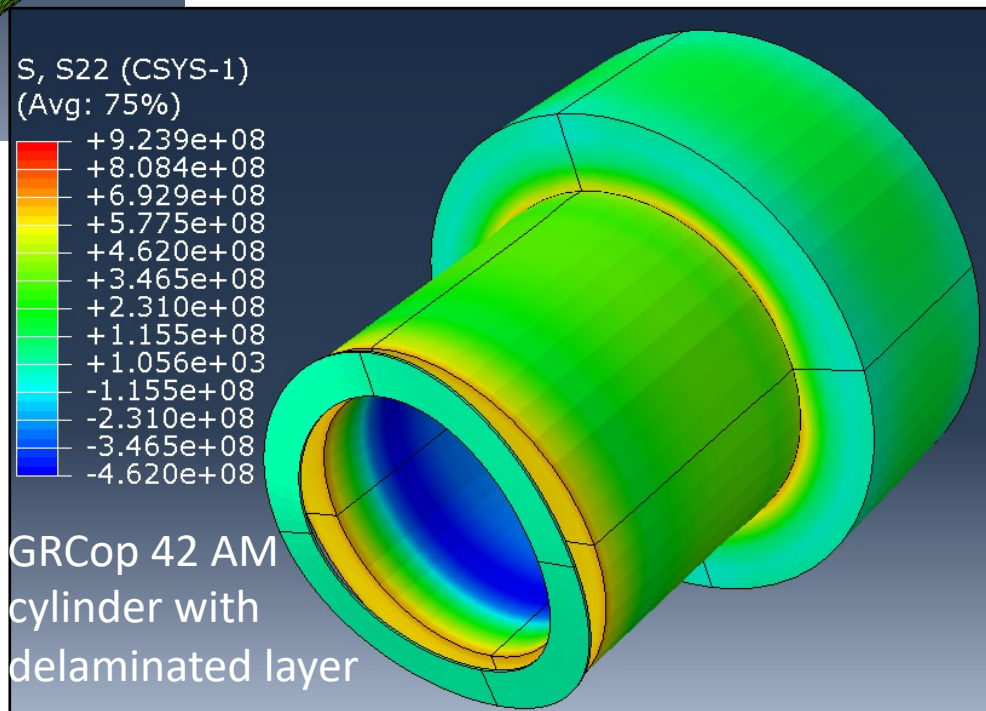
Hoop stress in an AM GRCop cylinder. One can see substantial hoop stress on the top of the structure (top plot). Adding Ni layer decreases hoop stress in the Ni layer (center and bottom plots)

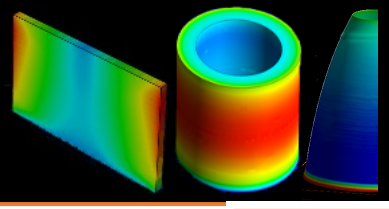


Hoop stress is presented as illustrative example. The same situation takes place for a radial stress. Axial stress is small since axial stress is normal to the surface

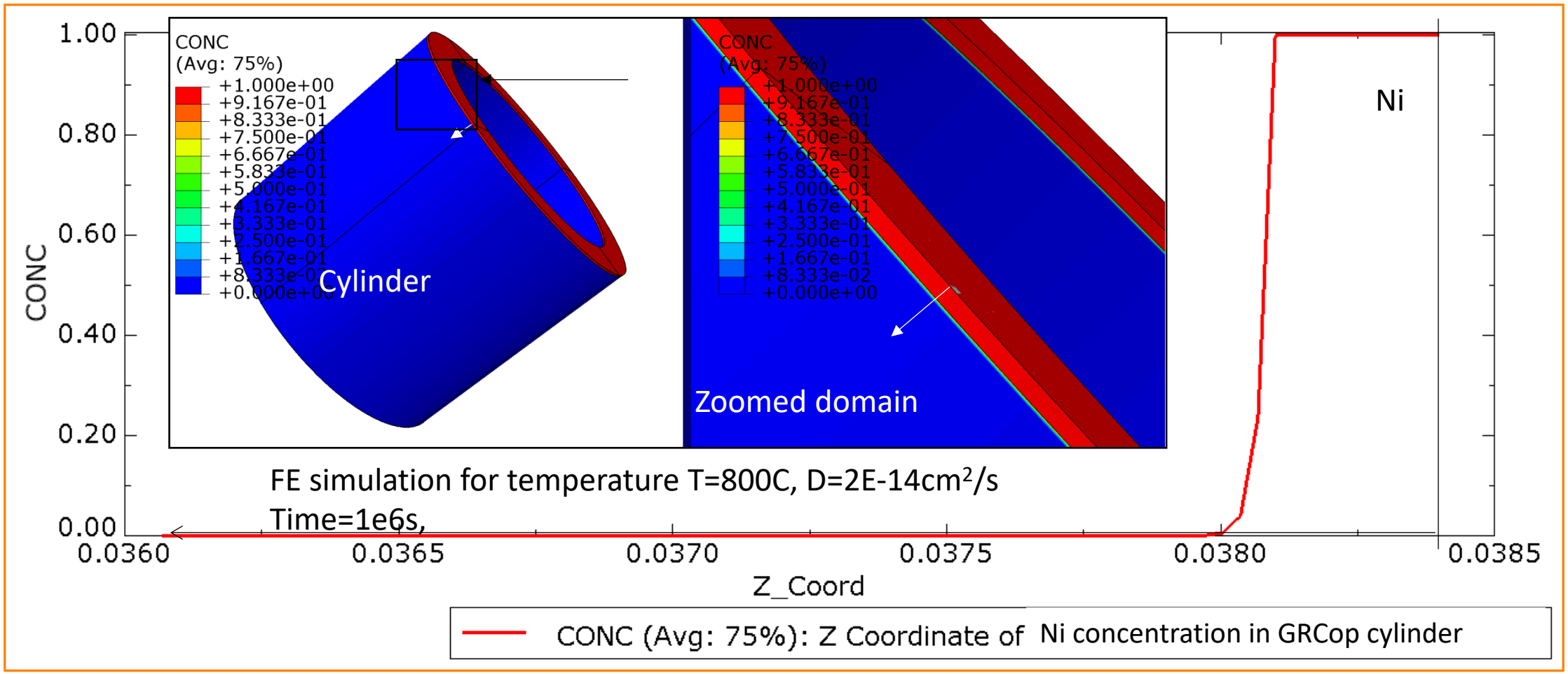


Small adhesion between Ni layer and GRCop 42 might lead to delamination of the cold sprayed Ni layer from the GRCop 42 cylinder and releasing the stresses in the Ni layer (compare stresses in the layer between left and hand side plots)

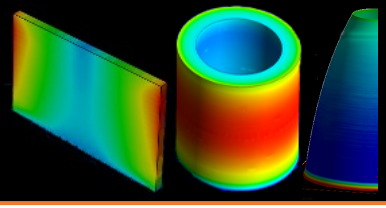




Simulation of Ni diffusion into GRCop-42



Ni adhesive layer strength might be increased by increasing diffusion length of the of Ni inside GRCop 42 structure. The finite element of diffusion process was simulated. Inserts to the linear plot show FE simulation of the Ni diffusion (red) insider GRCop concentration – blue. Linear plot (red line) corresponds to Ni concentration (white arrow on the contour plot). Obtained results depend strongly on experimental data of diffusion coefficient D depending on the temperature.



Accomplishments

Accomplishments

- Melt pool models developed and verified with published results
- Material thermal response characterization
- 3 coupons designed, manufactured and model predicted residual stresses verified
- Simulation models scaled up to part-scale
- Nozzle scale simulations performed in ANSYS Additive
- Bi-metallic coupon simulated